Salivary small non-coding RNAs as biomarkers for concussion management

By

Callum Nicholas Watson

UNIVERSITY OF BIRMINGHAM

A thesis submitted to the University of Birmingham for the degree of

Doctor of Philosophy

Institute of Inflammation and Ageing

College of Medical and Dental Sciences

University of Birmingham

August 2020

Abstract

Concussion occurs when a “biomechanical force, transiently disturbs normal brain function causing neurological, cognitive and behavioural signs and symptoms”. However, the diagnosis of concussion is imprecise and challenging.

Currently, there is a great deal of attention on concussion in contact sports due to the immediate and potential long-term effects on the brain. The transient and complex array of symptoms that occur, mean patient compliance is essential, to quantify the neurological deficit that enables an experienced assessor to diagnose accurately. The future in concussion diagnosis therefore lies in the development of a simple, relevant, rapid and objective assessment of the trauma to the brain. The most likely candidates are either brain imaging e.g. MRI, or measurement of a relevant biomarker or group of biomarkers. Rapid diagnosis is particularly needed in contact sports such as rugby and football to enable players to safely return to play. The development of an objective diagnostic test may also help to explain the longer-term impact of head injury, and be applicable to other sports and situations e.g. military or household accidents etc.

In this thesis, I have hypothesised that changes in small non-coding RNAs (sncRNAs) and extracellular vesicles (sEVs) in saliva may be used for the diagnosis of concussion. Changes in either or both of these in saliva could reflect rapid changes in the brain and systemic circulation due to the concussion. Understanding of mechanism through which these changes could occur is beyond the scope of this thesis.

The Study of Concussion in Rugby Union through MicroRNAs (SCRUM) (ISRCTN16974791) has used next Generation Sequencing (NGS) and qPCR validation steps to analyse 390 saliva

samples from the top two tiers of professional rugby in England. Samples were collected during training, 3 hours and 48-72 hours post-injury. Controls were taken from groups with musculoskeletal injury, uninjured players, and players in whom concussion had been suspected but ruled out on.

I have identified 12 sncRNAs that undergo up-regulation in saliva of players with concussion (ten in the immediate aftermath, two 48-72 hours post injury). Two sncRNA families had more than one member responding to injury, namely the RNU-6 snRNA and Let-7 miRNA families. Further work is required to confirm whether measurement of these, or a combination of sncRNAs, can be used to diagnose concussion. sEVs were measured in saliva using a new assay, the ExoView, but no clear pattern of change was observed. This is likely to reflect the complexity of sEVs which vary markedly in size and can be generated from multiple cell types.

Studies on miRNAs, were extended to a deceased group of patients who had been diagnosed with Alzheimer's disease (AD), in view of a possible historical link to concussion. Brain samples were obtained from the South West Dementia Brain Bank (SWDBB, University of Bristol). Two progressive stages of AD and a control group were assessed using qPCR. The Let-7 family miRNAs, hsa-let-7i-5p and hsa-let-7a-5p, were found to be differentially expressed in the brains of AD patients. Further work is required to understand the function of these two mRNAs in the brain.

In conclusion, this study has identified several sncRNAs that may change in saliva in response to concussion and which could form the basis of a future diagnostic test. This work has also provided preliminary evidence of changes in the Let-7 family of miRNAs in AD. Further work is required to understand the significance of changes in sncRNAs in concussion and AD, and a possible link between their role (if any) in these two disorders.

Publications arising from this thesis

Watson CN, Belli A, Di Pietro V. Small Non-coding RNAs: New Class of Biomarkers and Potential Therapeutic Targets in Neurodegenerative Disease. *Front Genet*. 2019;10:364. Published 2019 Apr 26. doi:10.3389/fgene.2019.00364

Yakoub KM, O'Halloran P, Davies DJ, Bentley C, **Watson CN,** et al. Study of Concussion in Rugby Union through MicroRNAs (SCRUM): a study protocol of a prospective, observational cohort study. *BMJ Open*. 2018;8(11):e024245. Published 2018 Nov 25. doi:10.1136/bmjopen-2018-024245

Yakoub KM, Davies DJ, Su Z, Bentley C, Forcione M, Toman E, Hammond D, **Watson CN,** et al. Investigation into repetitive concussion in sport (RECOS): study protocol of a prospective, exploratory, observational cohort study. BMJ Open. 2019;9(7):e029883. Published 2019 Jul 4. doi:10.1136/bmjopen-2019-029883

Acknowledgements

I would like to thank my primary supervisor, Professor Antonio Belli, for allowing me to undertake this project and acting as a figurehead throughout. I would also like to thank my secondary supervisor, Dr Valentina di Pietro, for supporting me on daily basis and for showing endless patience in my scientific ideas, I hope your first PhD student was not too hard work! I would also like to thank the Medical Research Council for funding me throughout my PhD.

I would like to thank my fellow PhD student, Dr Patrick O'Halloran, for his support through lunch club, the long car journeys to pick up samples and – in all seriousness – a colleague to talk to about the trials and tribulations of doing a PhD. I would also like to thank Dr Ghazala Begum for her help in designing and conducting numerous experiments with the Alzheimer's disease brain samples, without who this would have been a much more difficult challenge. I would also like to thank all members of the Neuroscience and Ophthalmology labs during my stay for their kindness and support, with a special mention to Dr Maryam Esmaeili for tidying up the mess I made when I had appendicitis.

I would also like to thank my vesicle colleagues in particular, Dr Paul Harrison, for his vision and enthusiasm for my project and vesicle's in general, and his support to allow for a visit to present at Nanoview Biosciences in Boston, USA. Also, I would like to thank Mr Joshua Price for his – quite frankly – ridiculous level of enthusiasm for science and particularly vesicles, which allowed for great chats and a very memorable trip to Boston.

I would like to thank Will for putting up with me as a housemate for this period, it has been a pleasure. I would also like to thank my girlfriend Emily for her care and support throughout allowing fun and laughter in what at times was a stressful period.

I would also like to thank my family for the endless level of support they give that has allowed me to succeed so thank you to my parents Anne and Steve Watson and my younger brother Sean who I must apologise to for leaving him as the only one without a PhD (hopefully).

Contents

Abbreviations

AD	Alzheimer's disease
AGO	Argounaute protein
BBB	Blood Brain Barrier
BCA	Bicinchoninic Acid
C	Concussion sample
CSF	Cerebral Spinal Fluid
CT	Computerized Tomography
CTE	Chronic Traumatic Encephalopathy
DAI	Diffuse Axonal Injury
ECM	Extracellular Matrix
FDR	False Discovery Rate
fMRI	Fluorescent Magnetic Resonance Imaging
HIA	Head Injury Assessment
HIA-	Concussion suspected and ruled out control
HK	Housekeeping gene
ILVs	Intraluminal vesicles
ImPACT	Immediate Post-Concussion Assessment and Cognitive Testing tool
miRISC	miRNA-induced silencing complex
miRNAs	MicroRNAs
MRI	Magnetic Resonance Imaging
mRNA	Messenger RNA
MSK	Musculoskeletal injury control
mTBI	Mild Traumatic Brain Injury
MVBs	Multi-vesicular bodies
ND	Neurodegenerative disease
NMDA	N-methyl-D-aspartate
PCA	Principal component analysis
piRNA	Piwi RNA
RECOS	Repetitive Concussion in sport
RFU	Rugby Football Union
SCRUM	Study of concussion in Rugby Union using microRNAs

sEVs	Small Extracellular Vesicles
SIS	Second Impact Syndrome
sncRNAs	Small non-coding RNAs
snoRNAs	Small nucleolar RNAs
snRNAs	Small nuclear RNAs
sTBI	Severe TBI
SWDBB	South West Dementia Brain Bank
TBI	Traumatic Brain Injury
tRNAs	Transfer RNAs
U	Uninjured control
UTR	Untranslated region

Chapter 1: Introduction

Concussion

Concussion, a type of mild traumatic brain injury (mTBI), is defined as a "clinical syndrome in which a biomechanical force, transiently disturbs normal brain function causing neurological, cognitive and behavioural signs and symptoms" by the Centre for Disease Control. [1].

Why is it a problem?

Currently concussion affects around 3.8 million sporting participants per year in the United States alone [2]. The exact figures are difficult to quantify due to; the transient nature of symptoms, the overlap of symptoms with other diseases and subjective diagnosis methods that require a highly skilled individual for diagnosis. Numbers could therefore be miss reported as a result of under-recognition of disease. Concussion makes up 20% of mild TBI (mTBI) forms and mTBI forms account for 80% of all TBI cases [3], which demonstrates the importance of effective mTBI diagnosis methods to manage such a wide population.

Typically, concussion symptoms resolve within two weeks, with minimal treatment, however 10-20% of all patients have prolonged symptoms. It is unclear why some patients have prolonged symptoms and not all symptoms are necessarily visible. However an early return to sport before a concussion has fully resolved is known to increase risk of new injury [4] and in extreme cases lead to second impact syndrome (SIS) [5]. Also, multiple concussions are associated with depression and chronic neurodegenerative diseases [6, 7]. The pathophysiological knowledge behind prolonged symptoms and long-term implications is limited so effective management is paramount to prevent repeat concussion to ensure patients are not put at any further risk.

Occurrence of concussion?

Concussion has as higher prevalence in contact sports (Rugby Union, Football and Boxing), front line military service and adolescents but occurs in recreational accidents as well as other settings [8]. Typically, an excessive trauma to the head or "whiplash" from extreme acceleration-deceleration forces are the main causes of concussion, and with all such injuries, there are two injury processes that occur.

Firstly, the initial blunt trauma causes direct injuries. The force of the direct injury initiates acceleration, deceleration and rotational forces that cause the brain to move inside the skull, putting both impact and stretching pressures across various areas of the brain (Figure 1). These pressures cause white matter changes over long-distance through axonal damage. The secondary injury is the physiological response to the damage caused by the primary injury that happens within seconds, minutes or hours after event e.g. inflammation and infection. The interplay between both primary and secondary injuries make for a complicated development of disease explaining the heterogeneity of concussion.

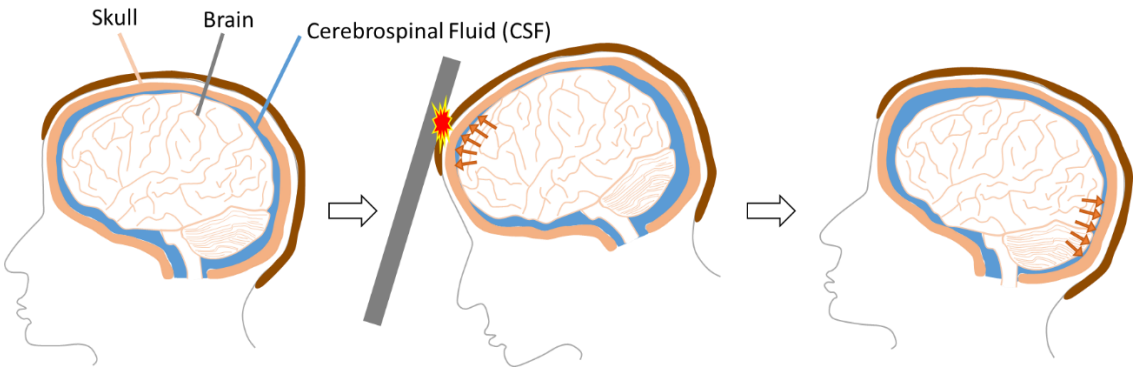

Figure 1 - Concussion Injury Mechanism. The impact on the head causes the brain to move inside the skull generating stretching pressures which cause the primary injury. The physiological response to this injury causes the secondary injury.

Pathophysiology

Ionic flux, neurotransmitter release and energy crisis

The initial biomechanical injury leads to “mechanoporation” of lipid membranes at a cellular level. This causes an efflux of intracellular potassium through voltage-gated channels, leading to neuronal depolarisation. This sustained response creates a feedback loop that increases the number of open voltage-gated channels, extracellular potassium, and depolarisation [9, 10].

Depolarisation promotes unselective release of neurotransmitters, including glutamate, from pre-synaptic terminals, extravasation from damaged cells and altered astrocytic reuptake. Extracellular glutamate induces receptor mediated potassium efflux through ligand-gated channels as well as binding N-methyl-D-aspartate (NMDA)-receptors that open K^+/Ca^{2+} channels to allow unrestricted flow of both ions. Intracellular calcium stores are released while voltage-gated calcium channels are activated leading to intracellular calcium accumulation, which can cause cellular damage through protease activation, reactive oxygen species and mitochondrial impairment [11, 12].

After initial excitation there is a neuronal depression throughout diffuse brain areas [13]. The continued ionic flux leads to an increased cellular metabolic demand, so the mitochondria increase ATP production. The cell attempts to restore ionic balance via the ATP dependent Na^+/K^+ pump [14, 15]. Glycolytic rate increases to meet energy demands of the cell, which produces lactate that cannot be removed in this state. The lactic acid accumulation leads to acidosis and possible BBB permeabilisation [16]. Eventually after a period of relative glucose hypometabolism, normal glucose utilisation returns [17].

Traumatic Diffuse Axonal Injury

Diffuse axonal injury (DAI), presents itself with extensive multifocal lesions throughout white matter tracts. Although not visible on conventional imaging techniques in mTBI, DAI is likely to be present to a lesser extent due to its importance in severe brain trauma [18]. These lesions cause varied neurological impairments dependent upon where they are located in the brain, with clusters forming more regularly in grey-white matter junctions, the brain stem and the splenium of the corpus collosum [19, 20].

There formation starts with the primary axotomy caused by initial impact that leads to rotational acceleration, which through tensile and compressive forces leads to damage in the axonal cytoskeleton. This interrupts transport and causes a secondary axotomy, an accumulation of neurotransmitters and β-amyloid precursor protein [21]. The altered calcium homeostasis, due to the release of glutamate, activates calpains that can further destabilise the cytoskeleton causing axonal undulation that is not all reversible [22, 23]. In some cases, the distal segments of an axon may undergo Wallerian degeneration, with loss of some diffuse synaptic connections [24, 25].

Blood Flow changes

In a healthy state, cerebral vasoreactivity monitors cerebral blood CO_2 concentration to maintain a consistent flow of oxygenated blood. Following mTBI, there are acute cerebral blood flow changes due to a decrease in the capacity of cerebral autoregulation [26]. In a lateral fluid percussion model cerebral blood flow was reduced and the return to normal was dependent on proximity to injury site [27]. Increased endothelial nitric oxide production from the trauma can also reduce cerebral vasoreactivity, which contributes to decreases in

endothelial and smooth muscle response. These effects can increase vulnerability to second injury, chronic injury or exertion related effects [28, 29].

Current management methods

Concussion is amongst the most complex injuries to diagnose. Most injuries happen without a loss of consciousness have little to no neurological signs and the initial signs of injury can be transient. As a result, current methods use a combined approach of neurocognitive testing, previous concussion and medical history, neurological imaging and symptomology to capture and monitor the heterogeneity of concussion manifestation.

Symptoms

Symptoms are used throughout the concussion management process from initial diagnosis through to return to play. Visible signs of initial injury can be short-lived and not always present with loss of consciousness and tonic posturing most noticeable. Symptoms after initial injury include; (1) cognitive (reaction time, memory, processing speed), (2) vestibular (dizziness, balance problems) and (3) psychological (anxiety, depression) impairments [30, 31]. The balance between these different symptom profiles can directly influence the recovery time, which normally take an average of two weeks to subside. An elongated recovery known as post-concussion syndrome occurs in 10-20% of the population [32]. This is more prevalent in patients with co-morbidity factors such as previous psychiatric history and psychosocial stressors [33]. Interpreting this information is important in the diagnosis of disease but it must be considered with caution due to its subjective nature.

Neurocognitive testing

Neurocognitive testing tools act as a standardised method to quantify the deficit that exists after the onset of a concussion alongside symptom profile measures. A combination of assessment tools are utilised to evaluate cognitive function at two stages: brief side line screening and lengthier neuropsychological testing.

Acute screening tools such as the sports concussion assessment tool 5 (SCAT5) (the most well established sideline assessment tool) use cognitive and neurological screening sections composed of tools such as digits backwards and a balance examination, to target neurocognitive symptom alterations. These tools, when used within hours of injury to assess the mental status, are widely agreed to be important in assisting with immediate management and aiding concussion diagnosis but have limited use after 3 days [34-37].

Lengthier neuropsychological tests can provide helpful information on both acute injury diagnosis and recovery from injury, after interpretation by a qualified neuropsychologist [38]. For example computerised cognitive testing in the acute period can identify athletes at risk of slower than expected recoveries [39] and identify deficits in patients who no longer report symptoms [40]. One such tool the Immediate Post-Concussion Assessment and Cognitive Testing (ImPACT) tool, that gives composite scores for verbal memory, reaction time, visual motor-speed and visual memory, has shown a significant decrease in verbal and visual memory with 72 hours of injury [41].

However there continue to be more general concerns of the lack of underlying clinical evidence for the basis of this testing [42]. Doubts exist in (1) whether available tests have robust enough psychometric properties to allow for accurate detection of neurological

change? (2) whether the false-positive and false-negative rates are good enough for accurate diagnosis and management? [43] Nonetheless they still provide clinical value to identify cognitive deficits over and above symptom reporting, especially within the first week after injury [44].

Neurocognitive tests offer benefits in concussion management due to their insight into cognitive deficits but do not offer a definitive answer. They are best used when accompanied with a multidimensional post-concussion assessment interpreted by a qualified neuropsychologist who understands the complexities of the data.

Neuroimaging

Conventional magnetic resonance imaging (MRI) as well as computed tomography (CT) scans are the most commonly used neuroimaging techniques after sustaining a concussion. They are used routinely to rule out more severe injury but do not help predict neurobehavioral dysfunction or recovery time [45]. With that in mind CT scans can rule out intracranial haemorrhage and skull fractures but cannot effectively resolve differences in the grey-white matter interface for mTBI, which MRI has far greater resolution [46]. So if the immediate concern of injury has passed, MRI is generally used to evaluate cerebral contusion and white matter injury [47] and can also indicate structural problems that may cause similar symptom profiles e.g. Chiari malformation to guide management. However, MRI still lacks resolution of the microstructure of the brain, which means, like CT, it is neither sensitive nor specific enough to identify mTBI related brain injury [48]. These limitations show that currently mTBI cannot be diagnosed by neuroimaging alone but it can guide concussion management alongside functional measurements. Novel adaptations of neuroimaging technology such as functional

MRI, diffusion tensor imaging with tractography and magnetic resonance spectroscopy may be able to act as future biomarkers [49, 50].

In summary, concussion management requires extensive tools to understand the functional and structural changes that take place, but the functional changes need to be accompanied to biological measurements to give relevance to the inner functioning of concussion signalling. Ideally this will lead to more consistent measurements that can guide diagnosis, prognosis and return to play more effectively.

Implementation of concussion diagnosis in Rugby Union

Head Injury Assessment (HIA)

In professional Rugby Union leagues across the world where an appropriate number of staff are available, the Head Injury Assessment (HIA) is performed to diagnose sports related concussion as effectively as possible. The World Rugby HIA process is a multifaceted assessment that consists of three time dependent stages, known as HIA1, HIA2 and HIA3 [51].

To enter the HIA process at HIA1, visible signs of concussion are suspected, and the player is immediately removed from play. If clear and obvious they will be removed for the rest of the match. If less clear, a 10-minute window is used for a secondary assessment that contains a small battery of neurocognitive tests including a tandem gait test and assessment of symptom profile are used to establish if a concussion is suspected. A player is then only returned to play if there are no abnormalities with testing.

HIA2 takes place within three hours of the injury for any player with a suspected or confirmed concussion using post-match video review among other things. This assessment uses SCAT 3

with a combination of symptoms and battery of neurocognitive tests. At this point any abnormal test result is considered a positive concussion assessment unless proven otherwise.

All players suspected or confirmed, like at HIA2, have an additional assessment at HIA3 stage that is 36-48 hours later after two nights rest. This includes an expanded SCAT 3 symptom checklist while using a computerised assessment tool such as CogSport and balance assessment.

Graduated Return to Play

In the immediate aftermath of a concussion, rest is recommended until the initial symptoms have subsided (24-48 hrs). After the immediate recovery period a six staged process is suggested whereby the athlete progresses to the next level if there are no recurrence of symptoms. A minimum of 24 hours is required before movement to the next stage. Stage 1 is a gradual return to normal cognitive and physical tasks e.g. normal daily activities. This is followed by a series of staged reintroduction of exercise, sub-symptomatic exercise is the only active therapy to show benefit [52], that test if symptoms reoccur if increased heart rate (Stage 2), movement (3), cognition (4) and contact (5) before full return to sport (6) are added sequentially with a delay if symptoms do reoccur before returning to full participation [53].

Clearly there are a lot of challenges to maintaining this level of management in a wider population and there is an over reliance on symptoms for recovery. Novel methods are therefore required to understand and management concussion more effectively.

Biomarkers

Concussion management is led by indirect multi-modal measures to create a wide-ranging understanding of the individual concussion. However, each method has a risk of subjectivity due to patient compliance or lack of resolution, even with expert and in-depth testing, while not being led by the underlying biology. These indirect measures result from physiological changes that are likely to cause acute unbiased measurable variations. Guiding management based on these objective changes (e.g. biomarkers or fMRI) could be the future to simpler, more effective non-biased methods.

Current Biomarkers

Several protein biomarkers have been looked into with targets for astrocyte (GFAP, S100β), axonal (Alpha-II-spectrin, Tau, Neurofilaments) and neuronal injury (NSE, UCH-L1) have had varied success (reviewed [54, 55]). However only two have been successfully FDA approved biomarkers for guiding whether a CT scan is required in mTBI, these are Glial Fibrillary Acidic Protein (GFAP) and UCH-L1 (Ubiquitin C-terminal Hydrolase).

A glial-derived biomarker stemming from the brain (GFAP) that has shown promise as a biomarker in adults and children. It is present within the serum within an hour after an mTBI injury and stays elevated for several days after injury. In the serum GFAP can distinguish mTBI patients from trauma patients who do not have a head injury. The same study showed GFAP was increased in mTBI patients with traumatic intracranial abnormalities on CT compared to those without with a sensitivity of 94-100% and could be used to predict who required surgical intervention [56].

The calcium-binding protein S100β is found in astrocytes and Schwann cells as well as chondrocytes and fat cells with levels measurable in serum, urine and CSF [57]. Numerous studies have demonstrated elevated S100β and abnormalities on CT imaging [58] and increased incidence of post-concussion syndrome [59]. However, questions still remain about specificity with elevated levels in polytrauma patients. When mTBI was compared to orthopaedic injury without head injury S100β had a sensitivity of 61% and specificity of 77% [60].

Tau is a protein involved in axonal transport and assembly of axonal microtubule bundles. Proteolytically cleaved tau (c-tau) is significantly upregulated in the CSF of TBI patients and correlate with poor outcome [61]. However, in blood, c-tau is a poor predictor in mTBI with an inability to accurately foresee traumatic lesions on CT and post-concussion syndrome [62, 63].

Neurofilaments are neurone cytoskeleton components. Following TBI, calcium influx causes a phosphorylation cascade that contributes to axonal injury [64]. Levels of hyperphosphorylated neurofilaments (p-NF) have been found to be elevated in the CSF of patients with sTBI when compared to controls [65]. In mTBI, p-NF serum levels have been shown to increase when compared to healthy controls at day 1 and day 3 [66]. The biomarker potential has not yet been fully explored and although this single study showed high sensitivity and specificity more studies are needed to prove its relevance.

The protein UCH-L1 is known to be highly abundant in neurons and is involved in the removal of ubiquitin from proteins that are going to be metabolised [67]. It has an important role in the removal of excessive, oxidised or misfolded proteins during normal functioning of neurons

[68]. Levels of UCH-L1 are elevated in the serum of mTBI patients within an hour of injury and seem able to distinguish between uninjured and trauma patients with an absent of head injury. Like GFAP, it has shown the capability to distinguish those patients with intracranial lesions on CT [69].

Although promising, none of these biomarkers have been produced for the purpose of diagnosing concussion, which may result from overlap with other populations or could be due to its complexity.

Novel Biomarkers (Small non-coding RNAs and Small extracellular vesicles)

All information obtained to manage concussion in patients is valuable. Protein biomarkers are playing their role in improving knowledge base and some candidates are proving possibilities in aiding the diagnosis process. However no current biomarker has the sensitivity or specificity to ably diagnose or manage concussion individually or as a group, which means concussion is still not led by invasive measurements. New potential markers of injury that have the sensitivity and specificity required to be used alone or in conjunction with other invasive measurements will allow a different angle to accompany the multi-modal testing procedure.

MicroRNAs

MicroRNAs (miRNAs) are short sequences of non-coding RNA comprising of around 20-22 nucleotides [70]. They act as messengers in response to undefined stimuli, which affect signalling within biological processes such as the cell cycle, cell metabolism, apoptosis and immune responses [71]. MiRNAs are expressed throughout the human body and have been shown to respond in numerous disease states including cancers and neurological diseases.

Concussion is a stimulus that miRNAs have been shown to respond to, with fluctuations in miRNA activity potentially demonstrating changes in disease state [71].

Biogenesis

MiRNA biogenesis commences through transcription – generally by RNA polymerase II – within the nucleus, producing a long primary miRNA (pri-miRNA) with a local stem-loop structure which contains the embedded miRNA sequences. This sequence (generally over 1kb) is excised by a microprocessor, a combination of the RNase III endonuclease Drosha and its cofactor DGC8, to produce the precursor miRNA (pre-mRNA), typically 60-70 nucleotides in length. The pre-mRNA is then exported, using translocation through a nuclear pore complex, into the cytoplasm by forming a transport complex with Exportin 5, where it then becomes cleaved by Dicer, an RNase III endonuclease, to produce the 20-22bp miRNA sequence. The miRNA sequence becomes adjoined to Argonaute (AGO) proteins to form the miRNA induced silencing complex (miRISC). MiRNAs, through imperfect binding, direct the miRISC complex to the specific messenger RNA (mRNA) sequence to regulate protein expression. (Figure 2) [72]

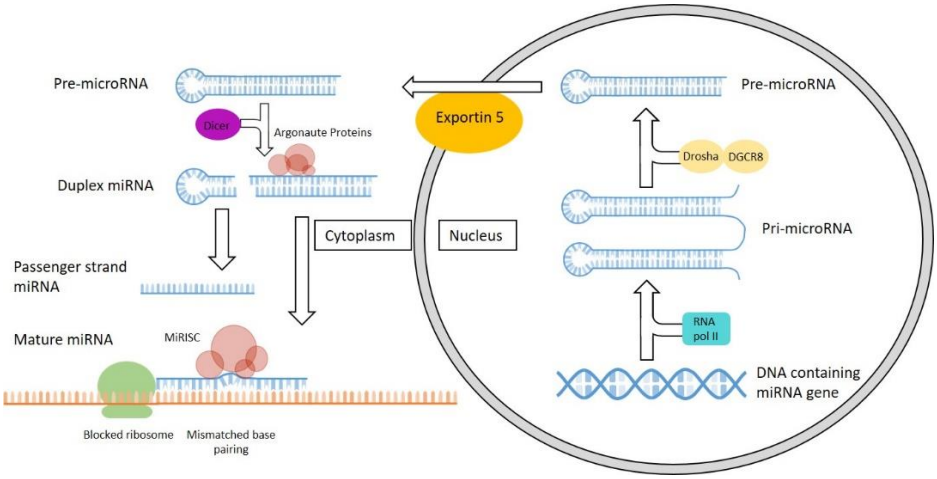

Figure 2 - MicroRNA biogenesis and mechanism of action - MicroRNAs are produced through transcription of the gene before numerous phases of cleavage – inside and outside of the nucleus – using different enzymes before the mature miRNA strand is produced. This strand can bind imperfectly

to mRNA to block the ribosome from completing translation to directly impact protein expression. Adapted from Figure 1 in [73].

Function

The MiRISC complex is integral to the functioning of miRNAs. The AGO proteins within it provide a multidisciplinary platform for cofactors to bind, interpreting these signals to direct miRISC gene expression. They combine with miRNA molecules, which accomplish target recognition using only the seed region (positions 2-8 at the 5' end), targets are found in the 3' untranslated region (UTR), 5' UTR and coding regions of mRNAs, to allow miRNAs to bind multiple targets due to requiring shorter sequence cross-over. As a result, they can detach and reattach to manufacturer control over numerous target molecules at any given time, influencing gene expression more greatly [74, 75].

MiRNA function in disease

An estimated 70% of all miRNAs are expressed in the brain. Dysregulation of these miRNAs, through a stimuli such as trauma, can lead to dysfunction of neuronal signalling within classical neurotransmitter and growth factor signalling in addition to neuronal excitability and intracellular signalling cascades due to their involvement in these processes (Reviewed here [76]).

Significant differences in miRNAs have been seen in mild to severe traumatic brain injury patients across different time points and bio-fluids such as serum, saliva and CSF. Original studies focussed largely on severe TBI (sTBI), with Patz et al. showing significant differences between miR-9 and miR-451 in vesicular packaged RNA of the CSF samples across a total of 28 patients [77]. MiRNAs differences were also shown by Yang et al. in the serum of sTBI patients across 114 patients with differences seen in miR-93, miR-191 and miR-499 and they peaked

between 2 to 7 days post injury [78]. These studies demonstrated miRNA changes in response to traumatic brain injury were present and measurable.

The idea progressed to mTBI with less invasive bio-fluids considered more relevant in this setting due to sampling capability. From this, Di Pietro et al. found 5 differentially expressed miRNAs (miR-27b-3p, miR-142-3p, let-7i-5p, miR-107 and miR-135b-5p) in the saliva of sports related concussion patients, 48 to 72 hours post-injury across 32 samples [79]. These markers showed more capability than protein markers to accurately diagnosis concussion. Other studies have found potential biomarkers (Table 1) but more work is required to get a consistent understanding of miRNA involvement.

Table 1 – Summary of studies to date that have found significant microRNA biomarkers for concussion. There are numerous potential markers but there is a lack of consistency due to differing methodologies and an emerging field.

Bio-fluid	Early (<4 days)	Longer (5+ days)
Serum/Plasma	miR-16 , miR-92a [80] miR-425-5p, miR-502 [71] miR-16, miR-27b, miR-532 [81]	miR-20a, miR-505*, miR-362-3p, miR-30d, miR-92a, miR-486, miR-195, miR-9-3p, miR-151-5p [82]
Saliva	miR-182-5p, miR-221-3p, mir-26b-5p, miR-320c, miR-29c-3p, miR-30e-5p [83] miR-27b-3p, let-7i-5p, miR-142-3p, miR-107, miR-135b-5p [79]	miR-320c-1, miR-133a-5p, miR-769-5p, let-7a-3p, miR-1307-3p [84]

Understanding the function of these differentially regulated miRNAs during concussion in humans is challenging due to the inability to take directly invasive measures, so functional analysis is largely bioinformatics based. This will not be discussed due to the lack of definitive evidence, however was reviewed here [85].

There has been little consistency in both method and outcome of experiments, which is likely due to the small number of studies. There are significant miRNA changes that warrant further investigation in a larger dataset. This combined with the stability of miRNAs as biomarkers and being an invasive measure with minimal collection difficulty, when compared to current methods, shows why this was an ideal target for biomarker research surrounding concussion.

Function of miRNAs in biofluids

Extracellular miRNAs have been shown to be present in numerous bio-fluids including but not limited to: saliva, urine, plasma and cerebrospinal fluid. Extracellular miRNAs, unlike cellular RNA species, are highly stable with the ability to withstand degradation at room temperature for a prolonged period [86].

Originally miRNA presence in extracellular bio-fluids was thought to be a dysregulated, unorganised response however overtime it has been realised that it is an organised response that may act as autocrine, paracrine or endocrine regulators to modulate cellular activities. This finding meant their transport and stability must be integral to their function. There are two active secretion methods known to transport miRNAs into extracellular bio-fluids, which maintain stability [87]. Firstly, via extracellular vesicles (EVs), which selectively package the miRNAs and encapsulate them to prevent degradation during delivery. Extracellular vesicles can vary in size dramatically and under physiological conditions are released from almost all cell types, which may partly explain the diverse signalling. Secondly via RNA-binding protein-dependent pathway with proteins such as Argonaute 2 (Ago2) combining to deliver the miRNA to its destination. Both methods are important in the control of secretion and may play a regulatory role in biological processes.

Both active secretion methods can allow extracellular miRNAs to be taken up at the site of interest. For extracellular vesicles markers on the surface of the EV can be recognised by the cell, which allows internalisation of the EV by phagocytosis, endocytosis or direct fusion that would allow action of the miRNA [88]. Likewise, AGO2 protein bound extracellular miRNAs can be taken up by cells using NRP1 as a high affinity receptor to extracellular miRNA associated with AGO2 [89].

The mechanisms that lead to a rapid increase in miRNAs in peripheral bio-fluids in response to head trauma are unclear. Several pathways have been proposed including: (i) direct release from the site of injury as result of cell death or secretion [90]; (ii) a neuroimmune response leading to increase sympathetic activity [91]; and (iii) stimulation of circulating blood cells with pre-packaged miRNAs [92]. These changes could lead to altered miRNA expression in blood, various organs, and glands, including salivary glands. These miRNAs could enter saliva transcellularly or paracellularly [93]. A slower change in miRNA secretion in bio-fluids could also occur because of transcriptional activity in injury and surrounding cells that induces secretion. Alternatively, there could be a post-transcriptional change that edits processing of miRNAs and therefore release [94].

Currently little is known about miRNA function once they are present in exterior bio-fluids or whether miRNAs are taken up into any cells to elicit their function. There function could stem from within the fluid or could be an offshoot from a response elsewhere e.g. brain functioning.

Other sncRNAs

There are many other families that have potential as biomarkers including small nuclear RNAs, small nucleolar RNAs, Y RNAs, piwi RNAs and transfer RNAs. These have not been discussed

here due to their limited study in concussion. However a review done by myself discusses their biogenesis pathways and involvement in neurodegenerative diseases [95].

Extracellular Vesicles/Exosomes

Biogenesis

Exosomes (30nm-120nm in diameter), microvesicles (50-1000nm) and apoptotic bodies (500-2000nm) are all forms of extracellular vesicles (EVs) that affect disease processes through their involvement in inter cell communication. Exosomes are the smallest form of EVs, unlike other EVs they derive from multi-vesicular bodies (MVBs). Upon release into the extracellular space, they convert from intraluminal vesicles (ILVs), to exosomes. Intraluminal vesicles are generated during the endocytic pathway, through budding of the external phospholipid bilayer. Upon delivery, they either degrade or get transported via MVBs to the cell surface for release [96] (Figure 3).

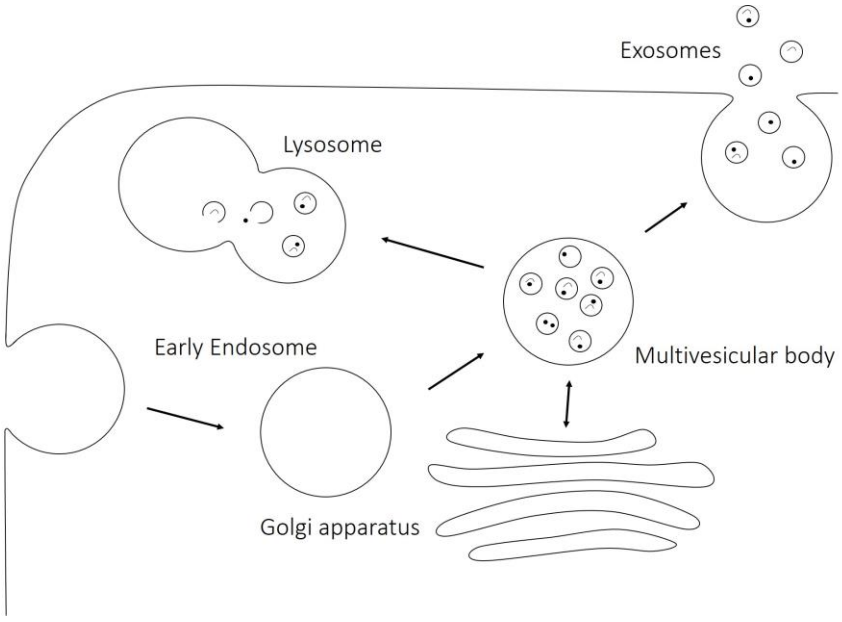

Figure 3 - Exosome biogenesis pathway - This process involves production of intralumincal vesicles (ILVs) packaged into the multivesicular bodies (MVBs), transport of MVBs to plasma membrane and fusion of MVBs to the plasma membrane leading to release of exosomes into the extracellular space.

Exosome secretion involves merging MVBs and the cell membrane, this is facilitated through numerous Rab GTPase proteins and enables the release of their contents into the extracellular space [97]. After release, cell surface molecules – including major histocompatibility complex (MHC) class I and II – target specific cells through antigen presentation [98]. Once targeted, cells are adhered to through a combination of tetraspanins, integrins and annexins. This contact enables the exosome and the cell membrane to merge causing release of their contents (that can be miRNAs, mRNAs or proteins) either through endocytosis, through merging of both membranes, or through cell surface receptors. These processes combine so exosomes can travel and exert their effects upon various cell types, making them attractive therapeutic vehicles due to their stable long-distance signalling.

Table 2 – Features of different vesicle types. There are three main groups exosomes, microvesicles and apoptotic bodies that in future will likely be sub-grouped further.

Characteristic	Exosome	Microvesicles	Apoptotic Bodies
Size (nm)	30-120	50-1000	500-2000
Origin	Multivesicular Body	Plasma membrane	Plasma membrane
Formation Mechanism	Exocytosis of MVB	Budding from PM	Budding from PM
Pathway	ESCRT-dependent, Tetraspanin-dependent	Ca^{2+}-dependent, stimuli and cell-dependent pathway	Apoptosis-related pathways
Markers	CD9, CD81, CD63, Alix and Tsg101	Selectins, integrin and CD40	Caspase 3, histones
Composition	Protein, lipids, RNA and DNA	Protein, lipids, cell organelles, RNA and DNA	Cell organelles, proteins, nuclear fractions, RNA and DNA

Potential as biomarker

Small extracellular vesicles are present in multiple bio-fluids such as saliva, urine, CSF and blood [99]. Their spherical lipid bilayer allows them to harbour internal signalling molecules such as miRNAs and protein receptors such as tetraspanins, which could specify subtypes of vesicles when analysed [100]. Tetraspanin markers (CD9, CD63 and CD81) for example are known to be highly prevalent on sEV's. The combination of diverse prevalence and contents offer a novel biological measure that could highlight concussion signalling.

How are they measured?

Small extracellular vesicles (sEV's) are around 50-200nm in size means they are too small to be measured using conventional flow cytometry making them difficult to study. Isolation methods have contaminants while quantification methods are not necessarily specific due to size limitations [101] (Figure 4).

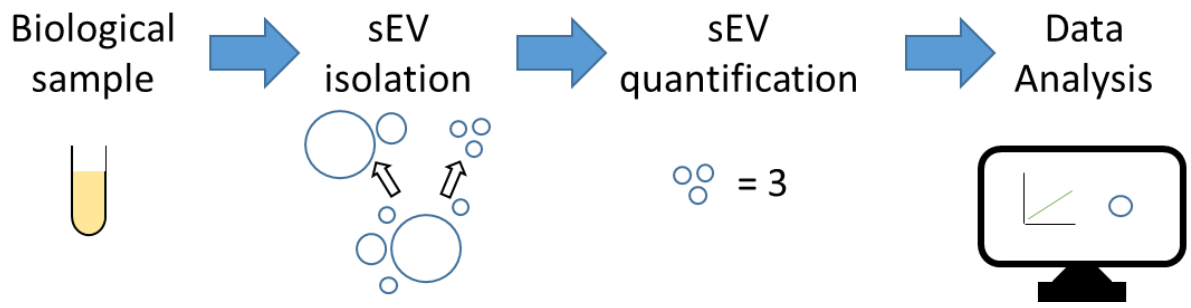

Figure 4 - Typical workflow for small extracellular vesicle analysis. Visual representation of the process with challenges generally found in the isolation and quantification steps.

Key challenges with the field are to find a combination of isolation and quantification that is specific, accurate, reproducible, not time-consuming and affordable. Through a combination of methodologies this is achievable with greater expense and a good level of understanding of the challenges of the field [102]. For the field to progress there needs to be shift away from

improving isolation to phenotypic experiments, so our knowledge of vesicles improves for future technological advances.

Bio-fluid of choice

Different bio-fluids signal for different reasons and in different ways. Therefore, a combination of bio-fluids would be the best method but this is not always achievable due to the limitations of collection methods as well as cost of analysis among other reasons.

Table 3 - Some advantages and disadvantages of different bio-fluids for biomarker analysis

Bio-fluid	Advantages	Disadvantages
Saliva	Easily obtainable, representative of the blood, invasive with potential links to the brain, concentrated with miRNAs/sEV's, stable at room temperature for longer	Not directly from the brain, collection procedure consistency
Blood – Serum/Plasma	Invasive measure, large knowledge base, considered normal	Requires training for removal of blood
Urine	Easily obtainable, representative of the blood	Concentration differences difficult to control, unlikely to represent the brain, dilute
CSF	Highly invasive, directly relevant to the brain	Overly invasive procedure to obtain

Saliva

Advantages of saliva include its fast, easy collection method that does not require specialist personnel as well as being easy to store and ship due to the absence of clotting [103]. Saliva

also offers a complex bio-fluid that crosses over with serum to reflect the physiological state of the body [104]. Finally, saliva contains a large concentration of miRNAs that make it ideal for this type of analysis.

Concussion and the impact long term

Studying the long-term impact of concussion is challenging due to the difficulty tracking disease development and an inability to accurately diagnose specific neurodegenerative diseases routinely before death. There is substantial evidence of moderate to severe traumatic brain injury (TBI) being a vital risk factor in neurodegenerative diseases such as Alzheimer's disease [105]. However, their link with concussion has been less well established with studies showing varied outcomes [106]. In recent years, mTBI injury has been shown to be of importance in chronic traumatic encephalopathy (CTE) and this has heightened the awareness of this field [107]. It appears CTE, a neurodegenerative taupathy, is a distinct pathology in athletes who have repeat trauma, its prevalence is unknown but may demonstrate a link between mTBI and ND's.

One systematic review [106] concluded that former athletes from contact sports suffer later in life from depression, cognitive deficits and there is an association between these deficits with multiple concussions. This longer-term symptom-based profile was in line with there being modest evidence showing neuroimaging based changes across some athletes, but conflicting data was present for the existence of NDs across a population of American football players. This demonstrates that there could be a subpopulation of athletes who are affected longer term.

Another more mechanistic study looked at Alzheimer's disease-vulnerable brain regions using MRI and showed a combination of mTBI exposure and high polygenic risk to Alzheimer's disease was associated with reduced cortical thickness [108]. As well as showing cortical thinning was hastened after mTBI injury. This demonstrates that there may be an involvement of mTBI in ND and may show where symptom-based changes derive. However, it is likely to be a subset of the population.

In summary, current evidence shows an unsubstantiated link between concussion and NDs, which is likely to be due to difficulties in studying methods as well as its role being part of a multifactorial causation. More evidence base is required to fully understand disease development and so in future patients can be better monitored who are in at risk professions or have pre-dispositions.

Alzheimer's disease

Alzheimer's Disease (AD) affects over 800,000 people within the United Kingdom and causes 62% of all dementia – an acquired progressive cognitive impairment that affects daily living – in patients, making it the most prevalent ND [109]. Categorising AD is done by the presence of amyloid beta (Aβ) plaques and hyperphosphorylated tau in the brain. Braak and Braak found that these changes are more widespread in the brain with increasing severity of disease, so are used to guide classification of the disease [110]. Six Braak tau stages (I-VI) and three Braak amyloid stages (A-C) split AD classification.

Tau Braak stages correlate with AD disease progression. Early stages can be asymptomatic, and it can take a long time for progression through the stages. Braak stages I and II are centred on the transentorhinal region with greater tau pathology in Stage II. At stage III, the pathology

is present at the entorhinal region with low levels seen in CA1 of the hippocampus and mild changes in the isocortex [110] (Figure 5). The hippocampus holds long-term memory, which correlates with the early mild cognitive impairment demonstrated by symptoms in Alzheimer's disease. In Stage IV there is increased pathology in the entorhinal region and CA1 hippocampus but there is no atrophy of the brain and as such does not meet the neuropathologic diagnosis of AD. At stage V, tau is found in almost all areas of the hippocampus and the isocortex with more severe demonstrations at stage VI [110] (Figure 5). The isocortex involvement corresponds with late AD and clinical diagnosis.

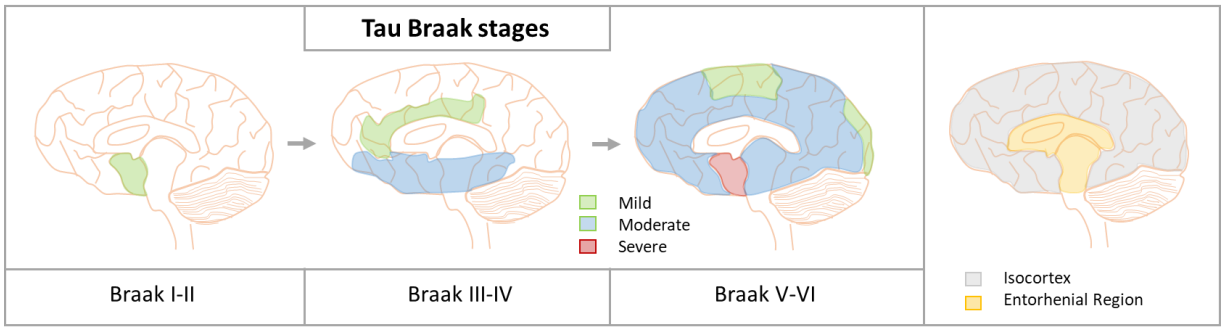

Figure 5 – Representation of Braak tau stages during development of Alzheimer's disease. The severity of the Braak stage correlates with the density of Tau protein present (Adapted from Figure 1 [111]).

MicroRNAs have been shown to be involved in development of disease with regulatory roles in Aβ production and clearance as well as regulation of tau balance. This has led to numerous studies finding differential expression across numerous bio-fluids (including brain tissues, CSF and serum) that have been extensively reviewed [95, 112, 113] (including by myself).

Importance of research

Best concussion management methods use a combination of functional testing, structural imaging and patient symptomology to give a qualified neuropsychologist the information, along with patient medical history, to best advise diagnosis and return to play. This

methodology was designed due to limitations in our ability to directly quantify the biological changes that occur throughout concussion development. An objective measure that is able to quantify biological changes will accompany functional and structural measurements to aid current concussion diagnosis.

The more direct nature of measurement may highlight diagnostic or prognostic differences, to aid initial diagnosis and return to play decisions that may not have been visible with traditional methods. The ultimate goal is for biological measures to be forefront of concussion to reduce the complexity of diagnosis and give prognostic information to guide return to play so patients can be more effectively managed across more settings.

Currently individuals who receive repeat head trauma e.g. professional rugby players do not routinely have check-ups of their long term risks due to limitations in technology as well as inconsistent biological evidence for a link between concussion and long term neurodegenerative disease. A greater pool of data is required to begin unpicking whether factors that signal during concussion can cause long term alterations. This would indicate whether routine monitoring would be essential (biological markers may act as an ideal platform for monitoring) and if so, would allow better guidance on return to play and retirement-based decisions for those at risk.

Overall research aims and hypotheses

Aims

- To investigate whether sncRNAs and/or small extracellular vesicles are differentially regulated in response to concussion
- To investigate the bioinformatics based biological functions of differentially regulated miRNAs during concussion

- To investigate the in vitro interactions of differentially regulated miRNAs during concussion
- To investigate whether differentially regulated miRNAs in concussion are differentially expressed in Alzheimer's disease brains

Chapter 2: Salivary small non coding RNA expression in concussion injury of professional athletes: implications for management techniques

Rationale

Concussion has a well-documented management challenge. A potential solution to this problem is biomarkers that offer a direct biological representation of the injury. Saliva is a non-invasive bio-fluid that is highly abundant in sncRNAs, which are stable markers and throughout preliminary data have demonstrated more consistent results than previously tested protein markers for concussion.

Aims

- To find differentially expressed miRNAs capable of distinguishing a specific post-injury concussion response when compared against uninjured, HIA- and MSK injured patients at time point b and c.
- To find differentially expressed miRNAs at baseline that show an association between patients that go onto to receive a concussion and those who do not.

Experimental guide

1. Next Generation Sequencing (NGS) to find differentially regulated miRNAs of interest
2. Validation of differentially regulated miRNAs in bigger cohort with qPCR methodology
    a. Phase I – 200 microRNAs (193 samples)
    b. Phase II – 94 microRNAs (376 samples)
3. Final data analysis – 56 miRNAs (396 samples)
    a. SncRNA differences in post-injury response (316 samples)
    b. SncRNA differences in pre-season (80 samples)

Statement of Contribution

The experimental design for both the NGS and both validation phases were completed by Marker Health with the experimentation completed by Qiagen. I was part of the team integral to collection and processing of samples that were sent to Qiagen for analysis. At the end of

data collection, I completed the statistical analysis methods for all data represented in this chapter. Statisical analysis guidance was sourced from Dr Animesh Acharjee.

Methods

SCRUM study

Rationale

The Study of Concussion in Rugby Union through MicroRNAs (SCRUM) study utilises the top two tiers of English Rugby. Rugby Union has a high prevalence of concussion being the 3rd most played sport across England and the combative contact nature of the sport means the players are liable to repetitive contact and in the professional game this is repeated game after game, week after week. This repeat contact leads to inevitability of head trauma, which can cause concussion more routinely than average with 21.5 injuries per 1000 player match hours [114]. Also, the Rugby Football Union (RFU) has a stringent Head Injury Assessment (HIA) to diagnose concussion as accurately as possible. So, the high number of players, the accuracy of diagnosis and the high number of injuries make it an ideal platform for observational study and sample collection.

Ethics

The SCRUM study was conducted as part of the ReCoS (The REpetitive COncussion in Sport) research programme [115]. The study was authorised by the University of Birmingham Research Ethics Committee and by the East of England NHS Ethics Committee (Ref. 11-0429AP28). All subjects gave written informed consent in accordance with the Declaration of Helsinki.

The study was pre-registered with the International Standard Randomised Controlled Trials Number in February 2018 (ISRCTN16974791). This study followed the Strengthening the Reporting of Observational Studies in Epidemiology (STROBE) reporting guideline and the full methodology, including the analysis plan, was published in 2018 [116].

Participants

A total of 1028 participants were recruited to the study. During Season 1, 22 out of 24 clubs (92%) from the Premiership and Championship participated. One club withdrew after baseline collection due to lack of resources so 21 clubs collected from HIA events. The demographics of patients collected from the first season of the study can be seen in Table 4.

Table 4 – Demographics of patients from season 1 of SCRUM study

	n	Range	Mean	SD
Age (yrs)	186	18-39	26.52	3.77
Height(cms)	182	162-208	186.65	7.49
Weight(kg)	182	82-134	105.56	12.07

Collection and Classification Process

Post-injury

Throughout the season, samples were collected when club medical staff assessed players for concussion using World Rugby's standardised Head Injury Assessment (HIA) Protocol, which has a clearly defined definition for sports-related concussion to be used for this study.

Patients undergoing the HIA process provided saliva and urine samples at HIA1 (Timepoint A), HIA2 (Timepoint B) and HIA3 (Timepoint C) [117]. Patients that had a concussion confirmed at any stage throughout the HIA process formed the HIA+ group, while if concussion was ruled

out, they made up the HIA- group. This was confirmed by video footage of two experienced sports medicine doctors who were blinded to any results.

In addition to concussion samples, players who completed equivalent number of minutes and sustained a musculoskeletal injury (MSK) as well as non-concussed players (Uninjured) were collected, to rule out effects that have no neurological basis, including exertion related effects. These patients gave samples at time point b and time point c.

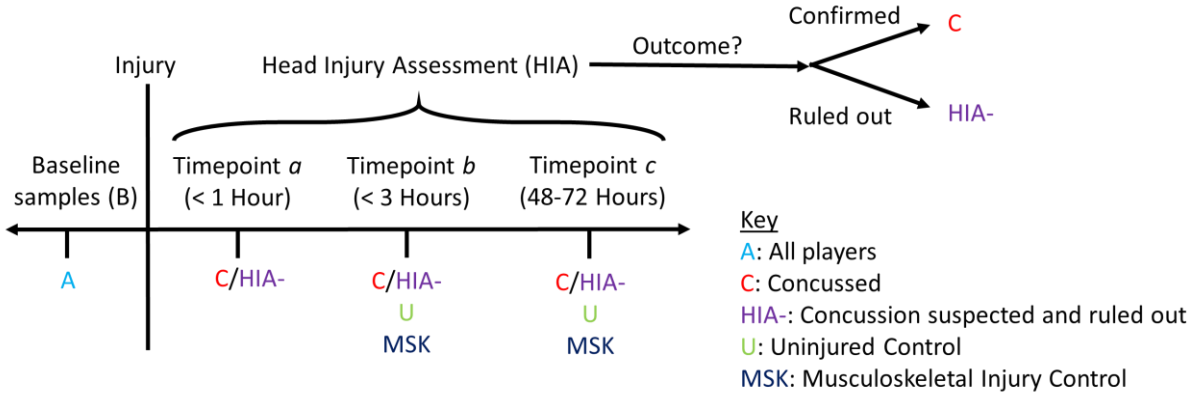

Figure 6 - Timeline for sample collection during the SCRUM study. Baseline samples were collected during pre-season. Samples were collected at three time points following concussion injury at time point A (<1 hour), time point b (<3 hours) and time point c (36-48 hours) in line with the Head Injury Assessment procedure. Control samples were collected from the same matches with three control groups present; (1) Musculoskeletal, (2) Uninjured and (3) Concussion suspected and ruled out.

Pre-season (Baseline)

Pre-season saliva and urine samples (baseline) were taken. After the season these were classified into individuals who had at least one concussion during that season (BC) or those who did not have an injury during the season (BU) (Figure 7). Only premiership samples were used for this due to the effectiveness of diagnosis across the whole season.

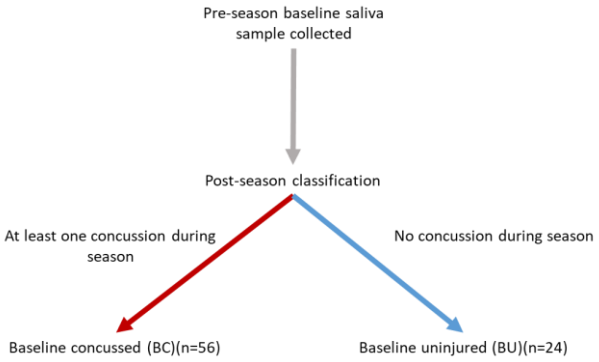

Figure 7– Post-season classification of baseline saliva samples. After the season completion samples were classified based on whether an individual had a concussion during the season. This left two groups for analysis baseline concussed (n=56) and baseline uninjured (n=24).

Data Collection

Medical and demographic data of participants were collected. Factors such as age, height, weight and ethnicity. Also, the number of minutes played was calculated for each incident.

Saliva Collection

Medical staff at each club were trained in the collection methodology. A 2ml sample of saliva was produced by patients using natural stimulation methods, it was then collected in the Oragene®-RNA RE-100 collection kit containing a stabilising solution (DNA Genotek). Samples were stable at room temperature for eight weeks, enabling transport to the University of Birmingham. Saliva samples were then warmed at 50°C for one hour to allow the samples to become homogenous, before freezing at -20°C indefinitely. This was in line with the manufacturer's protocol. The second season saw the Oragene®-RNA RE-100 collection kit discontinued so it was replaced with the CP-190, an equivalent product.

Next Generation Sequencing process

Rationale

Next Generation Sequencing (NGS) was the most advanced and high throughput technology available. Hence the most efficient way to quickly discover potential targets of interest and therefore was used for the discovery phase.

Samples

Fifty samples from the SCRUM study were selected for the discovery phase using 200bp as a cut off so it was a small non-coding RNA Next Generation Sequencing (NGS). These were 15 Baseline samples, 15 concussed samples (HIA+), 10 musculoskeletal controls (MSK) and 10 uninjured controls (U). All samples from the HIA process were collected at time point *b*.

RNA preparation

Samples were transported to QIAGEN, Germany. RNA was prepared by QIAGEN Genomic Services using the DNA Genotek recommendations with the use of the miRNeasy extraction kit (Qiagen).

Library Preparation

After a quality control (QC) check, 5µl of the extracted RNA was used to create NGS sncRNA library using a QIAseq miRNA library kit (Qiagen). Adapters that contained unique molecular identifiers (UMIs) were ligated to RNA to ensure that they could be distinguished. RNA was then converted to cDNA using reverse transcription before amplification using PCR (22 cycles). During this, PCR indices (indexes) were added to 'label' the sequence and the quality of the sample preparation was tested on either the Bioanalyser 2100 (Aligent) or the Tapestation 4200 (Aligent). Based on the quality of the inserts and concentration measurements,

calculated using the qPCR ExiSEQ LNA Quant kit (Qiagen), the libraries were pooled to equimolar concentrations.

Sequencing

The library pool was then sequenced on a NextSeq500 sequencing instrument according to the manufacturer instructions (NEBNext Multiplex Small RNA Library Prep Set for Illumina) to make approximately 163-175 base pair sized libraries. Data was de-multiplexed and FASTQ files for each sample were generated using the bcl2fastq software (Illumina inc.). Data was provisionally checked using the FastQC tool.

Mapping

A reference profile of sequencing data was obtained using the whole human genome sequence GRCh37, downloaded from the Genome Reference Consortium and mirbase_20 as an annotation reference. Bowtie2 (2.2.2) was then used to map the reads. The criteria for mapping reads to spike-ins, abundant sequences and miRBase databases was they must be a perfect match to the reference sequence. While matching to the genome a single mismatch was permitted within the first 32 bases of the read, no indels were allowed however. Unaligned reads were mapped against the human genome and used as input for mirPara and miRBase to predict putative miRNAs [118].

Normalisation

EdgeR statistical software package (Bioconductor, http://www.bioconductor.org/) was used to count aligned reads and perform differential expression analysis using false discovery rate according to the Benjamini-Hochberg method. P-values for the significantly differentially expressed sncRNAs were estimated by an exact test on the negative binomial distribution. For

normalisation, the trimmed mean of M-values method based on log-fold and absolute gene-wise changes in expression levels between samples (TMM normalisation) was used. This accounted for library size, sequencing depth and sampling differences to produce less skewed data with fewer false positive results.

qPCR validation of predicted markers identified by RNA sequencing

Rationale

NGS is a great technique to ably identify novel molecules, including miRNAs, but it is known to produce false positives. The sample cohort that the NGS was based upon was a small sub-population so further qPCR analysis was required to validate the initial findings and establish, which sncRNAs are of interest.

Samples and Analysis

All qPCR validation experiments were conducted at QIAGEN genomic services. There were two phases of analysis, which in total 396 samples were analysed. The decisions made for samples to be used as well as targets was made by a commercial company (Marker Health).

Phase I

All sncRNAs that were found to be differentially regulated between HIA+ and MSK+U groups at time point *b* were selected for analysis in 193 samples. These included 38 microRNAs, 233 put-miRs and 168 other small non-coding RNAs.

Phase II

Phase I limited the number of sncRNAs to 92 through their ability to distinguish concussed subjects. This was made up of 30 microRNAs, 28 other small non-coding RNAs and 34 put-miRs. They underwent further analysis 376 independent samples.

Procedure

Reaction

14µl of prepared RNA was reverse transcribed in 70µl reactions using the miRCURY LNA RT Kit (Qiagen). cDNA was diluted 50x and assayed in 10µl PCR reactions according to the protocol for miRCURY LNA miRNA PCR; each miRNA was assayed once by qPCR on the miRNA Ready-to-Use PCR custom panel using miRCURY LNA SYBR Green master mix (Qiagen). Negative controls excluding template from the reverse transcription reaction were performed and profiled like the samples. The amplification was performed in a LightCyclerp 480 Real-Time PCR System (Roche) in 384 well plates.

Analysis format

Amplification curves were analysed using the Roche LC software, for determination of Cq (by the 2nd derivative method) and for melt curve analysis. The amplification efficiency was calculated using algorithms similar to the LinReg software. All assays were inspected for distinct melting curves (Tm) to ensure the Tm was within known specifications for the assay. Assays had to be more than the negative control based on 0 Cq but less than 37 Cq to be included in the data analysis.

Normalisation

Normalization was performed based on the average of hsa-miR-29c-3p and hsa-let-7b-5p, the two most stable miRNAs identified across all samples by Normfinder software to be housekeeping genes (HK) [119]. Normalized Cq values were calculated by the difference between the two most stable miRNAs (HK) mean Cq and the assay Cq (miRNA of interest). After normalization, 20 was added to the normalized ΔCq values to shift the numbers in a positive range to allow using the qPCR analysis pipelines according Qiagen procedures. While processing the data in the qPCR pipeline a minus is inserted before the normalized ΔCq value. (Equation 1) A higher value indicates that the miRNA is more abundant in that sample.

Equation 1 – Equation used to find Normalised ΔCq. This method uses the ΔCq from the miRNA of interest and from the housekeeping gene (HK) to produce a normalised ΔCq value.

$$Normalised\ \Delta Cq\ value = -((Average\ HK\ Cq - miRNA\ of\ interest\ Cq) + 20)$$

Data analysis

Small non-coding RNA selection

All data was collected and normalised for 92 sncRNAs. At this point sncRNAs were only taken forward if they were present in at least 66% of all patients, which limited the selection of sncRNAs from 92 to 56 the final list for testing. This was made up of 23 microRNAs, 6 put-miRs and 29 other small non-coding RNAs. At this point any further analysis was carried out by me with no commercial interest in mind.

Statistical analysis

Normalised ΔCq values were found not to be normally distributed using the Shapiro-Wilk test. A Mann-Whitney U test procedure was carried out to compare means of paired groups.

Two forms of analysis were carried out:

1. The concussed group was compared against HIA-, Uninjured + MSK at time point *b* and *c* to understand any immediate response to injury. (Concussed vs. Uninjured at time point b and c, Concussed vs. HIA- at time point b and c, Concussed vs. MSK at time point b and c)
2. The baseline concussed during the season (BC) and uninjured during the season (BU) were compared using a Mann-Whitney U test to establish if there were pre-season differences. (BC vs. BU at baseline)

Volcano plots were produced using Graphpad Prism.

R software programming language was used to produce the PCA plots. All missing data points were accounted for using multivariate imputation by chained equations (mice) and the predictive mean matching (PMM) method for correction.

Results

Next Generation Sequencing

This experiment was to find potential sncRNA biomarkers.

Analysis using NGS compared 15 concussion samples against 20 controls (composed of 10 MSK and 10 uninjured samples) at time point *b.* This exploratory analysis found several possible miRNAs that could differentiate between groups. Data of individual sncRNAs that were selected can be found in the supplementary materials.

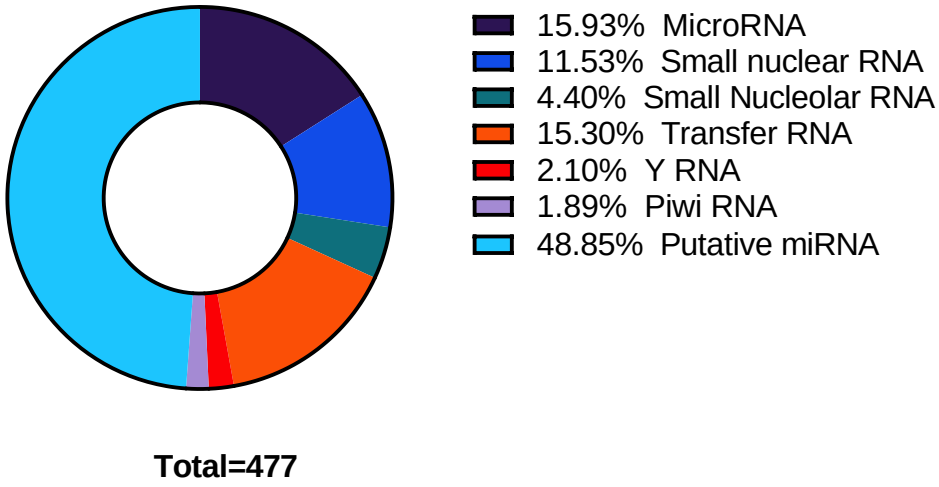

Figure 8 – Pie chart showing the percentage proportions of different small non-coding RNAs (SncRNAs) selected after Next Generation Sequencing (NGS) analysis. After the NGS analysis 477 sncRNAs were selected for further analysis after an assessment of their biomarker potential. The proportion of each category of sncRNA are shown here.

A large number of potential putative microRNAs (put-miRs) found in this study 233 out of 477 (48.85% of all sncRNAs), which were found to have similar structures to miRNAs. This was an unexpected finding and demonstrated that there were novel mechanisms taking place. However, it must be considered that these put-miRs may not be present across all samples, have primers with untested stability for qPCR and could be false positives as a result of the low selection threshold. For these reasons the number of put-miRs was likely to drop off through selection more starkly than other sncRNAs, some were still likely to be some useful, novel miRs.

MicroRNAs of known origin were the next most prevalent (76), perhaps unsurprising given they are the most studied. There are also others present, which could demonstrate that like concussion manifestation the response is individual and there may be many different elements that make up a differential response with Small nuclear RNAs (SnRNA)(64), Small

nucleolar RNAs (SnoRNA)(21), Transfer RNAs (tRNA) (73), Piwi RNAs (piRNA)(9) and YRNAs (10) found at this stage.

The total number of sncRNAs with potential relevance being so high (477) led to a significant challenge of limiting this number to a manageable number for future qPCR steps. As a result, a further reduction during phase I was essential.

qPCR Validation of predicted markers identified by RNA sequencing

This experiment was to validate the markers previously found using NGS.

Phase I

A further 193 samples were tested using qPCR using 477 sncRNAs selected based on their differential expression from NGS. The aim was to limit the number of sncRNAs while beginning to build a dataset to be used for later analysis. There were 94 sncRNAs found to be relevant for phase II of qPCR validation.

After phase I, 385 different sncRNAs were dropped from further analysis, which left 30 microRNA, 13 Small nuclear RNA, 3 Small nucleolar RNA, 9 Transfer RNA, 3 Y RNA, 1 Piwi RNA and 35 Putative miRNAs. The proportions of putative miRNAs decreased by the largest with transfer RNAs also showing a marked decrease comparative to the other sncRNAs.

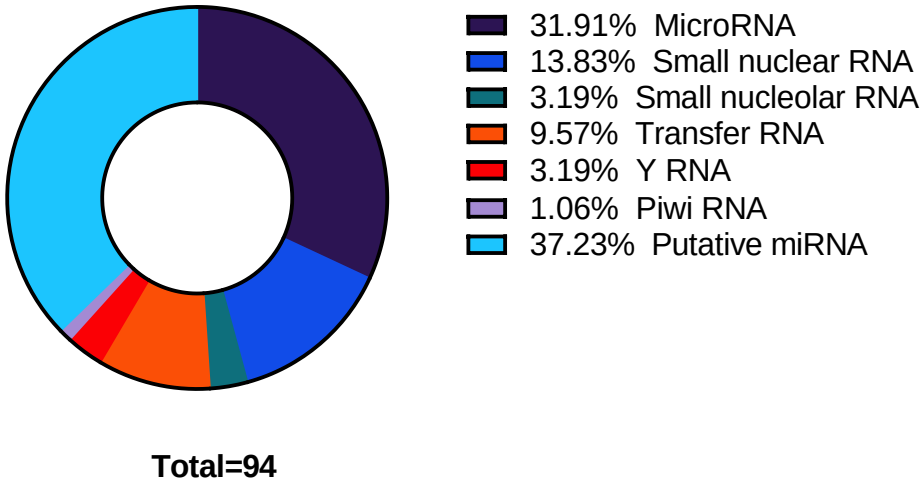

Figure 9- Pie chart showing the proportion of different small non-coding RNA (sncRNA) subtypes that were selected for further qPCR validation after completion of Phase I. After phase I of validation there were 94 sncRNAs selected for further validation after assessment of their biomarker potential. The proportion of each sncRNA category is displayed above.

Table 5- Showing the small non-coding RNAs (sncRNAs) selected for qPCR analysis validation Phase II.

sncRNA name	**sncRNA family**	Total
hsa-let-7a-5p, hsa-let-7b-5p, hsa-let-7f-5p, hsa-let-7i-5p, hsa-mir-103a-3p, hsa-mir-107, hsa-mir-1246, hsa-mir-126-3p, hsa-mir-126-5p, hsa-mir-1271-5p, hsa-mir-135b-5p, hsa-mir-142-3p, hsa-mir-142-5p, hsa-mir-143-3p, hsa-mir-144-3p, hsa-mir-144-5p, hsa-mir-148a-3p, hsa-mir-16-1-3p, hsa-mir-206, hsa-mir-21-5p, hsa-mir-29c-3p, hsa-mir-339-5p, hsa-mir-34b-3p, hsa-mir-425-5p, hsa-mir-449a, hsa-mir-497-5p, hsa-mir-671-3p, hsa-mir-6748-3p, hsa-mir-92a-3p, hsa-mir-934	microRNA	30
put-mir-1003, put-mir-1080, put-mir-1084, put-mir-1098, put-mir-1130, put-mir-1146, put-mir-1204, put-mir-1207, put-mir-1306, put-mir-1352, put-mir-161, put-mir-166, put-mir-188, put-mir-209, put-mir-219, put-mir-293, put-mir-323, put-mir-325, put-mir-410, put-mir-444, put-mir-465, put-mir-468, put-mir-469, put-mir-476, put-mir-594, put-mir-6, put-mir-71, put-mir-742, put-mir-750, put-mir-806, put-mir-856, put-mir-893, put-mir-92, put-mir-958, put-mir-961	Putative microRNA	35
RNU4-6P, RNU6-4, RNU6-45, RNU6-6, RNU6-7, RNU6-73, U2.3, U4.64, U6.1249, U6.168, U6.375, U6.428, U6.601	Small nuclear RNA	13
SNORA57, SNORD3B2, snoU13.120	Small nucleolar RNA	3
tRNA-120-Ala-AGC, tRNA-18-Arg-CCT, tRNA-27-Met-CAT, tRNA-2-Leu-TAA, tRNA-73-Arg-CCG, tRNA-84-Glu-TTC, tRNA-8-Ala-TGC, tRNA-8-Thr-AGT, tRNA-9-Tyr-GTA	tRNA	9
uc022cjg1	piRNA	1
Y_RNA.245, Y_RNA.255, Y_RNA.684	Y RNA	3

Phase II

Phase II measured 94 sncRNAs after selection from Phase I in 376 independent samples. Phase I and Phase II were combined to produce a larger dataset with the 94 sncRNAs. To produce a valid dataset at this point sncRNAs were only accepted if they were present in at least 66% of all patient samples. After this there were 56 sncRNAs remaining across at dataset of 396 samples, which are shown in Table 6 with their relative proportions shown in Figure 10. This dataset was used for all further analysis.

Table 6- Showing the small non-coding RNAs selected for final data analysis after completion of qPCR validation experimentation

sncRNA name	**sncRNA family**	Total
hsa-let-7a-5p, hsa-let-7b-5p, hsa-let-7f-5p, hsa-let-7i-5p, hsa-miR-103a-3p, hsa-miR-107, hsa-miR-1246, hsa-miR-126-3p, hsa-miR-1271-5p, hsa-miR-135b-5p, hsa-miR-142-3p, hsa-miR-142-5p, hsa-miR-143-3p, hsa-miR-144-3p, hsa-miR-148a-3p, hsa-miR-16-1-3p, hsa-miR-21-5p, hsa-miR-29c-3p, hsa-miR-339-5p, hsa-miR-34b-3p, hsa-miR-425-5p, hsa-miR-497-5p, hsa-miR-92a-3p,	microRNA	23
put-miR-1130, put-miR-1204, put-miR-1207, put-miR-325, put-miR-594, put-miR-893	Putative microRNA	6
RNU4-6P, RNU6-4, RNU6-45, RNU6-6, RNU6-7, RNU6-73, U2-3, U4-64, U6-1249, U6-168, U6-375, U6-428, U6-601	Small nuclear RNA	13
SNORA57, SNORD3B2	Small nucleolar RNA	2
tRNA18-ArgCCT, tRNA27-MetCAT, tRNA2-LeuTAA, tRNA73-ArgCCG, tRNA84-GluTTC, tRNA8-AlaTGC, tRNA8-ThrAGT, tRNA9-TyrGTA	tRNA	8
uc022cjg1	piRNA	1
Y_RNA.245, Y_RNA.255, Y_RNA.684	Y RNA	3

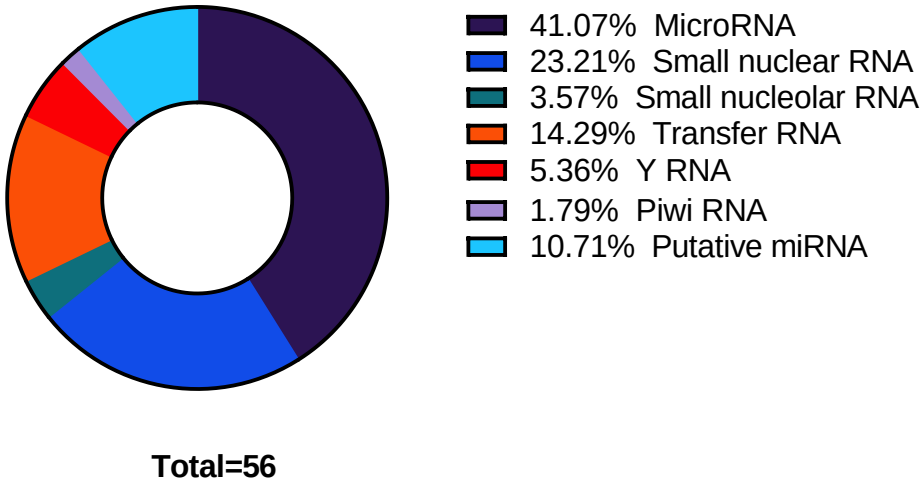

Figure 10 – Pie chart showing the percentage proportion of different small non-coding RNA subtypes selected for final data analysis. After phase II of qPCR validation, the sncRNAs with biomarker potential were reduced from 94 to 56. The proportion of each sncRNA category is displayed above.

Statistical analysis after qPCR validation completion

Samples used for analysis

A total of 396 samples were analysed at baseline, time point b and time point c (resent throughout collection.

Table 7) much larger than any other previous study. These were split to reveal similar numbers across each time point. Smaller numbers of HIA- and MSK samples were analysed due to a smaller number of these samples being present throughout collection.

Table 7 – Total number of samples used for the analysis. The samples were split across three time points; baseline, time point b and time point c. Samples were further classified into four sub-groups of concussed, uninjured, HIA- and MSK to assess differences between samples. Baseline had no HIA- or MSK due to the design of the study.

	Concussed	Uninjured	HIA-	MSK	Total
Baseline	56	24	N/A	N/A	80
Time point b	53	61	25	31	170
Time point c	55	46	20	25	146
Total	164	131	45	56	396

SncRNA differences in post-injury response

The concussed group was compared against uninjured, HIA- and musculoskeletal controls. Differentially regulated microRNAs are not necessarily present across all groups. This could demonstrate that there are different types of regulation between groups. However, any significant value was noted for discussion later.

Two time points were considered for post-injury response analysis:

1. Time point b (Immediately Post match)
    a. This experiment was to establish if there were statistically significant sncRNAs at time point b
2. Time point c (36-48 hours Post match)
    a. This experiment was to establish if there were statistically significant sncRNAs at time point b

Time point b

Time point b gives an indication of the immediate response to injury.

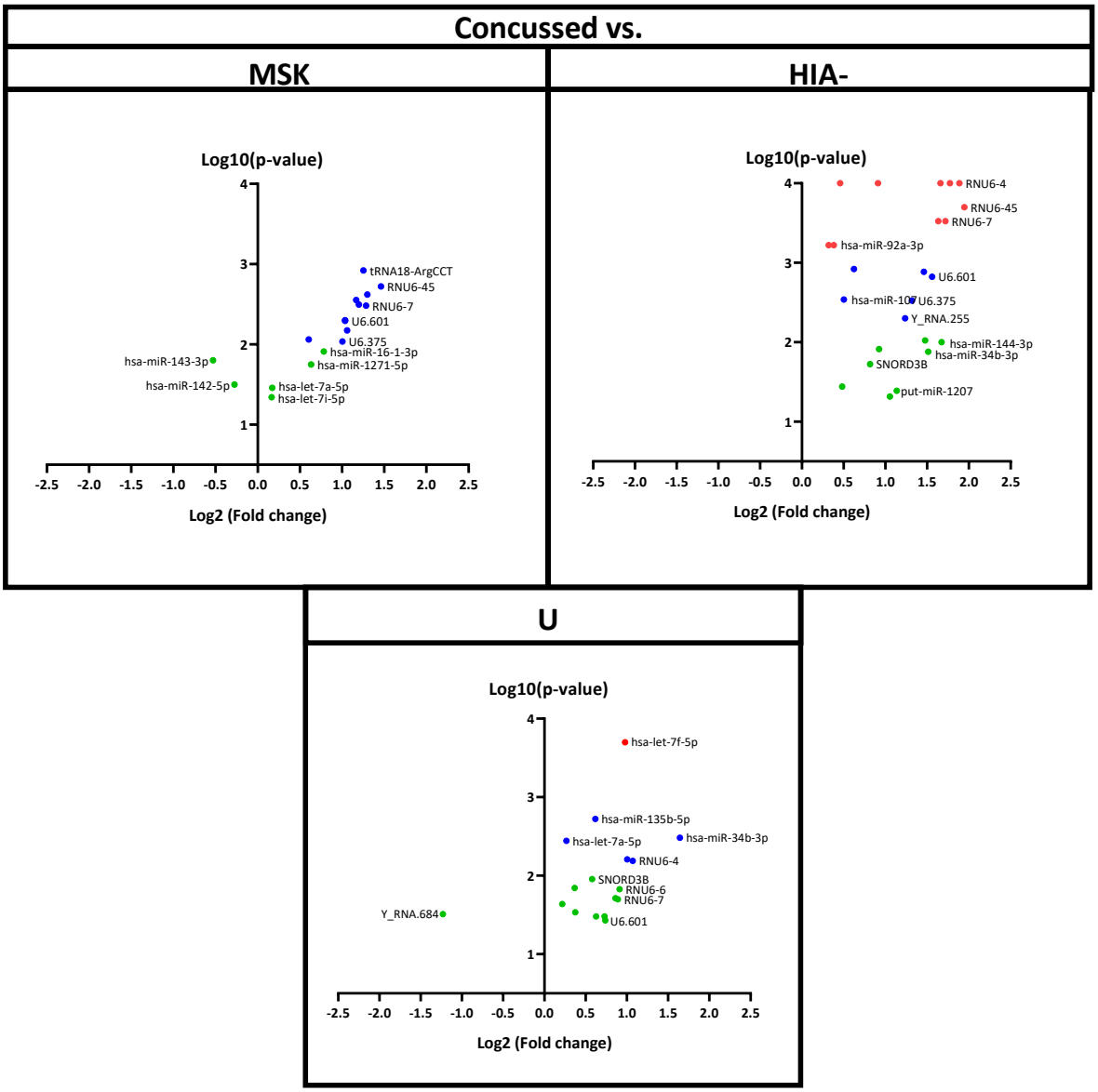

Figure 11 - Volcano plots showing the log10(p-value) against log2(fold change) of significantly different small non-coding RNAs (sncRNAs) in concussed athlete saliva samples at time point *b.* A volcano plot was displayed for differences between the concussed group and each control group (MSK: Musculoskeletal, U: Uninjured and HIA-: Concussion suspected and ruled out). The most significant associations can be seen when compared to the HIA- control group. Significantly different sncRNAs were calculated using Mann-Whitney U tests between the concussed group and each control group separately. A p-value of less than 0.05 was considered significant. Red spot p<0.001, blue spot p<0.01 and green spot p<0.05.

Table 8 – Showing small non-coding RNAs that were significantly different in the concussed group when compared control groups at time point *b.* p-value of less than 0.05 was significant. A Mann-Whitney U test was used to compare means between the concussed group and each control group separately. C: Concussed, MSK: Musculoskeletal, HIA-: Suspected but not concussed and U: Uninjured.

sncRNA	Time point b Average dCT				Standard Deviation				Fold changes			p-values		
	C	MSK	HIA-	U	C	MSK	HIA-	U	MSK/C	HIA- /C	U/C	MSK/C	HIA-/C	U/C
hsa-let-7a-5p	-20.09	-20.26	-20.55	-20.36	0.49	0.70	0.41	0.37	1.13	1.37	1.20	0.0348	0.0001	0.0036
hsa-let-7f-5p	-16.24	-16.40	-17.90	-17.22	1.28	1.59	0.55	1.31	1.12	3.16	1.97		0.0001	0.0002
hsa-let-7i-5p	-18.49	-18.66	-18.81	-18.71	0.41	0.62	0.48	0.48	1.12	1.25	1.16	0.0456	0.0006	0.023
hsa-miR-103a-3p	-19.70	-19.82	-20.33	-20.08	0.87	0.77	0.62	0.77	1.08	1.54	1.30		0.0012	0.0293
hsa-miR-107	-19.30	-19.41	-19.80	-19.61	0.92	0.79	0.51	0.73	1.08	1.42	1.24		0.0029	
hsa-miR-1271-5p	-13.08	-13.71	-13.23	-13.35	1.73	1.16	0.69	1.34	1.55	1.11	1.21	0.0178		
hsa-miR-135b-5p	-14.17	-14.47	-15.08	-14.79	0.89	1.20	0.50	0.96	1.24	1.88	1.53		0.0001	0.0019
hsa-miR-142-5p	-20.82	-20.55	-20.74	-20.77	0.96	0.74	0.70	0.89	0.83	0.94	0.96	0.0317		
hsa-miR-143-3p	-18.17	-17.64	-17.93	-18.00	0.91	1.01	0.80	0.98	0.69	0.85	0.89	0.0158		
hsa-miR-144-3p	-14.19	-13.33	-15.87	-14.15	2.57	2.51	2.67	2.68	0.55	3.19	0.97		0.01	
hsa-miR-148a-3p	-19.31	-19.31	-19.79	-19.68	1.13	1.04	0.75	1.07	1.00	1.40	1.29		0.0362	0.0144
hsa-miR-16-1-3p	-14.16	-14.94	-14.14	-14.27	1.40	1.34	1.46	1.35	1.72	0.99	1.08	0.0123		
hsa-miR-34b-3p	-12.33	-12.84	-13.84	-13.97	1.99	1.55	2.16	2.46	1.42	2.86	3.12		0.0132	0.0033

hsa-miR-92a-3p	-20.38	-20.40	-20.76	-20.51	0.50	0.63	0.56	0.64	1.01	1.30	1.10		0.0006	
put-miR-1207	-13.48	-13.09	-14.62	-14.21	3.33	2.59	1.94	2.60	0.76	2.20	1.66		0.0409	
RNU6-4	-19.90	-21.20	-21.79	-20.97	2.17	2.06	1.62	1.76	2.46	3.70	2.10	0.0024	0.0001	0.0065
RNU6-45	-18.86	-20.32	-20.81	-19.86	2.17	2.18	1.69	2.18	2.75	3.85	2.01	0.0019	0.0002	0.0062
RNU6-6	-19.79	-20.98	-21.56	-20.70	1.99	2.07	1.60	1.77	2.30	3.42	1.88	0.0032	0.0001	0.0149
RNU6-7	-19.82	-21.11	-21.54	-20.72	1.99	1.74	1.66	1.75	2.43	3.29	1.85	0.0033	0.0003	0.02
RNU6-73	-19.76	-20.93	-21.39	-20.62	1.85	1.97	1.71	1.78	2.25	3.10	1.82	0.0028	0.0003	0.0194
SNORA57	-20.82	-21.33	-21.15	-20.96	1.14	1.11	1.16	1.08	1.43	1.26	1.10	0.0501		
SNORD3B-2	-19.25	-19.70	-20.07	-19.83	1.60	1.47	1.05	1.25	1.36	1.76	1.49		0.0189	0.0111
tRNA18-ArgCCT	-22.31	-23.57	-23.77	-22.80	1.79	1.43	1.63	1.66	2.38	2.75	1.40	0.0012	0.0013	
tRNA27-MetCAT	-18.36	-18.74	-19.28	-18.60	1.86	1.08	1.28	1.46	1.30	1.90	1.18		0.0122	
tRNA73-ArgCCG	-16.65	-17.44	-18.12	-17.08	2.29	1.40	1.68	1.81	1.73	2.78	1.35		0.0095	
U2-3	-26.58	-26.66	-27.64	-27.16	2.11	2.02	0.94	1.67	1.05	2.08	1.49		0.0484	
U6-168	-16.74	-17.78	-17.46	-17.16	1.66	1.60	1.46	1.50	2.05	1.64	1.33	0.005		
U6-375	-16.38	-17.39	-17.70	-17.01	1.75	1.48	1.55	1.45	2.01	2.49	1.54	0.0092	0.003	0.0332
U6-601	-18.17	-19.21	-19.73	-18.91	1.94	2.04	1.72	1.73	2.05	2.95	1.67	0.0051	0.0015	0.0372
uc022cjg1	-22.04	-22.65	-22.18	-22.28	1.04	0.97	0.80	0.97	1.52	1.10	1.18	0.0087		
YRNA-255	-23.71	-24.77	-24.94	-24.44	1.75	1.64	1.37	1.63	2.09	2.35	1.66	0.0067	0.005	0.0332
YRNA-684	-12.30	-11.65	-11.64	-11.07	2.65	2.78	2.09	2.68	0.64	0.63	0.43			0.031

At time point *b,* when compared to MSK control group there were 17 differentially regulated sncRNAs (6 miRNAs, 8 snRNAs, 1 tRNA, 1 piRNA and 1 YRNA). Out of these sncRNAs 15 (88%) were upregulated with the strongest response being RNU6-45 (fold change: 2.75) (Table 8) (Figure 11). There are 6 sncRNAs that show no cross-over with other groups, which would indicate they are likely to be responding the MSK injuries. The PCA plot showed little separation based on the significant markers showing a more specific panel of markers would be required to strategically separate these data points (Figure 12).

The comparison between the HIA- and concussed group is the most interesting diagnostically. There were 24 significantly different sncRNAs between these groups (10 miRNAs, 8 snRNAs, 3 tRNAs, 1 YRNA, 1 snoRNA and 1 put-miR). All sncRNAs were upregulated compared to HIA- with RNU6-45 showing the largest increase (fold change: 3.85) (Table 8). The discrimination – shown by PCA – between these groups was clearer than the other control groups (Figure 12), which is likely due to their diverging signalling that is masked in the other control groups by other factors. As a result, it seems these groups seem to be largely separable.

When compared to the uninjured group there were 17 differentially regulated sncRNAs (7 miRNAs, 7 snRNAs, 1 snoRNA and 2 YRNAs). YRNA-684 was the only value to significantly decrease (fold change: 0.43) in the concussed group whereas all others increased with hsa-let-7f-5p showing the largest, most consistent change (fold change: 1.97) (Table 8). There was little separation when using PCA analysis (Figure 12), which demonstrates that the diverging response found between concussed and HIA- is likely to have the uninjured response between them.

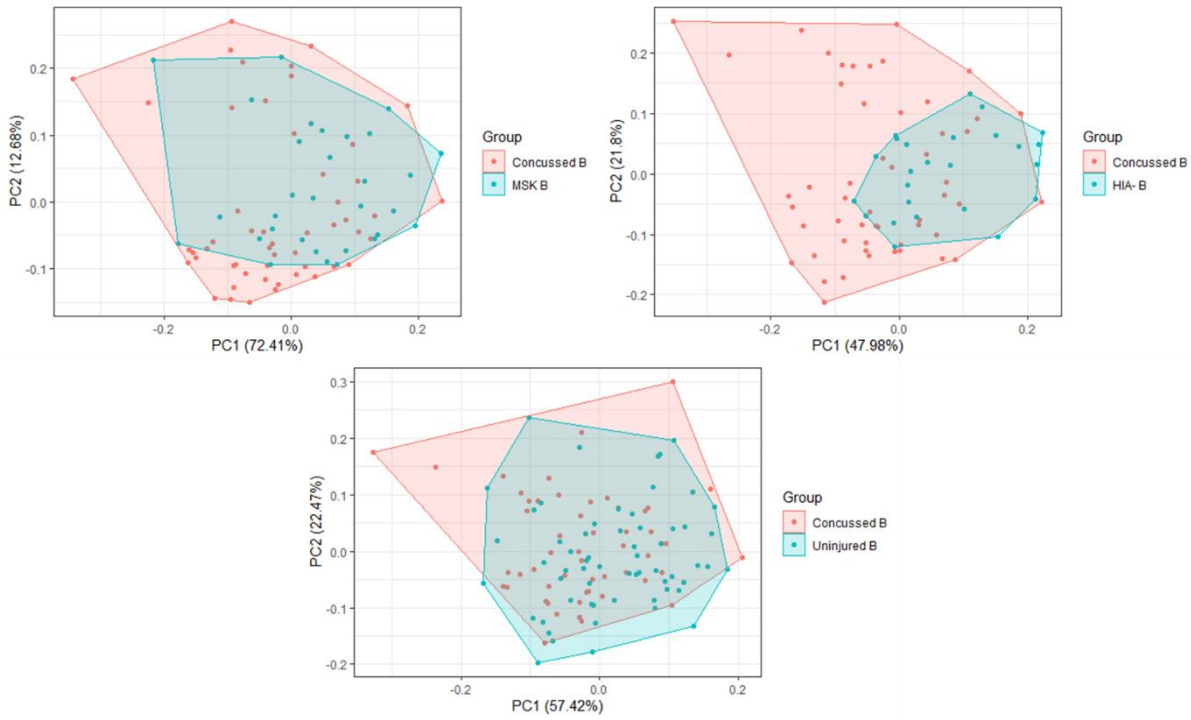

Figure 12 – Principle Component Analysis (PCA) plots showing separation of concussed group when compared to three control groups at time point b. Significantly different small non-coding RNAs (sncRNAs) were calculated using Mann-Whitney U tests between the concussed group and each control group separately, $p<0.05$ was considered significant. These were then used to produce three separate PCA plots against the relevant controls with the largest separation seen when compared to HIA- control group. (MSK: Musculoskeletal, U: Uninjured and HIA-: Concussion suspected and ruled out)

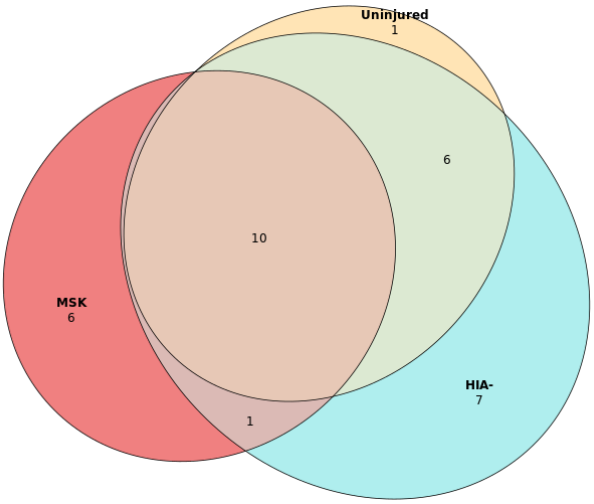

Figure 13- Venn diagram showing the cross-over of differentially regulated small non-coding RNAs (sncRNAs) by their control group at time point b. Significantly different sncRNAs calculated when means were compared using Mann-Whitney U testing are shown. There was a large cross-over between all groups.

When comparing across all groups there are 10 different sncRNAs (2 miRNAs, 7 snRNAs and 1 YRNA) that are significant (Figure 13). These can be considered specific to the concussion related response at time point *b.* All 10 increase in the concussion group when compared to all other groups. Perhaps the most interesting observation was all 7 snRNAs are related to the U6 snRNA (RNU6-4, RNU6-45, RNU6-6, RNU6-7, RNU6-73, U6-375 and U6-601), which demonstrates a likely upregulation of U6 snRNA in response to concussion immediately post-match. This time point shows the strongest regulation demonstrating an early time point may be essential in correct diagnosis based on early indicative biological signalling.

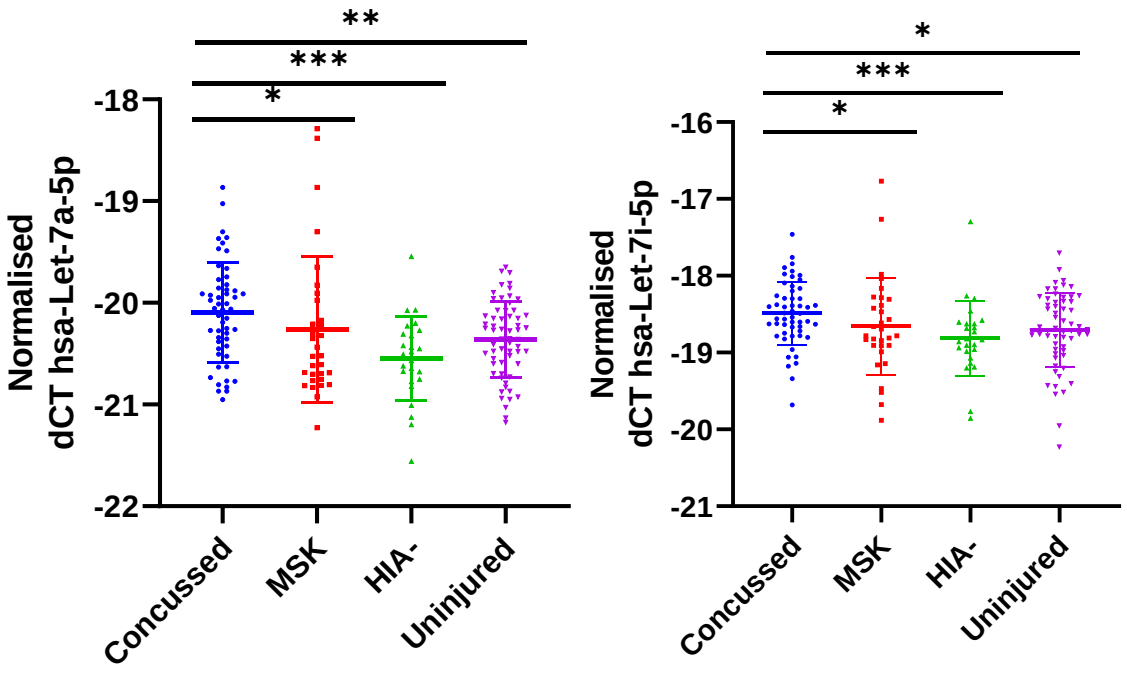

Figure 14 – Showing an interleaved scatter plot of significantly associated microRNAs when compared to all control groups at time point *b*. The graph shows mean±SD. Statistical analysis shown was a Mann-Whitney U test when means were compared each control group individually. *p<0.05, **p<0.01 and ***p<0.001. (MSK: Musculoskeletal, U: Uninjured and HIA-: Concussion suspected and ruled out)

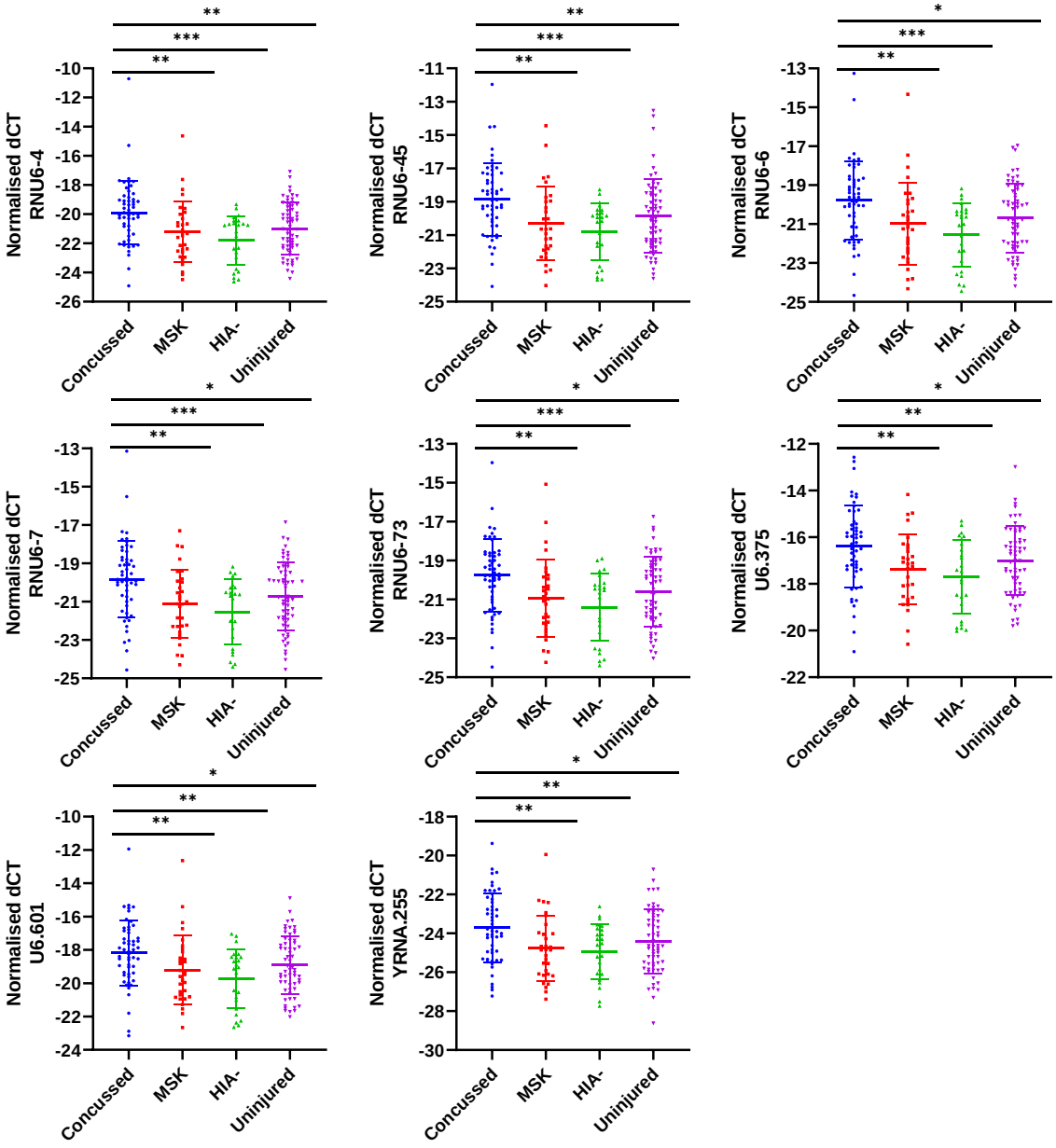

Figure 15 – Showing an interleaved scatter plot of all other small non-coding RNAs that were statistically different when compared against all control groups at time point b. The graph shows mean±SD. Statistical analysis shown was a Mann-Whitney U test when means were compared each control group individually. *p<0.05, **p<0.01 and ***p<0.001. (MSK: Musculoskeletal, U: Uninjured and HIA-: Concussion suspected and ruled out)

Time point c

Time point c demonstrates a slightly more delayed response to injury and could highlight different targets, while being potentially more achievable for collection in the community.

Table 9 - All significantly different small non-coding RNAs found between concussed and either MSK, HIA- or uninjured at time point *c.* p-value of 0.05 was considered significant. A Mann-Whitney U test was used to compare means between the concussed group and each control group separately. C: Concussed, MSK: Musculoskeletal, HIA-: Suspected but not concussed and U: Uninjured.

sncRNA	Time point c Average dCT				Standard Deviation				Fold changes			p-values		
	C	MSK	HIA-	U	C	MSK	HIA-	U	MSK/C	HIA- /C	U/C	MSK/C	HIA- /C	U/C
hsa-let-7a-5p	-20.33	-20.28	-20.62	-20.49	8.28	7.14	7.46	6.91	0.97	1.22	1.11		0.0113	
hsa-let-7f-5p	-16.33	-15.49	-18.16	-16.95	8.57	3.11	7.63	9.22	0.56	3.55	1.54	0.006	0.0001	0.0143
hsa-let-7i-5p	-18.54	-18.68	-18.74	-18.66	9.43	8.55	7.91	9.94	1.10	1.15	1.09		0.0016	
hsa-miR-107	-19.31	-19.27	-19.85	-19.45	9.96	8.08	8.33	7.22	0.97	1.45	1.10		0.0021	
hsa-miR-126-3p	-13.00	-13.12	-13.51	-13.37	6.61	7.16	7.32	5.22	1.08	1.42	1.29		0.0217	
hsa-miR-135b-5p	-14.95	-14.08	-15.24	-14.88	7.47	7.68	8.08	5.64	0.54	1.22	0.95	0.0021		
hsa-miR-144-3p	-12.54	-14.57	-14.01	-13.95	6.73	8.49	8.20	6.20	4.10	2.78	2.66	0.001	0.0138	0.0014
hsa-miR-148a-3p	-19.09	-19.16	-19.62	-19.28	9.23	10.06	10.08	7.27	1.05	1.45	1.14		0.0367	0.0158
hsa-miR-16-1-3p	-13.80	-15.06	-13.86	-14.11	6.99	8.18	7.55	5.56	2.40	1.05	1.25	0.0006		
hsa-miR-21-5p	-21.88	-21.40	-22.55	-22.05	10.53	11.20	11.70	8.12	0.72	1.59	1.12	0.031	0.0055	
hsa-miR-34b-3p	-12.34	-12.25	-13.99	-13.04	6.95	7.11	8.03	5.25	0.94	3.12	1.62		0.0371	
hsa-miR-425-5p	-18.47	-19.20	-18.58	-18.61	8.91	10.13	9.65	6.84	1.66	1.08	1.11	0.0009		
hsa-miR-92a-3p	-20.47	-20.49	-20.72	-20.61	9.94	10.62	10.57	7.36	1.02	1.19	1.11		0.0468	
RNU4-6P	-16.98	-16.23	-17.61	-16.69	1.48	1.07	1.45	0.99	0.59	1.55	0.82		0.0441	
RNU6-45	-19.22	-20.14	-20.51	-19.65	2.03	2.40	1.41	2.36	1.89	2.45	1.34	0.0318	0.0113	
RNU6-6	-20.09	-20.98	-21.24	-20.45	1.80	2.07	1.39	2.02	1.86	2.23	1.29	0.0446	0.0121	
RNU6-7	-20.13	-20.96	-21.17	-20.45	1.77	2.07	1.43	1.99	1.78	2.06	1.25		0.0189	
RNU6-73	-20.02	-20.88	-21.08	-20.39	1.78	2.06	1.45	1.95	1.81	2.08	1.29		0.0231	
SNORA57	-20.64	-21.42	-20.91	-20.74	1.19	1.03	0.76	1.07	1.72	1.21	1.07	0.008		
tRNA18-ArgCCT	-22.59	-23.74	-23.08	-22.60	2.14	1.57	1.25	1.57	2.22	1.41	1.01	0.0345		
tRNA27-MetCAT	-18.53	-19.42	-18.98	-18.64	1.74	1.50	1.30	1.10	1.85	1.36	1.08	0.0393		
U6-375	-16.53	-17.05	-17.41	-16.92	1.81	2.14	1.32	1.65	1.43	1.84	1.31		0.0441	
U6-428	-13.10	-14.26	-13.05	-13.27	1.51	1.55	1.45	1.38	2.24	0.97	1.13	0.0075		
U6-601	-18.42	-19.22	-19.46	-18.70	1.87	1.72	1.61	1.89	1.74	2.05	1.21		0.0372	
YRNA-255	-23.91	-25.06	-24.45	-23.99	1.75	1.44	1.26	1.95	2.22	1.45	1.05	0.0028		
U6-168	-16.78	-17.60	-17.37	-17.04	1.56	1.88	1.40	1.62	1.77	1.51	1.20	0.0493		

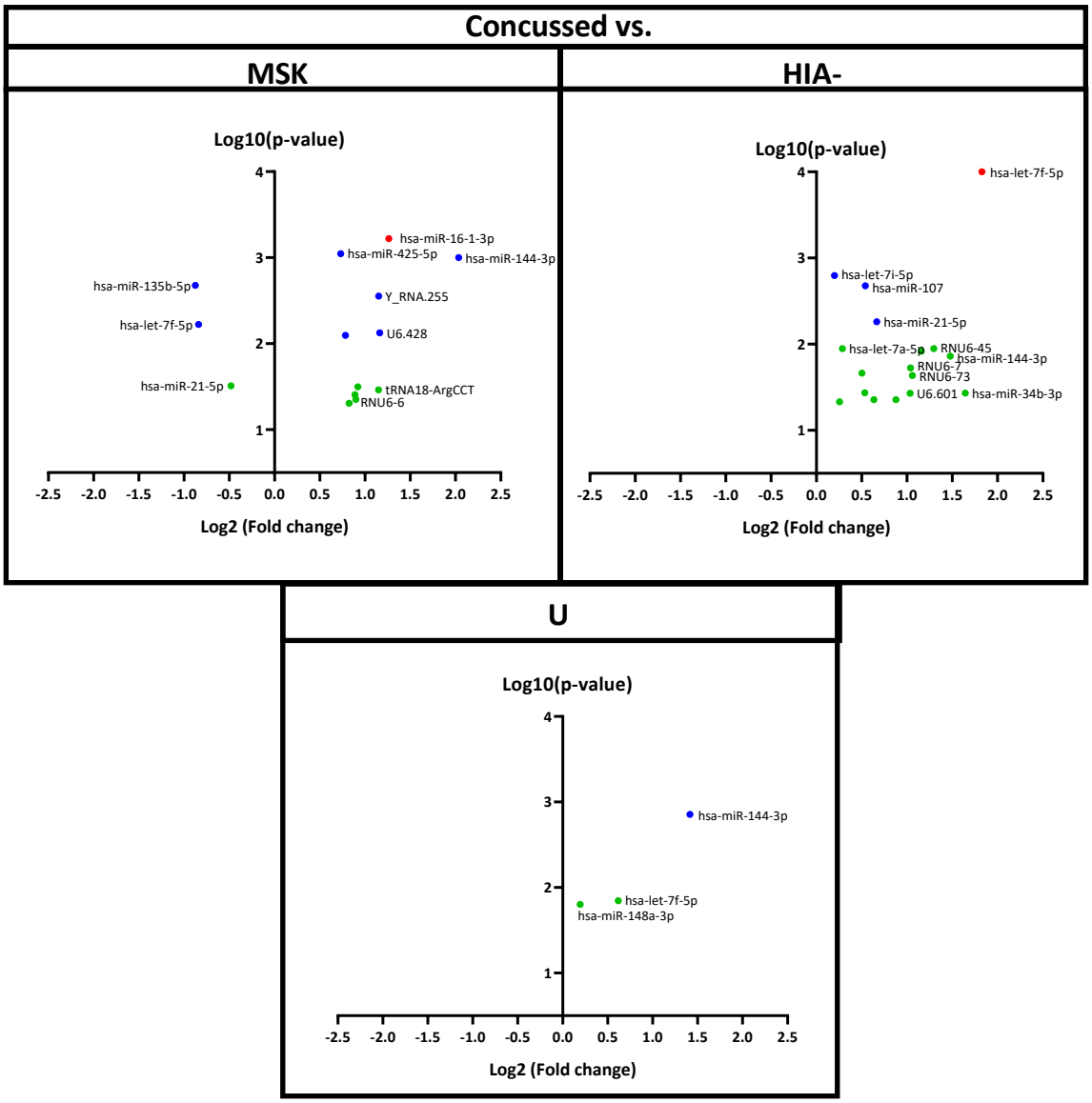

Figure 16 – Volcano plots showing the log10(p-value) against log2(fold change) of significantly different small non-coding RNAs (sncRNAs) in concussed athlete saliva samples at time point *c.* A volcano plot was displayed for each control group (MSK: Musculoskeletal, U: Uninjured and HIA-: Concussion suspected and ruled out). The most significant associations can be seen when compared to the HIA- and MSK control groups. Significantly different sncRNAs were calculated using paired Mann-Whitney U tests between the concussed group and each control group individually. A p-value of less than 0.05 was considered significant. Red spot p<0.001, blue spot p<0.01 and green spot p<0.05.

When compared to MSK at time point c there were 14 significantly different sncRNAs (6 microRNAs, 4 snRNAs, 1 YRNA, 1 snoRNA and 2 tRNAs). Three decreased expression within the concussed group with the largest being hsa-miR-135b-5p (fold change: 0.54) (Figure 16). All others increased with the largest increase being hsa-miR-144-3p (fold change: 4.10). There is quite varied signalling demonstrating a more controlled response. The PCA plot shows a little amount of separation (Figure 17).

Comparing to the HIA- control group there were 17 differentially expressed sncRNAs (10 miRNAs and 7 snRNAs). All increased in expression in the concussion group with hsa-Let-7f-5p showing the largest increase (fold change: 3.55) (Figure 16). A PCA plot demonstrates a separation between the groups that was also seen at time point *b* (Figure 17), which shows there is differential signalling between these two groups.

Comparing against the uninjured control group there were 3 differentially regulated sncRNAs, all of which were miRNAs (Table 9). All three increased in expression with hsa-miR-144-3p showing the largest increase (fold change: 2.66) (Figure 16). PCA showed little separation, which is unsurprising due to the number of sncRNAs. Three sncRNAs was much smaller number than other groups and time points, which is likely due to more varied signalling that is not concussion specific.

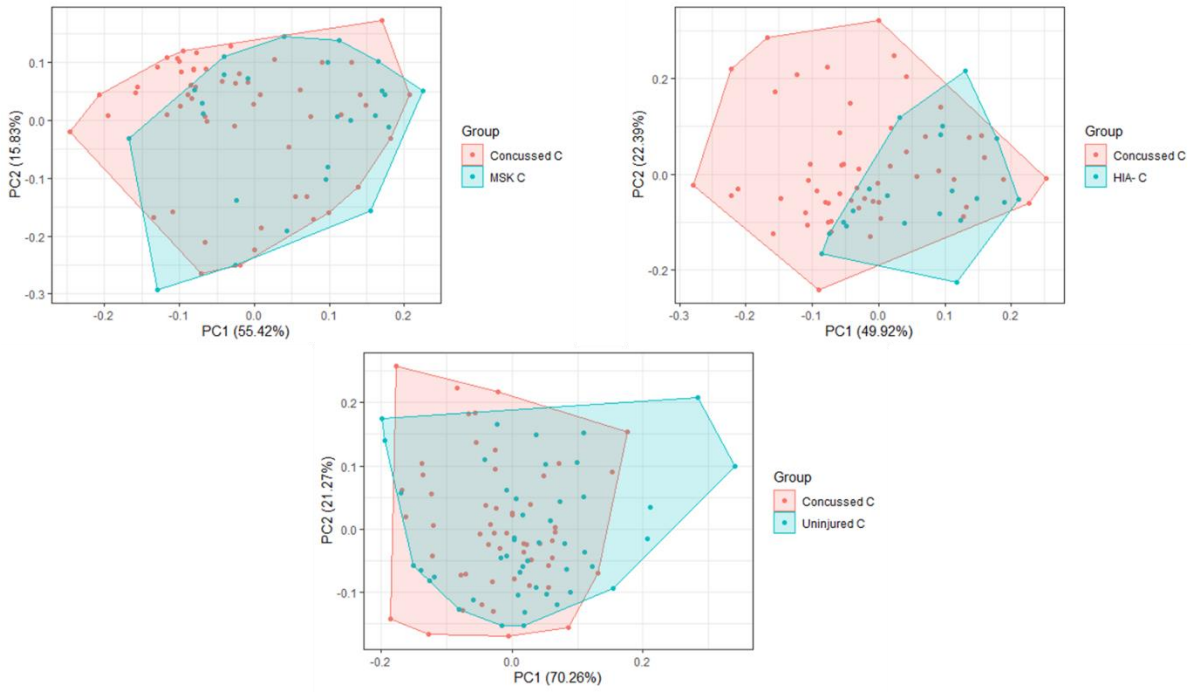

Figure 17 – Principle Component Analysis (PCA) plots showing the separation between groups using the significant small non-coding RNAs of the compared control group at time point *c.* Significantly different sncRNAs were calculated using Mann-Whitney U between the concussed group and each control group individually, $p<0.05$ was considered significant. These were then used to produce three separate PCA plots against the relevant controls with the largest separation seen when compared to HIA- control group. (MSK: Musculoskeletal, U: Uninjured and HIA-: Concussion suspected and ruled out)

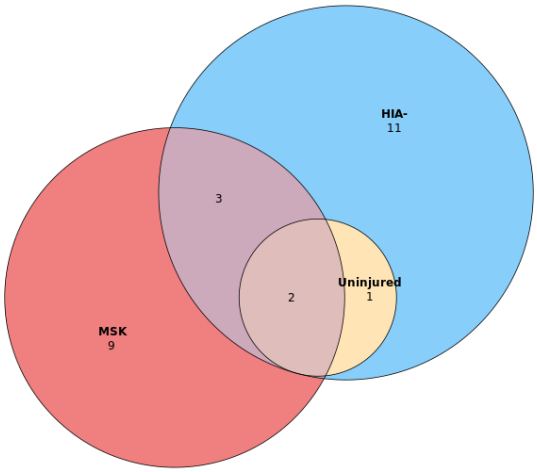

Figure 18– Venn diagram showing the cross-over of differentially regulated small non-coding RNAs (sncRNAs) by their control group at time point c. Significantly different sncRNAs calculated when means were compared using Mann-Whitney U testing are shown. A p value of <0.05 was considered significant. There was a small amount of cross-over at this time point.

There were 2 miRNAs that were significant across all groups at this time point. These were hsa-miR-144-3p (MSK: 0.001, HIA-: 0.0138 and uninjured: 0.0014) and hsa-let-7f-5p (MSK: 0.006, HIA-: 0.0001 and uninjured: 0.0143). They show different responses when compared to the groups with the concussed hsa-miR-144-3p group increasing compared to all others, which looks as if it true concussion signalling (Figure 19). However, in hsa-let-7f-5p the MSK group is larger than the concussed group, which demonstrates that this signal may be a trauma response at this time point (Figure 19).

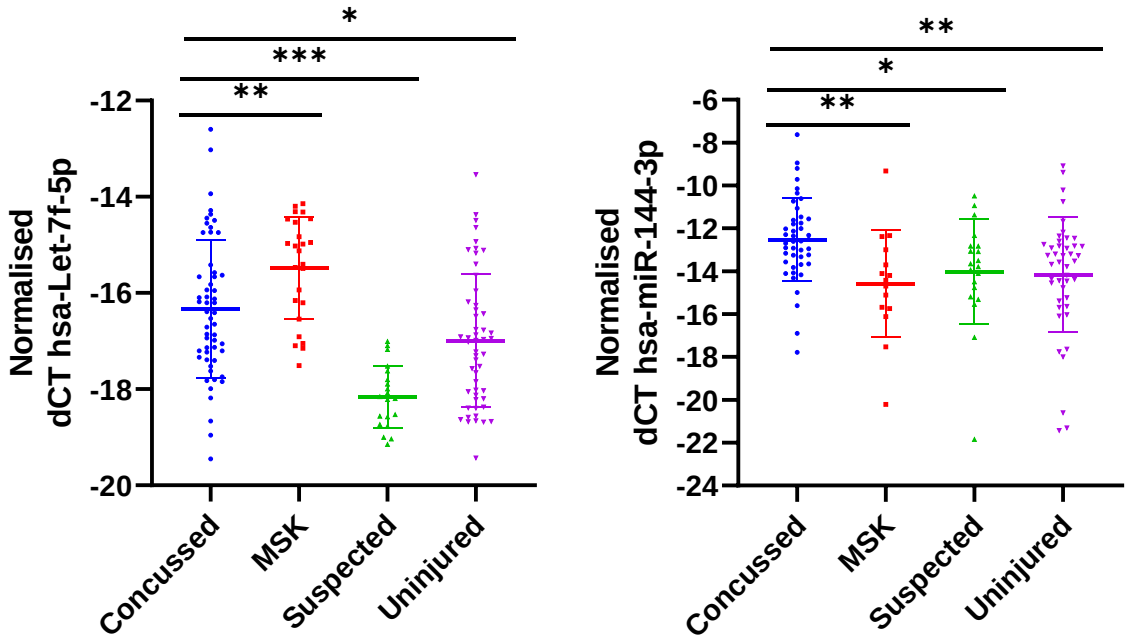

Figure 19 – Showing an interleaved scatter plot of differentially expressed microRNAs when compared to all control groups at time point c. The graph shows mean±SD. Statistical analysis shown was a Mann-Whitney U test when means were compared each control group individually. *p<0.05, **p<0.01 and ***p<0.001. (MSK: Musculoskeletal, U: Uninjured and HIA-: Concussion suspected and ruled out)

SncRNA differences during pre-season

This experiment was to establish if sncRNA levels were differentially expressed before the onset of concussion.

The differences found in the post-injury response led to the question as to whether these sncRNAs could have more far-reaching roles, and therefore potential as biomarkers. Baseline samples were grouped based on their classification from events later in the season. To establish if pre-analytical miRNA changes could be indicative of prior injury or be predictive markers of concussion.

Baseline

Of the 56 sncRNAs tested for there were nine significantly different sncRNAs between groups. This was composed of seven miRNAs (one that was putative) and two small nuclear RNAs that were U2 and U4 spliceosome components respectively. Eight of the differentially expressed sncRNAs were upregulated in the baseline concussed group when compared to the baseline uninjured group (Table 10) the most significant upregulated sncRNA being RNU4-6P (p=0.005). The most significant interaction was found to be – a novel miRNA – put-miR-325 (p=0.0027) that was downregulated in the baseline concussed group (Figure 20).

Table 10 – Showing significant small non-coding RNAs between baseline concussed and baseline uninjured. Mann-Whitney U tests were carried out to establish differences between groups. p<0.05 was considered significant.

MicroRNA	Baseline Concussed		Baseline Uninjured		ddCT	Fold Change	P-value
	Mean	Standard deviation	Mean	Standard deviation			vs. Uninjured
put-miR-325	-18.90	2.47	-17.34	1.48	1.56	0.34	0.0027
RNU4-6P	-16.47	1.25	-17.15	0.67	-0.68	1.60	0.0050
hsa-let-7f-5p	-17.23	1.43	-18.11	1.02	-0.88	1.85	0.0069
hsa-miR-103a-3p	-19.98	0.7	-20.31	0.45	-0.33	1.26	0.0099
hsa-miR-107	-19.54	0.66	-19.88	0.42	-0.34	1.26	0.0127
hsa-miR-148a-3p	-19.49	0.71	-19.89	0.36	-0.40	1.32	0.0182
hsa-miR-143-3p	-17.33	1.28	-18.05	0.89	-0.72	1.65	0.0199
U2.3	-26.71	1.47	-27.51	0.86	-0.80	1.74	0.0311
hsa-miR-92a-3p	-20.38	0.43	-20.53	0.33	-0.16	1.11	0.0328

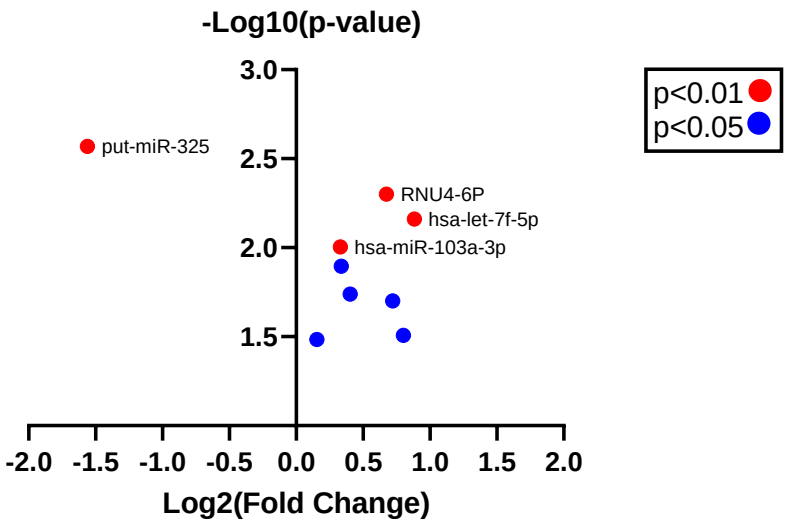

Figure 20 - Volcano plot showing the significantly different small non-coding RNAs in saliva of athletes between baseline concussed and baseline uninjured. The most significant downregulation in the baseline concussed group was put-miR-325. All other sncRNAs were upregulated with the most significant upregulation being RNU4-6P. Mann-Whitney U tests were used to calculate statistical differences between the concussed group and each control group individually. P<0.05 was considered significant.

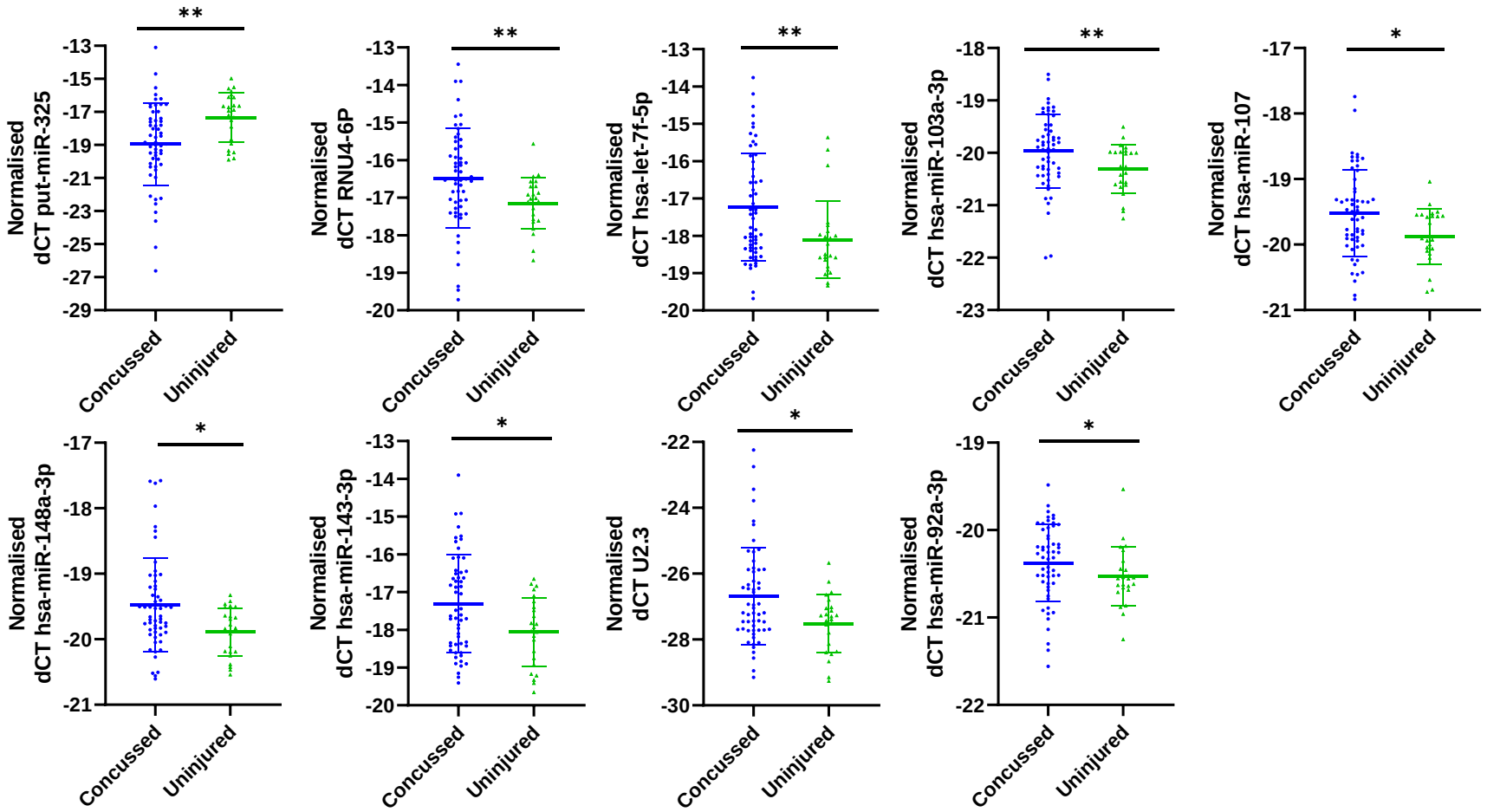

Figure 21 – Showing an interleaved scatter plot of significant small non-coding RNAs between baseline concussed and baseline uninjured. Mann-Whitney U tests were used to establish differences between the concussed group and each control group individually. **p<0.01, *p<0.05. Graphs show Mean±SD.

Separation of differentially expressed sncRNAs by retrospective concussion classification

PCA was used to establish if individuals could be classified at pre-season into whether they went on to get a concussion or not based on the differential regulation in the significant sncRNAs (Table 10). In Figure 22 there was a much less variation in the athletes that went uninjured. There were 25/56 (44.7%) that directly overlapped between groups. This leaves 31/56 (55.3%) that may be able to be separated at during pre-season.

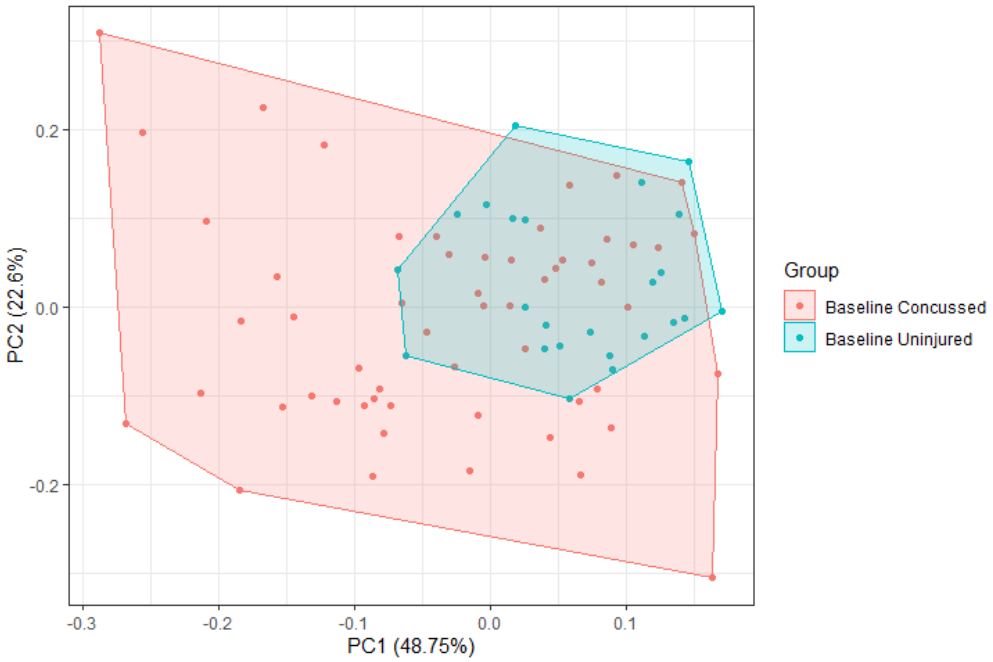

Figure 22 - Principal component analysis (PCA) using nine significantly differentially regulated small non-coding RNAs to demonstrate separation between groups. Significantly different sncRNAs were calculated using Mann-Whitney U test in paired groups between concussed and controls, $p<0.05$ was considered significant.

Discussion

SncRNAs were found to be differentially regulated across all three time points (Baseline, time point b and c). The most significant changes were witnessed at time point b and these changes may indicate underlying mechanistic information that could be useful in diagnostics and ongoing management in the case of baseline measurements.

Differential expression of sncRNAs after concussion-based injury

In this study, salivary sncRNA markers were looked at after concussion-based injury for potential as biomarkers. SncRNAs are considered novel biomarkers with miRNAs in particular having shown potential in identification of clinical disease states including concussion [95]. Saliva – also considered novel – has value in this field based on previous studies [79, 120] as it shows crossover with blood and can diagnose other systemic disorders.

Our results found salivary sncRNAs that were differentially regulated between concussed and all three control groups at time point b and time point c.

At time point b (immediately post-match) the results showed a differential expression of two hsa-let-7 miRNA family members (hsa-let-7a-5p and hsa-let-7i-5p), seven U6 small nuclear RNAs (RNU6-4, RNU6-6, RNU6-7, RNU6-45, RNU6-73, U6.375 and U6.601) and one YRNA (YRNA.255). This differential expression highlights these sncRNAs are involved in early-stage concussion development and potential biomarkers for diagnosis.

At time point c there are two miRNAs that were significantly different; hsa-let-7f-5p and hsa-miR-144-3p. No other forms of sncRNAs were significantly altered that demonstrates they are not involved in this time point. Overall, there are fewer sncRNAs differentially regulated at this later time point that may demonstrate an early time point is important in the search for a biomarker. Also, the lack of cross-over between two time points is perhaps unsurprising but demonstrates a multifaceted sncRNA response that is time-dependent.

The miRNA changes support hsa-let-7 family involvement in the specific response to concussion with previous studies showing hsa-let-7i-5p was shown to have concussion changes in saliva within 2-3 days post injury [79]. Likewise, hsa-let-7a-5p has been shown to

correlate with prolonged symptoms of concussed paediatric patients [84]. Unlike the earlier time point hsa-let-7f-5p – at time point c – has no literature-based data to further demonstrate its involvement, which aligns with the data to suggest it is a more generic trauma response. A consistent pool of data shows that the let-7 family is involved in saliva after concussion but currently the exact involvement is unclear although early responses seem to be more specific for biomarkers. Future functional assessment of potential roles could be of value.

The later time point differentially regulated hsa-miR-144-3p is considered to be brain specific. This may indicate that the later response is mediated with evidence that hsa-miR-144-3p can promote β-amyloid accumulation-induced cognitive impairments in traumatic brain injury [121]. However, the function of this response is unclear and even though hsa-miR-144-3p increases in response to concussion – like the study – this response may still be protective reacting to injury or damaging because of injury.

These results also demonstrate a novel role of U6 snRNA participation in concussion pathogenesis. U6 snRNA had previously been thought to be an optimal normalisation gene for miRNA experimentation via qPCR however more recently this has been realised to be outdated [122], which this data supports. The prevalence of multiple significantly implicated U6 snRNAs demonstrates their potential as biomarkers in general, but particularly in concussion. Additionally, this reveals the major spliceosome as a likely responder to the early stages of injury, which may associate RNA splicing as important at this time point. Although a novel finding RNA binding motifs 5 and 10 have been shown to be upregulated in response to TBI between 48-72 hours in mice that would appear to support a role for RNA splicing role in the immediate aftermath of head trauma [123].

The combination of both hsa-let-7 family and U6 snRNA upregulation could be attributed to oligo-uridylylation that has been shown to upregulate let-7 biogenesis as well as U6 snRNA maturation [124]. This could be an important pathway at the early stage of disease development to cause the upregulation that is seen.

There was a differential expression of a Y-RNA, which have also shown potential as biomarkers in other diseases such as coronary heart disease [125]. The function of this change is currently unknown but Y-RNAs have been shown to be involved in short- and long-term neuronal stresses through binding with neuronal ELAV proteins that may prevent their actions via mRNA targets [126]. As a result of this and their novel nature the role they play should be considered further.

Differential expression of sncRNAs during pre-season

At the moment the ongoing management of concussion risk in settings that receive repeat head trauma is minimal and inconsistent, due to a lack of an objective quantifiable measure to predict ongoing concussion risk.

This study has shown statistically significant differences in nine different salivary sncRNAs (6 known miRNAs, 2 snRNAs and 1 putative miRNA). This demonstrates a differential signal can be detected during pre-season that may illustrate protective signalling, represent sub-concussive or incomplete recovery from injury. These factors may increase individual risk of concussive injury over the forthcoming season and demonstrate a non-invasive biologically relevant method for monitoring concussion risk.

The putative miRNA change (put-miR-325) opposes the other miRNAs in their response however nothing is currently known about its function – due to its novel nature – so little can

be interpreted at this stage. The small nuclear RNA changes are at two different spliceosome fragments; U2 and U4, which are different to the U6 that respond in the immediate aftermath of injury. Although both snRNAs have no literature-based involvement in neurological based trauma this is perhaps unsurprising as snRNAs are relatively novel in research. These snRNA changes demonstrate – like in post-injury – an involvement of the major spliceosome that can effect RNA splicing and gene expression [127]. This information in the form of a biomarker may help in assessment of ongoing risk of concussion and in future may lead to mechanistic understanding of their role.

Two of the known miRNAs (hsa-miR-103a-3p and hsa-miR-107) found in this study have previously been found to be differentially regulated in saliva of concussed athletes within 2-3 days [79]. While all miRNAs were found to be differentially regulated in the post-injury response against a control group within this study, which demonstrates their relevance to concussion. Their role in the post-injury response depicts a diagnostic role when in fact they may have been pre-existing ongoing changes. This may explain the inconsistent presence as the control groups may contain at 'risk' individuals.

Perhaps more worryingly differential regulation of hsa-let-7f-5p, hsa-miR-103a-3p and hsa-miR-107 have consistently been found in peripheral blood circulation of Alzheimer's disease patients [128, 129]. Although this is a different bio-fluid it raises questions as repetitive concussion has been linked to neurodegenerative diseases such as Parkinson's, Alzheimer's and chronic traumatic encephalopathy (CTE) [130-133].

One miRNA was differentially expressed in the post-injury response across all control groups as well as within this baseline analysis. This was hsa-let-7f-5p, which may demonstrate a sub-

concussive response that could show an individual is at further risk of injury. The unique characteristics of this miRNA may lend itself to an ongoing biomarker and its function must be considered in more detail.

Why are there sncRNA changes in saliva?

This study has strengthened the concept that sncRNAs are responding to concussion. However, the causation as to why they exist in saliva and their function, are not fully solved. Intuition would suggest that owing to the fast nature of the response they are likely to be indirect readouts from a biological process elsewhere in the body, not directly related to the site of injury. This is a gap in this study but has given a platform for those questions to be asked in the future.

Alternative Analyses

The design of data handling in this study utilised the key changes with respect to all control groups. Owing to the number of control groups this could mask concussion related signal. So, further analysis could be done to establish if there are specific sncRNAs that are changing in levels between time points. Even though there are only two time points of direct comparison it may demonstrate sncRNA signalling patterns that could be integral to understanding the pathophysiological signalling in response to concussion.

Impact of study design

When doing a study of this size there is always a compromise to be struck to get a balance on the scientific aspects, while suiting the group of individuals aiding you in the task of collection and supplying samples for you. In this case, to be keep in line and maximise compliance the time points were selected in line with the HIA process.

The pitfalls of this are the lack of controls at time point A (HIA1), but you must consider there is no viable way of obtaining such a sample. So, there was a reliance on time point b and time point c that align with the HIA2 and HIA3 respectively. Time point b being immediately post-match is an ideal time point as this is consistent and a realistic sampling time point for a diagnostic test. Time point c has a much larger variability in time between 48-72 hours, this could mean other factors are at play and this variability may explain why there were fewer significant values at this time point. Nevertheless, to do a more defined study you would not be able to complete it on such a large scale because without ease to the operator, compliance would fall, and this should be considered when designing a study.

It is clear to me, there is a sncRNA response to concussion, but there is still a large cross-over between groups on any given sncRNA and when sncRNAs are combined. This can largely be explained by the transient and inconsistent nature of concussion, but that does not help in diagnostic terms. So, based on the data received from this study there is a basis for a highly complex test but that requires money, time and expertise to accurately diagnose, not ideal for clinical use. So, in my opinion, to make progress in this environment sub-classification of disease is key to then diagnose based on individual sncRNAs and simplify a testing strategy to be used clinically.

Based on this, I believe in the future diagnosis using sncRNAs maybe possible with technological improvements and increased biological understanding but there is still a lot of work to maximise the potential of salivary sncRNAs in concussion.

Limitations

This study was designed as an exploratory study, so it is not definitive. This would require confirmation in an independent setting.

The HIA process, which is used as the 'gold standard' for the diagnosis of concussion in this study, is not perfect. The inherent error rate in the gold standard would inevitably lead to some miss-classification within the study. There may be discrepancies between leagues as well given the Premiership utilises video footage analysis to verify the diagnosis of concussion and is reported to have a lower misdiagnosis rate than the championship [51].

Another source of possible error is the change in saliva collection kits between season 1 and season 2, which was beyond our control. The two kits yield slightly different recovery rates for the sncRNAs of interest (data not shown), which introduces a potential element of heterogeneity in the methodology.

This study was finically supported by an external company (Marker Health) during the NGS and subsequent validation steps. This allowed more far-reaching capabilities of work but may have limited scientific input at some points.

The study did not lend itself to an elongated time course due to the lack of time points. A future study could address this more specifically by taking a defined set of patients with samples given at 2-hour intervals to assess directional changes, with the sncRNAs to be used as a guide for that.

Finally, the NGS was done based on Time point b (HIA2) samples alone. This may be a reason why there was a larger population of significant sncRNAs at time point b over time point c. So there could be more sncRNAs that exist at the later time point.

Overall

This research has shown that differential expression exists before concussion injury at baseline as well as in a time-dependent manner post injury, which demonstrates its diagnostic testing capabilities. Although the pool of participants was very specific due to the constraints of the study – and has not directly tested specificity and sensitivity – this has put the building blocks in place to create a sncRNA diagnostic test, for which the function can be expanded in future.

It has also demonstrated Let 7 miRNA family, RNU6 snRNA and Y-RNA involvement in the post injury response that could depict the underlying pathophysiology of concussion. While some of the miRNAs involved in the pre-season differential expression have shown links to neurodegenerative disease, which must be investigated further. This information has opened a new chapter in concussion investigation that could be integral in the pathogenesis.

Future work

The aim of future work would be to test the effectiveness of these biomarkers as a diagnostic test. If effective then applying this to different cohorts would be an essential step to making it applicable to the whole population of demographics including but not limited all genders, ethnic groups and ages for use in a healthcare setting. As well as that looking into the role of these miRNAs in pathways through bioinformatics databases or in vitro analysis would have use in understanding the pathophysiology of concussion.

Future work should also look to address (1) Where the differentially expressed sncRNAs have come from to be expressed in saliva? (2) Are they directly related to the site of injury? Or are they indirect readouts from other biological processes? This work has overlooked this step due to a combination of complexities of analysis and immediate success of saliva. However, it

is an important step in the understanding of disease manifestation and how to best utilise any test in a clinical decision-making environment.

Chapter 3: Bio-informatics based function of salivary microRNAs involved in concussion injury response

Rationale

In the first chapter there were salivary sncRNAs found to be differentially regulated during concussion. The function of these differentially regulated sncRNAs in concussion is unknown. Bioinformatics tools clarify the potential function of the miRNAs within this group, through their interaction with mRNAs. Other sncRNAs have limited bioinformatics capability currently so bioinformatics tools were used to understand the function of the differentially expressed miRNAs to highlight important mechanisms that may have miRNA involvement.

Aims

To find potential functions for the differentially expressed miRNAs at different time points and how they may relate to concussion.

Create a list of pathways, and from that mRNA targets for microRNAs, that could be functioning in response to concussion to guide future experimentation.

Statement of Contribution

I completed all the work in the chapter. Dr Valentina Di Pietro guided and supported throughout.

Methods

Downstream signalling analysis

Bioinformatics miRNA tools to help analyse to begin to understand the function of the salivary miRNAs during concussion.

Diana Tools mirPath v.3

Differentially regulated miRNAs found in results chapter 2 were used to visualise KEGG pathways that were overexpressed based on their predicted mRNA targets. Diana tools mirPath v.3 was used, which uses the micro-T prediction algorithm (>0.8) to produce a gene target list for each miRNA. Based on this list across different miRNAs the gene targets that are overrepresented it shows the most present KEGG pathways. The gene union tool was used that produced a final p-value that was corrected using a false discovery rate method. A p-value of less than 0.05 was considered significant.

Technique used for analysis

Using all differentially expressed miRNAs

All differentially expressed miRNAs against each control group were used to create a list of significantly impacted KEGG pathways. The KEGG pathways that were present when compared to all control groups were considered the pathways specifically signalling in response to concussion.

Using individual miRNAs differentially expressed across all groups

MiRNAs that were significant across all groups in chapter 2 were considered alone. These miRNAs are already functioning alone in the concussion group. Due to the different analysis method at the baseline time point miRNAs two miRNAs were selected for further interrogation based on interest from the data.

Differentially expressed miRNAs used for analysis

Below are the miRNAs used for analysis in this study, by time point.

Time point b

At time point b there are numerous different markers that show significant differences when compared against all groups.

Table 11 – Showing differentially regulated microRNAs found in chapter 2 at time point b, which were used for downstream analysis.

	vs. MSK	vs. HIA-	vs. Uninjured
Significant microRNAs	hsa-let-7a-5p, hsa-let-7i-5p, hsa-miR-1271-5p, hsa-miR-142-5p, hsa-miR-143-3p, hsa-miR-16-1-3p	hsa-let-7a-5p, hsa-let-7f-5p, hsa-let-7i-5p, hsa-miR-103a-3p, hsa-miR-107, hsa-miR-135b-5p, hsa-miR-144-3p, hsa-miR148a-3p, hsa-miR-34b-3p, hsa-miR-92a-3p	hsa-let-7a-5p, hsa-let-7f-5p, hsa-let-7i-5p, hsa-miR-103a-3p, hsa-miR-135b-5p, hsa-miR-148a-3p, hsa-miR-34b-3p
Total	6	10	7

Time point c

At time point c there were a large number of miRNAs differentially regulated.

Table 12 – Showing significantly different microRNAs found in chapter 2 at time point c used for downstream analysis.

	vs. MSK	vs. HIA-	vs. Uninjured
Significant microRNAs	hsa-let-7f-5p, hsa-miR-135b-5p, hsa-miR-144-3p, hsa-miR-21-5p, hsa-miR-16-1-3p, hsa-miR-425-5p	hsa-let-7a-5p, hsa-let-7f-5p, hsa-let-7i-5p, hsa-miR-107, hsa-miR-126-3p, hsa-miR-144-3p, hsa-miR-148a-3p, hsa-miR-34b-3p, hsa-miR-21-5p, hsa-miR-92a-3p	hsa-let-7f-5p, hsa-miR-144-3p, hsa-miR-148a-3p
Total	6	10	3

Baseline

Differentially expressed miRNAs were used to establish potential mechanisms that could be involved in a mechanism that may put individuals at risk of concussion (Table 13).

Table 13 – Showing the significantly different microRNAs found at baseline in chapter 1 used for downstream analysis.

	vs. Uninjured
Significant microRNAs	hsa-let-7f-5p, hsa-miR-103a-3p, hsa-miR-107, hsa-miR-148a-3p, hsa-miR-143-3p and hsa-miR-92a-3p
Total	6

Results

The bioinformatics tools for miRNAs are becoming ever more sophisticated. However, for other sncRNAs there is a lag behind due to less interest in them. As a result, miRNA bioinformatics tools were used throughout this chapter.

Post injury response

Time point b

There are numerous KEGG pathway changes at time point b. The significance of each KEGG pathway against each group can be seen in Figure 23. The overall trend is that the pathway significance associated with uninjured and HIA- are much more closely aligned than MSK, which is perhaps unsurprising.

The KEGG pathway with the highest combined significance across all groups was ECM-receptor interaction (MSK p-value: 1.77E-09, HIA- p-value: 1.63E-15, Uninjured p-value: 2.14E-19), which demonstrates a likely miRNA mediated extracellular matrix response to injury. Unlike other time points the thyroid hormone signalling pathway was present at time point b (MSK p-value: 7.19E-08, HIA- p-value: 0.000286, Uninjured p-value: 0.001509) that could demonstrate that miRNAs mediate an initial thyroid hormonal response to injury.

Table 14 - KEGG pathways associated with differential microRNA expression across all three control groups at time point b. Diana mirPath V.3 was used for analysis and a FDR corrected p-value of less than 0.05 was considered significant.

KEGG pathway	MSK			HIA-			Uninjured		
	p-value	#genes	#miRNAs	p-value	#genes	#miRNAs	p-value	#genes	#miRNAs
ECM-receptor interaction	1.77E-09	20	6	1.63E-15	32	10	2.14E-19	27	7
Prion diseases	2.69E-16	8	4	1.26E-08	4	3	8.01E-11	1	1
Thyroid hormone signaling pathway	7.19E-08	36	6	0.000286	42	9	0.001509	31	6
Proteoglycans in cancer	0.004514	46	6	2.92E-13	85	10	4.11E-11	63	7
Melanoma	0.004514	23	6	0.010901	26	9	0.013903	20	6
PI3K-Akt signaling pathway	0.00709	79	6	0.000118	107	10	0.000194	83	7
Signaling pathways regulating pluripotency of stem cells	0.013252	37	6	3.89E-10	61	10	7.87E-12	52	7
Pathways in cancer	0.018357	90	6	0.000664	122	10	0.001509	92	7
Colorectal cancer	0.018357	18	6	0.010085	24	9	0.001611	21	6
AMPK signaling pathway	0.019771	32	6	0.002942	45	10	0.009447	34	7
mTOR signaling pathway	0.021313	19	6	0.000299	28	10	0.000382	24	7
Wnt signaling pathway	0.031631	33	6	0.003265	44	10	0.002095	34	7
Prostate cancer	0.031631	26	6	0.003618	34	10	0.004757	27	7
Glioma	0.039444	17	6	0.000119	26	10	0.000715	20	7
Platelet activation	0.040277	31	6	0.002075	44	10	0.005637	33	7
Type II diabetes mellitus	0.020683	16	5	0.034199	18	9	0.041558	14	6

Numerous other signalling pathways were predicted to have interactions with these miRNAs, which could demonstrate how miRNAs impact signalling during concussion. The strongest two were the AMPK signalling pathway and PI3K-Akt signalling pathway, which could illustrate the importance of these pathways during the initial stages.

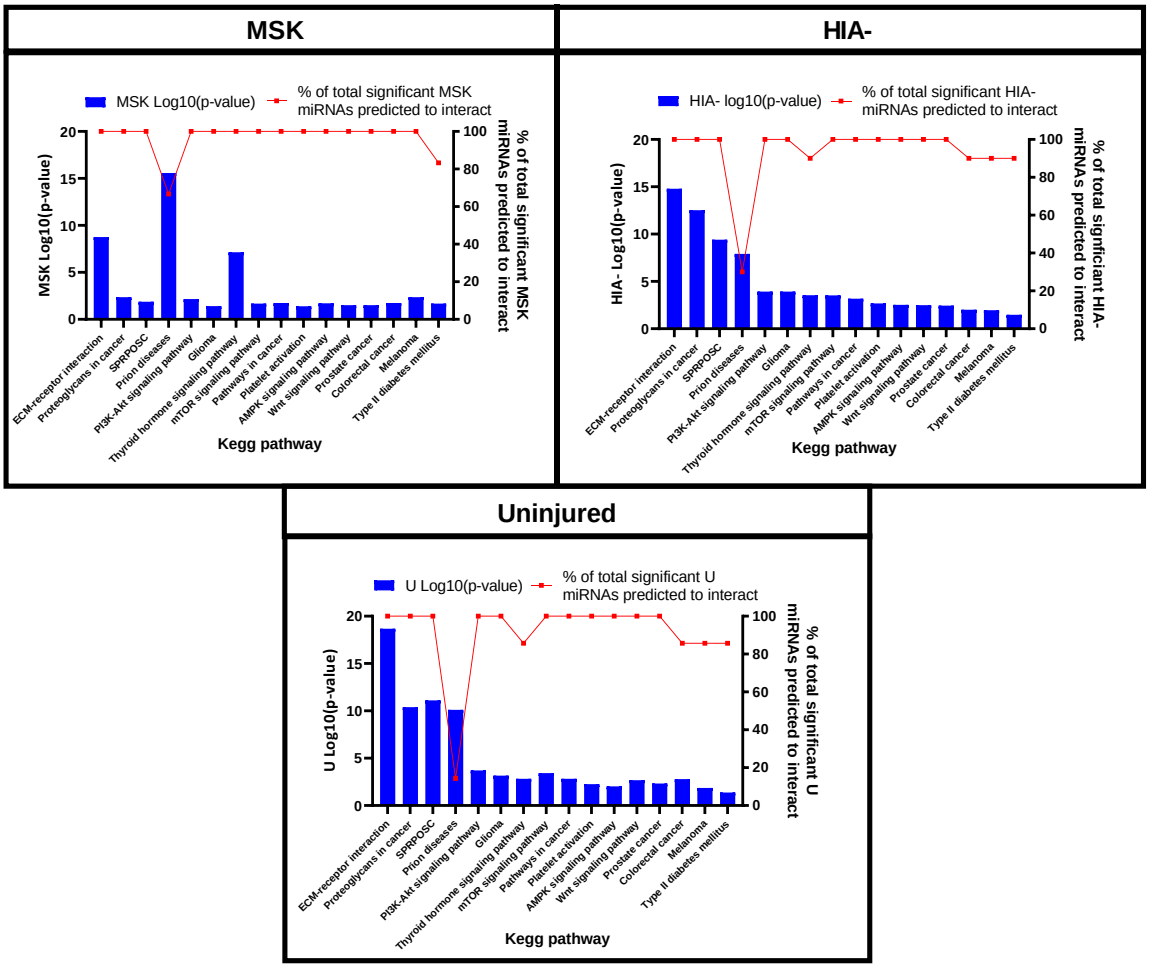

Figure 23 – KEGG pathways significantly associated with differential microRNA expression in the concussed group when compared against controls at time point b. This visual representation shows the similarity when compared to the uninjured and HIA- control groups. Diana mirPath V.3 was used for analysis and a FDR corrected p-value of less than 0.05 was considered significant. Significant microRNAs from chapter 2 were used for analysis in this figure.

Individual microRNA responses

Two miRNAs were statistically significant across both groups, hsa-let-7a-5p and hsa-let-7i-5p.

hsa-let-7a-5p

Table 15 – KEGG pathway interactions of targets from hsa-let-7a-5p. Created using pathways union tool in Diana tools with FDR corrected p-value of less than 0.05 considered significant.

KEGG pathway	p-value	#genes	#miRNAs
ECM-receptor interaction	1.88E-22	10	1
Mucin type O-Glycan biosynthesis	0.001423	4	1
Glycosaminoglycan biosynthesis - chondroitin sulfate / dermatan sulfate	0.001423	3	1
Amoebiasis	0.001423	10	1
Signaling pathways regulating pluripotency of stem cells	0.004393	16	1
PI3K-Akt signaling pathway	0.019567	28	1
p53 signaling pathway	0.028031	10	1
Transcriptional misregulation in cancer	0.041664	15	1
Wnt signaling pathway	0.042665	11	1

hsa-let-7i-5p

Table 16 – KEGG pathway interactions of targets from hsa-let-7i-5p. Created using pathways union tool in Diana tools with FDR corrected p-value of less than 0.05 considered significant.

KEGG pathway	p-value	#genes	#miRNAs
ECM-receptor interaction	3.86E-19	8	1
Glycosaminoglycan biosynthesis - chondroitin sulfate / dermatan sulfate	3.25E-05	4	1
Mucin type O-Glycan biosynthesis	0.000617	4	1
Amoebiasis	0.000753	10	1
Signaling pathways regulating pluripotency of stem cells	0.002083	16	1
Protein digestion and absorption	0.028632	11	1

These miRNAs were considered together due to their similarity in both family and KEGG pathway results. Both miRNAs show interaction with ECM-receptor interaction (hsa-let-7a-5p p-value: 1.88E-22, hsa-let-7i-5p p-value: 3.86E-19), glycosaminoglycan biosynthesis (hsa-let-7a-5p p-value: 0.001423, hsa-let-7i-5p p-value: 3.25E-05) and mucin o-glycan biosynthesis (hsa-let-7a-5p p-value: 0.001423, hsa-let-7i-5p p-value: 0.000617) with hsa-let-7i-5p showing

a stronger interaction. This indicates a likely role in extracellular matrix control in early response to injury.

Hsa-let-7a-5p shows a more diverse range of signalling with p53 signalling pathway (p-value: 0.028031) and PI3K-Akt signalling pathway (p-value: 0.019567), these signalling pathways may be equally important so although these miRNAs are similar, they may have slightly diverging roles.

Time point c

At time point c there are numerous KEGG pathways that are significantly impacted. The pattern of significant Just like at time point b, ECM-receptor signalling was the most significant across all groups (MSK p-value: 2.66E-10, HIA- p-value: 9.11E-15, Uninjured p-value: 2.01E-16). This change like at other time points seems important throughout concussion.

Table 17 – KEGG pathways significantly associated with differential microRNA expression across all control groups at time point c. Diana mirPath V.3 was used for analysis and a FDR corrected p-value of less than 0.05 was considered significant.

KEGG pathway	MSK			HIA-			Uninjured		
	p-value	#genes	#miRNAs	p-value	#genes	#miRNAs	p-value	#genes	#miRNAs
ECM-receptor interaction	2.66E-10	23	6	9.11E-15	27	10	2.01E-16	19	3
Proteoglycans in cancer	8.74E-06	56	6	1.09E-10	80	9	4.44E-05	44	3
Signaling pathways regulating pluripotency of stem cells	5.46E-06	45	6	2.81E-07	54	9	0.000519	35	3
Focal adhesion	0.000607	58	6	0.000283	68	10	0.00077	47	3
PI3K-Akt signaling pathway	0.001456	80	6	0.000928	97	10	0.002142	66	3
Amoebiasis	0.00077	28	6	0.007672	30	9	0.002353	22	3
Renal cell carcinoma	0.009812	21	6	0.001773	26	9	0.002443	19	3
Glioma	0.001096	20	6	0.001015	23	9	0.003263	16	3
ErbB signaling pathway	0.019287	24	6	0.005964	30	9	0.003532	22	3
MAPK signaling pathway	0.002668	61	6	0.006356	70	9	0.005126	49	3
Prolactin signaling pathway	0.001528	22	6	0.005964	25	9	0.00755	18	3
FoxO signaling pathway	0.000607	42	6	0.000424	51	10	0.008288	32	3
Hippo signaling pathway	0.000256	36	6	4.80E-06	47	9	0.014353	28	3
Glutamatergic synapse	0.013181	28	6	0.032277	31	9	0.025173	21	3
Platelet activation	0.003714	35	6	0.025926	39	9	0.02814	28	3
Endocrine and other factor-regulated calcium reabsorption	0.003714	14	6	0.022001	15	7	0.033835	12	3
Pathways in cancer	0.004985	90	6	0.003222	108	10	0.04184	67	3
Melanoma	0.003714	23	6	0.0152	24	8	0.04688	16	3
AMPK signaling pathway	0.006108	33	6	0.0152	40	10	0.048534	25	3

The significant miRNAs interact with numerous pathways including ErbB signalling pathway, hippo signalling pathway and AMPK signalling pathway, which all may have individual roles in the response to concussion. The glutamatergic synapse KEGG pathway (MSK p-value: 0.013181, HIA- p-value: 0.032277, Uninjured p-value: 0.025173) was significantly associated across all groups, which demonstrates that the miRNAs could be responding in the brain due to the high abundance of glutamatergic synapses within the brain.

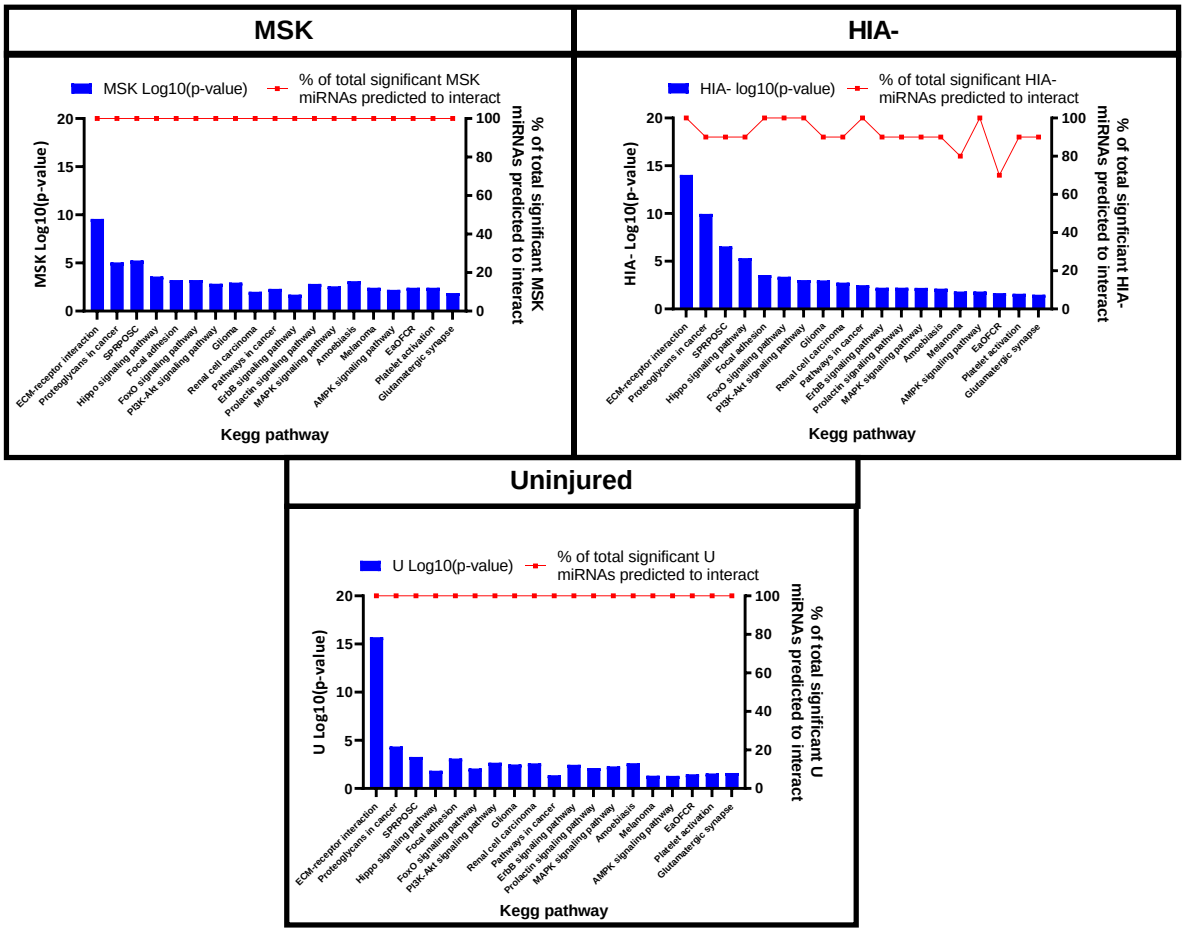

Figure 24 - KEGG pathways significantly associated with aberrant microRNA expression in the concussed group when compared against each control group at time point c. There is relative similarity of the significance of each pathway interactions across all three control groups. Diana mirPath V.3 was used for analysis and a FDR corrected p-value of less than 0.05 was considered significant. Significant microRNAs from chapter 2 were used for this analysis.

Individual miRNAs responses

There were two miRNAs that were present across all control groups, hsa-miR-144-3p and hsa-let-7f-5p.

hsa-mir-144-3p

Table 18 - KEGG pathways that are predicted to interact with hsa-miR-144-3p. Created using pathways union tool in Diana tools with FDR corrected p-value of less than 0.05 considered significant.

KEGG pathway for hsa-mir-144-3p	p-value	#genes	#miRNAs
Gap junction	0.004056	10	1
Glutamatergic synapse	0.004056	16	1
Dopaminergic synapse	0.004056	20	1
Prolactin signaling pathway	0.004056	12	1
Adrenergic signaling in cardiomyocytes	0.005341	19	1
cAMP signaling pathway	0.005458	27	1
Endocrine and other factor-regulated calcium reabsorption	0.008589	9	1
Proteoglycans in cancer	0.012018	23	1
cGMP-PKG signaling pathway	0.025277	20	1
Serotonergic synapse	0.025277	14	1
ErbB signaling pathway	0.031223	11	1

Hsa-miR-144-3p has a more clearly defined role in synaptic transmission with significant interactions with the glutamatergic synapse (p-value: 0.004056), dopaminergic synapse (p-value: 0.004056) and serotonergic synapse (p-value: 0.025277). This demonstrates hsa-miR-144-3p alters signalling at this later time point, which is likely to be causing a neurological

change in response to injury. Other different pathways not present at time point b are present here including cAMP signalling pathway and cGMP-PKG signalling pathway.

hsa-let-7f-5p

Table 19 – KEGG pathways interaction based on hsa-let-7f-5p targets. Created using pathways union tool in Diana tools with FDR corrected p-value of less than 0.05 considered significant.

KEGG pathway for hsa-let-7f-5p	p-value	#genes	#miRNAs
ECM-receptor interaction	2.27E-19	9	1
Amoebiasis	0.000482	11	1
Mucin type O-Glycan biosynthesis	0.000834	4	1
Glycosaminoglycan biosynthesis - chondroitin sulfate / dermatan sulfate	0.000879	3	1
Signaling pathways regulating pluripotency of stem cells	0.000957	17	1

Hsa-let-7f-5p also specifically signals at time point c in response to concussion. Like other members of the hsa-let-7 family the role of this miRNA seems to be largely to do with ECM-receptor interaction (p-value: 2.27E-19) and glycan biosynthesis (Mucin type O-Glycan biosynthesis p-value: 0.000834 and Glycosaminoglycan biosynthesis p-value: 0.000879), which demonstrates the early changes are persisting at this time point although with a different miRNA. It also shows it is unlikely to be one miRNA working at a specific time point and is more dynamic. This miRNA may be enabling the physical changes to let hsa-miR-144-3p elicit its effects.

Post-injury response pathway cross-over

There is a large cross-over between the time point b and time point c. Pathways such as ECM-receptor interaction, PI3K-Akt signalling pathway and AMPK signalling pathway are present

across both time points. However, some pathways such as thyroid hormone signalling pathway are present at time point b that demonstrates some time-dependent responses. Time point c shows more specific signalling that could demonstrate the start of a recovery response with pathways such as ErbB signalling pathway and FoxO signalling pathway.

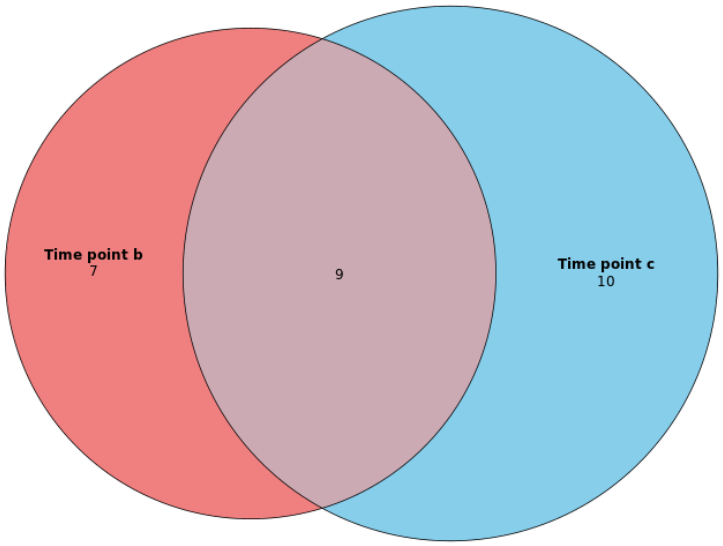

Figure 25- Venn diagram showing the crossover of pathways between time point b and time point c. There was a fair proportion of pathways (9/26 = 35%) that crossed over between both time points that may demonstrate some similar signalling pathways.

Pre-injury differential signalling

The most significantly associated pathway was ECM-receptor interaction (p=1.12E-16) (Figure 6) with four separate miRNAs interacting with this pathway individually (Figure 7). There seems to be a role for fatty acids with both biosynthesis (p=1.39E-12) and metabolism (p=0.003) showing significant interactions. Other signalling pathway such as Hedgehog signalling pathway and MAPK signalling pathway may indicate some of the differences that may exist. However, the presence of prion diseases pathway (8.36E-12) should be investigated

further to understand if the interaction with hsa-miR-148a-3p could illustrate a more substantial signalling change.

Table 20 –KEGG pathways that were significantly associated with differential microRNA expression when compared to the uninjured cohort, at baseline. Diana mirPath V.3 was used for analysis and a FDR corrected p-value of less than 0.05 was considered significant.

KEGG pathway	p-value	#genes	#miRNAs
ECM-receptor interaction	1.12E-16	26	6
Fatty acid biosynthesis	1.39E-12	3	5
Prion diseases	8.36E-12	3	3
Signaling pathways regulating pluripotency of stem cells	1.64E-07	48	6
Proteoglycans in cancer	2.59E-06	58	6
PI3K-Akt signaling pathway	7.44E-05	88	6
Focal adhesion	0.000863	58	6
Fatty acid metabolism	0.002808	9	6
Renal cell carcinoma	0.002808	22	6
Amoebiasis	0.005627	27	6
FoxO signaling pathway	0.00592	41	6
Glioma	0.007187	19	6
Pathways in cancer	0.008286	92	6
Hedgehog signaling pathway	0.010057	18	6
Wnt signaling pathway	0.010585	34	6
Dilated cardiomyopathy	0.014526	27	6
Platelet activation	0.014526	35	6
Regulation of actin cytoskeleton	0.014526	53	6
Basal cell carcinoma	0.018483	18	6
Hypertrophic cardiomyopathy (HCM)	0.018483	25	6
MAPK signaling pathway	0.018483	58	6
Dorso-ventral axis formation	0.029847	11	6
Prolactin signaling pathway	0.036946	19	6
Hippo signaling pathway	0.045554	41	6
mTOR signaling pathway	0.045554	19	6
Thyroid hormone signaling pathway	0.045554	28	6

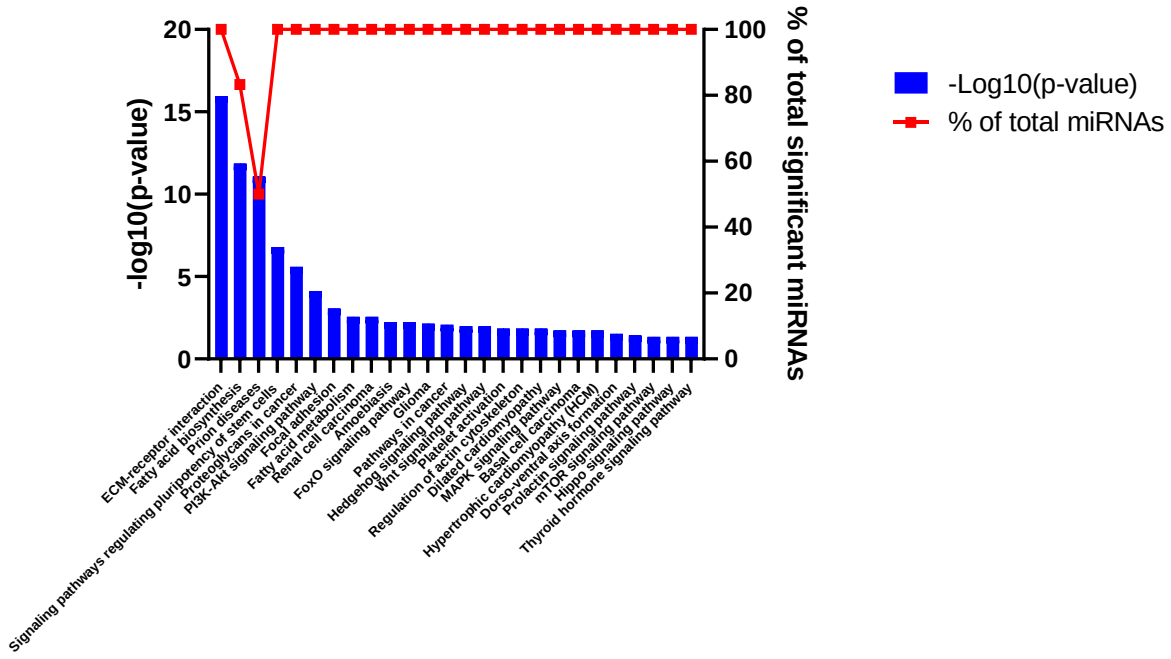

Figure 26 – Twenty-five most significant KEGG pathways associated with differentially regulated miRNAs. Diana mirPath V.3 was used for analysis and a FDR corrected p-value of less than 0.05 was considered significant.

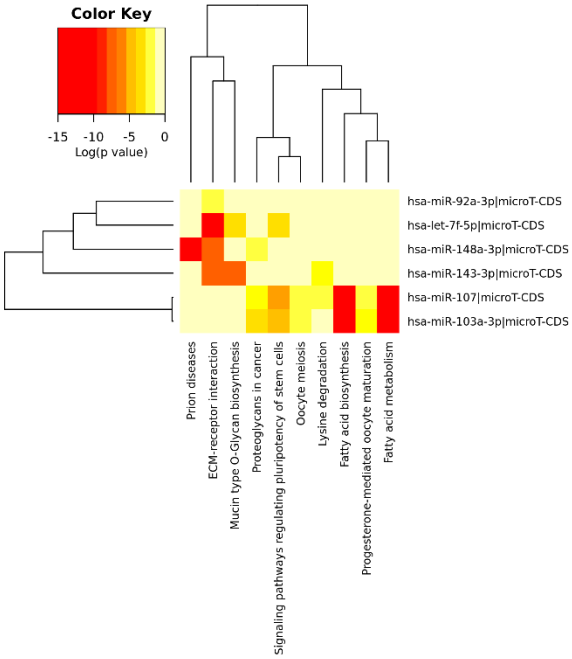

Figure 27 – Heat map showing KEGG pathways and their miRNA association. Using the pathways intersection tool in Diana tools mirPath v.3 miRNAs that interact with the same pathways can be seen to give an understanding of the microRNAs that may be working together.

Figure 27 shows that hsa-miR-107 and hsa-miR-103a-3p are working in similar ways with shared pathways in fatty acid biosynthesis and metabolism. Whereas all other miRNAs show interactions with ECM-receptor interaction that might demonstrate two different types of miRNA-based responses.

Individual miRNA responses

Two miRNAs were selected because of their interesting interactions and previous relevance to the study.

hsa-miR-148a-3p

Table 21 -KEGG pathways associated with hsa-miR-148a-3p. Created using pathways union tool in Diana tools with FDR corrected p-value of less than 0.05 considered significant.

KEGG pathway for hsa-mir-148a-3p	p-value	#genes	#miRNAs
Prion diseases	6.04E-35	1	1
ECM-receptor interaction	1.09E-08	8	1
Renal cell carcinoma	0.001491	8	1
Other glycan degradation	0.006916	1	1
FoxO signaling pathway	0.013648	13	1
MicroRNAs in cancer	0.017402	13	1
Glioma	0.025754	6	1
PI3K-Akt signaling pathway	0.036544	21	1
Proteoglycans in cancer	0.036544	13	1
Hypertrophic cardiomyopathy (HCM)	0.038988	9	1

The miRNA hsa-mir-148a-3p shows these pathway interactions (Table 21). One of particular interest is Prion diseases (Figure 26), which within it has PRNP gene as a validated interaction. This could implicate that this miRNA is interacting with neuroprotective signalling in the brain. Other pathways include ECM-receptor interaction that could contribute to physical extracellular matrix changes that may indicate previous injury or pre-dispose to future.

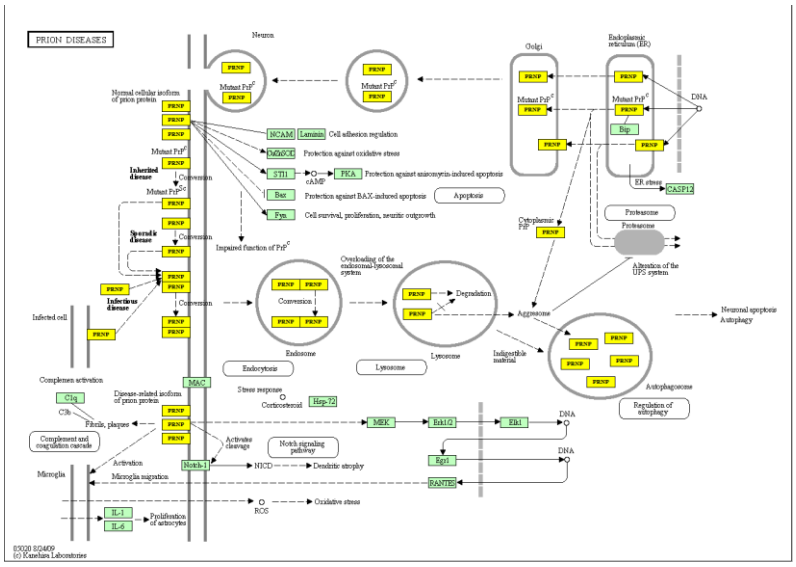

Figure 28 - Prion disease KEGG pathway – PRNP (highlighted in yellow) – a target of miR-148a-3p – is involved in the prion disease pathway. It may be illustrating that there is underlying pathology that may be making individuals susceptible to neurodegeneration or neurodegenerative diseases

hsa-let-7f-5p

Table 22 – KEGG pathway interactions of hsa-let-7f-5p. Created using pathways union tool in Diana tools with FDR corrected p-value of less than 0.05 considered significant.

KEGG pathway for hsa-let-7f-5p	p-value	#genes	#miRNAs
ECM-receptor interaction	2.27E-19	9	1
Amoebiasis	0.000482	11	1
Mucin type O-Glycan biosynthesis	0.000834	4	1
Glycosaminoglycan biosynthesis - chondroitin sulfate / dermatan sulfate	0.000879	3	1
Signaling pathways regulating pluripotency of stem cells	0.000957	17	1

The most relevant change here is the presence of ECM-receptor interaction, which could demonstrate physical extracellular matrix changes that could result from previous trauma or make an individual more susceptible to future injury.

Discussion

There are many signalling pathways that are partaking in the concussion-based response based on this evidence. Therefore, to understand the potential involvement of miRNAs, pathways with comprehensible links based on current knowledge will be discussed throughout.

For all pathways discussed throughout this section differential miRNA functioning is assumed to have stemmed and be functional in the brain. Clearly, this a large assumption and they could be demonstrative of signalling in the salivary gland or other places. This should be considered with any interpretation of this section.

Concussion based signalling at both time points

There are specific pathways that signal in the post-injury concussion response, the most significant from this study was ECM-receptor interaction. All three hsa-let-7 family members – that were significant across all control groups – showed ECM-receptor interaction.

The finding of ECM-receptor involvement is unsurprising as the extracellular matrix (ECM) makes up one-fifth of total brain volume. It functions as structural support – using glycosaminoglycans (GAG), proteoglycans (PG) and glycoproteins (GP) as its component parts – and to modulate intracellular communication [134]. The ECM has previously been shown to have an involvement in TBI with secondary inflammatory molecule release increasing

synthesis of extracellular matrix molecules to remodel the ECM, which has mixed consequences for recovery of function [134, 135]. Although this is not concussion based there are likely to be similarities in pathogenesis, which strengthens the relevance of these salivary miRNAs. This may demonstrate the ECM response may be important in the immediate aftermath from injury and could offer a therapeutic target that has previously been preliminary tested in an animal model [136].

Linked to ECM are both the mucin type o-glycan biosynthesis and glucosaminoglycan biosynthesis pathways that are component parts of the ECM [134, 137]. The hsa-let-7 family members that are individually significant against all control groups – hsa-let-7a-5p, hsa-let-7i-5p and hsa-let-7f-5p – have these pathways present that further states the potential ECM involvement.

Another pathway of significance across both time points was AMPK signalling pathway. AMPK is a serine/threonine kinase that under low-energy conditions becomes phosphorylated to actively supress energy consumption and boost ATP production [138]. After concussion-based injuries there is a stereotypical energy crisis that leads to a requirement for ATP production. This may demonstrate that the level of AMPK phosphorylation could be impacted after a concussion, which could be contributing to the energy crisis. This has been shown in an animal model with AMPK phosphorylation reduced in the hippocampus after mTBI [139] and may provide a novel treatment target to increase ATP production and improve recovery [140].

The PI3K-Akt signalling pathway was also present across both time points. PI3K-Akt signalling pathway is integral in the regulation of cell growth and survival of neurons and can be modulated through glutamate receptor signalling [141]. This pathway has been shown to be

upregulated in response to TBI [142, 143], which accompanied with our data may suggest concussion related injury may have a PI3K-Akt signalling pathway response within the first three days. The impact of these signalling changes have shown conflicting results in the way they impact neuronal and functional recovery [144, 145]. However it seems their roles may be through managing autophagy [146]. So, drug treatments targeting this pathway may be useful, but the complexity of concussion may limit their implementation of a population wide basis.

All mentioned pathways have had a previous association with head trauma and although they may have a much less impactful role in concussion it still demonstrates potential clinical targets and usefulness of salivary based markers. Although this is bioinformatics analysis it still provides valuable insight into the potential implications of concussion-based signalling.

Concussion based signalling specific to time point b

The thyroid hormone signalling pathway was significant at time point b only, which could mean there is a miRNA mediated specific thyroid hormone-based response within the first hours of injury that is not maintained. Thyroid signalling has been shown to be impacted after concussion previously, however the changes are not designated to a specific time point [147-149]. This could demonstrate the miRNA signalling may precede the longer-term thyroid hormone signalling. They may also impact the length and symptom burden with FT4 – a hypothalamic-pituitary-thyroid (HPT) axis hormone – correlated to higher somatic symptoms at lower concentrations [147]. This could offer potential treatment target to affect these symptoms profiles to have an early impact and prevent further symptomology.

Concussion based signalling specific to time point c

The glutamatergic synapse KEGG pathway was present at time point c only, which may demonstrate that glutamate based synaptic signalling changes are not immediately altered post-injury and take time to develop. There is a typical immediate increase in glutamate so this may demonstrate that miRNA signalling could be responding at the synaptic level in response to this initial increase as glutamate levels [13]. As there is evidence of reduced glutamate levels in some brain areas in the first week of injury [150]. These changes may be important in the development of disease and may demonstrate longer term changes so understanding the relevance of hsa-miR-144-3p – that is one such miRNA involved when compared to all controls – could illustrate concussion-based responses.

Pre-concussion injury signalling that may highlight risk

The signalling pathways involved are similar and not distinguishable from those in the post-injury response, which demonstrates they are relevant to concussion. Further study would help to evaluate the subtle differences between the different groups. However perhaps most worryingly prion diseases is present that could demonstrate a longer term consequence of differential signalling as PRNP has shown to be involved in the development of Alzheimer's disease [151]. As a result, the role of hsa-miR-148a-3p – a miRNA that targets PRNP – should be considered carefully.

The ECM-receptor interaction is also involved at this preliminary time point. This may demonstrate an incomplete recovery from injury due to its presence in the post-injury response and could highlight a mechanism that may put individuals at risk of a future concussion-based injury.

This study is limited by its bioinformatics origin, so this data does not have the accuracy of an in vitro analysis and relies on the micro-T algorithm for selection of targets. However, as it was an exploratory analysis these are understood and expected limitations.

Several miRNAs are involved at different time points so the combination of these produce a diverse picture. As a result, this should be considered as a guide for potential pathways that could be involved with in vitro interactions to prove an interaction. Furthermore, the method used here is highly dependent upon what is known, and little is known about miRNA function specifically in saliva and concussion.

Bioinformatics based analysis is only as good as the algorithm that selects the targets. The way miRNAs target multiple mRNA sequences makes designing that algorithm very challenging. These tools will get more advanced as time moves forward to allow more accurately designed in vitro assessments following on from it.

Overall

Overall, this bioinformatics analysis demonstrates that salivary miRNA biomarkers may have an important role in illustrating disease changes. Differential pathways at both time points – ECM receptor interaction and AMPK signalling pathway – or more specifically across individual time points – Thyroid signalling pathway and Glutamatergic synapse – have given an insight into concussion pathogenesis, pathways that may make individuals susceptible to concussion or neurodegenerative disease while offering potential time specific treatment targets.

Future work

Future research could utilise these pathways to establish whether a miRNA can impact that signalling of that pathway to further understand miRNA involvement in the concussion response more greatly.

They could use a differentially regulated miRNA from chapter 2 and test a target or multiple targets that is associated with a pathway of choice. For example, I would look at targets for hsa-let-7a-5p in the ECM receptor interaction pathway to establish the role at time point b.

Additionally, the bioinformatics tools do not exist for small nuclear RNAs. If these tools did become available, it would be of interest to investigate the role of the RNU-6 small nuclear RNA sub family to understand the ramifications of this signalling more closely.

Chapter 4: The in vitro interactions of concussion injury related salivary miRNAs

Rationale

Differentially regulated miRNAs were found in the saliva of concussed athletes. To understand their function, it was important to find if any biological interactions could be found in vitro. Predictive bioinformatics tools are good for finding context of overall biological functioning but finding validated mRNA targets could pinpoint the actual biological processes behind concussion or certainly begin to unpin this response, which little is known about.

Aims

To establish mRNA targets of a selection of the differentially regulated miRNAs found in SCRUM.

Statement of Contribution

I completed all work stated in this chapter. Dr Valentina Di Pietro offered support and guidance throughout.

Methods

Experimental guide

1. Differentially regulated miRNAs used
2. Finding of mRNA targets using bioinformatics tool
3. Luciferase assay analysis of targets tested

Differentially regulated miRNAs

Owing to the design of the study the selection of differentially regulated miRNAs occurred halfway through miRNA analysis. At that point, the two strongest candidate markers were hsa-

miR-144-3p and hsa-miR-135b-5p. Both markers are significant across a selection of groups. Hsa-let-7i-5p was selected based on previous data.

Finding mRNA targets using bioinformatics tool

To predict potential mRNA targets the more up to date miRWalk database was used. The criteria used for this assessment was a miRWalk prediction score of >0.95 of binding to the 3'UTR region, while also being present in at least one of the miRDB or TargetScan databases. This list was then limited down based on previous findings to create a manageable list.

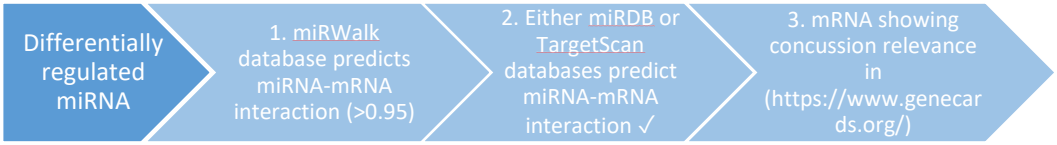

Figure 29 - Workflow carried out to search for mRNA targets - For differentially regulated miRNAs found in the SCRUM study the miRWalk database (http://mirwalk.umm.uni-heidelberg.de/) was used to find probable mRNA targets using the sequence of events shown above. Confirmation of whether mRNAs were targets was carried out using the luciferase assay.

Cell Culture

Materials

Adenocarcinomic human alveolar basal epithelial cells (A549 cells) were washed using sterile Dulbecco's phosphate buffered saline (PBS) without calcium and magnesium chloride. Dulbecco's Modified Eagle Medium (DMEM) (Gibco) was supplemented with 10% foetal bovine serum (Sigma) and 1% Penicillin Streptomycin (PS) (10,000U/mL Penicillin and 10mg/ml Streptomycin) (Sigma), this supplemented media is referred to as growth media. Cell culture flasks (T-75) and conical centrifuge tubes were purchased from Sarstedt Ltd. Multiwell plates (96 well) for cell culture from Grenier.

A549

Adenocarcinomic human alveolar basal epithelial cells (A549 cells) derived from cancerous lung tissue that are known to be capable of withstanding transfection. A549 cells were grown in growth media (DMEM, 10% FBS and 1% PS) and were used between the passages 2-6 for all experiments.

Thawing and Plating A549 cells

Cryopreserved vials of A549 cells were stored at -80^{o}C upon arrival. After removing the vial, it was thawed at room temperature, re-suspended in 5ml of growth media and centrifuged at 300xg for 5 minutes (10^{o}C) (Beckmann Coulter Allegra X-12R, Beckmann Coulter). The supernatant was poured away to remove traces of Dimethyl sulfoxide (DMSO) and the cell pellet was re-suspended in 2ml of growth media before plating on a T-75 flask with an additional 13ml of growth media. The T-75 flask containing the cells was then stored in normal cell culture conditions at 37^{o}C with 5% CO_2 within an incubator (Panasonic). Growth media was changed routinely, and cells were passaged after becoming 90-100% confluent. A549 cells were sub-cultured and when they reached 90% confluency they cryopreserved during early passages.

Cryopreservation of A549

To cryopreserve A549 cells, growth media containing 10% DMSO (Freezing media) was prepared on the day of use and cooled to 4^{o}C. DMSO was used to prevent cell damage or death through ice crystal formation during freezing. Cells were detached and pelleted as stated previously (see Thawing and Plating A549 cells). Pre-cooled freezing media was then added to the cell pellet such that 3.0 x 10^5 cell density per 1ml aliquot before transferring to

cryogenic storage vials (Grenier bio-one). Cryogenic storage vials were then transferred to a cryo freezing container (Nalgene™, Mr. Frosty™, Thermo Fisher Scientific) filled with 250ml 100% isopropyl alcohol (Thermo Fisher Scientific) and stored at -80°C until required.

Luciferase Assay

Materials

Appropriate mRNA targets were chosen using the miRWalk database. Subsequently LightSwitch™ GoClone® reporters, LightSwitch™ miRNA mimics, DharmaFECT® Duo transfection reagent and LightSwitch™ Luciferase Assay reagent were selected and obtained (Active Motif). On receipt, the LightSwitch™ GoClone® reporters, DharmaFECT® Duo transfection reagent and LightSwitch™ Luciferase Assay reagent were kept at -20°C until use, as per the manufacturer's instructions. MiRNA mimics (5nmol) were defrosted at room temperature before resuspension in 500µL of RNase-free water (10µM) for storage at -80°C, in aliquots of 20µL. Before use, miRNA mimics were defrosted at room temperature and diluted 1:4 in RNase free water to make a working concentration (2µM).

Table 23 - Example list of reagents for luciferase assay. All purchased from Active Motif.

Reagent	Example	Stock concentration	Working concentration
MicroRNA mimic of interest	hsa-let-7i-5p	10µM	2µM
Non-target miRNA mimic	Non-targeting miRNA mimic V1	10µM	2µM
Target reporter	hsa-let-7i-5p target reporter	30ng/µl	5ng/µl
Positive Control	LightSwitch™ Beta-actin 3'UTR	30ng/µl	5ng/µl
Negative Control	LightSwitch™ Random 3'UTR	30ng/µl	5ng/µl
Background Control	LightSwitch™ Background 3'UTR	30ng/µl	5ng/µl
GoClone 3'UTR Target reporter	IL13 GoClone® 3'UTR reporter	30ng/µl	5ng/µl

Experimental Setup

After the mRNA targets were selected from the differentially regulated miRNA found within the SCRUM study the luciferase assay was used to quantify whether these interactions were reproducible in vitro. Experiments were run jointly with miRNA mimic and miRNA of interest to assess target miRNA interaction. Controls used included Beta-actin (housekeeping gene), random reporter vector (Negative control) and Empty 3'UTR vector (positive control). A target reporter gene for the miRNA of interest was then used to assess the endogenous level of miRNA and a target of interest to see if it interacts.

pLightSwitch_3UTR reporter vector

The RenSP luciferase reporter vector was used for all assays (Figure 30) (Active Motif). The reporter vector contains a promoter region, optimised RenSP luciferase gene, poly A region

and a target of interest e.g. IL13. Target reporter genes were present in the 3'UTR region to understand whether miRNA mimics block their action in this region where they commonly elicit their actions.

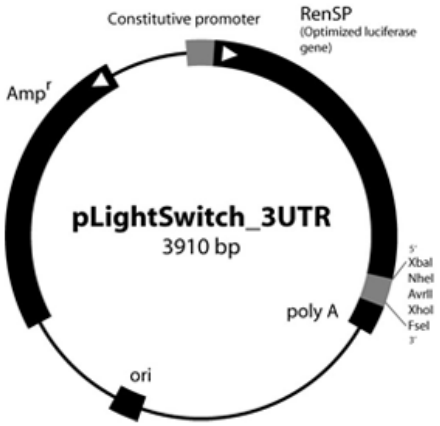

Figure 30 - RenSP luciferase reporter vector – Showing the constitutive promoter upstream of the optimised luciferase gene as well as the 3'UTR region with the target of interest. (https://switchgeargenomics.com/resources/science-technology)

Cell preparation

Cells were grown up as per the methodology stated previously (Figure 29). Once enough cells were grown up, they were re-suspended in growth media at 15,000 cells/well and plated on a 96-well plate (Grenier).

Transfection

Between 24-48 hours later the A549 cells were 90-100% confluent verified using an Eclipse TS100 inverted microscope (Nikon), at this stage the growth media was removed. A miRNA mimic, target reporter and serum free media (100% DMEM) mixture was prepared for each GoClone reporter. The DharmaFECT Duo mixture – the transfection reagent – was prepared with serum free media and allowed to incubate for 5 minutes before mixing with the GoClone reporter mixture. The DharmaFECT duo and GoClone reporter mixture was allowed to

incubate for a further 20 minutes before the addition of 400µl of antibiotic free growth media (DMEM + 10% FBS). Aliquots of 100µl from this mixture were added to each well containing only cells and allowed to incubate at 37°C for 24h hours.

Luminescence

After 24 hours fresh LightSwitch™ luciferase assay reagent was added to each well, which after a 30-minute incubation in a light protected setting was read on a luminometer (PHERAstar). Each well was measured for one second using the LUM plus optic.

Results were then normalised using the manufactures guidance and statistical analysis was run using an independent T-test in IBM SPSS Software.

Normalisation

$$\text{Control 1 miRNA mimic ratio (Repeat for all controls)} = \frac{\text{Control 1 miRNA mimic}}{\text{Control 1 average}}$$

$$\text{Average control ratio } = (\text{All controls miRNA mimic ratio})/\text{n}$$

$$\text{Target miRNA normalised data} = \text{ miRNA mimic result/ Average ratio}$$

Equation 2 – Normalisation method used from Active motif – To equate the luciferase assay data this normalisation method was used for all samples. This is an example using miRNA mimic and this must be repeated for the target miRNA.

Statistical analysis

An independent t test was used to compare means between groups.

SPSS was used for all statistical testing with GraphPad Prism used for data visualisation.

Results

MicroRNA selection

Two miRNAs were chosen in the first instance based on phase I of experiments. These were hsa-miR-143-3p and hsa-miR-135b-5p, which were the most significant following this phase I. Both were differentially regulated at the final analysis step. Hsa-let-7i-5p was selected based on previous data but SCRUM data has been shown below.

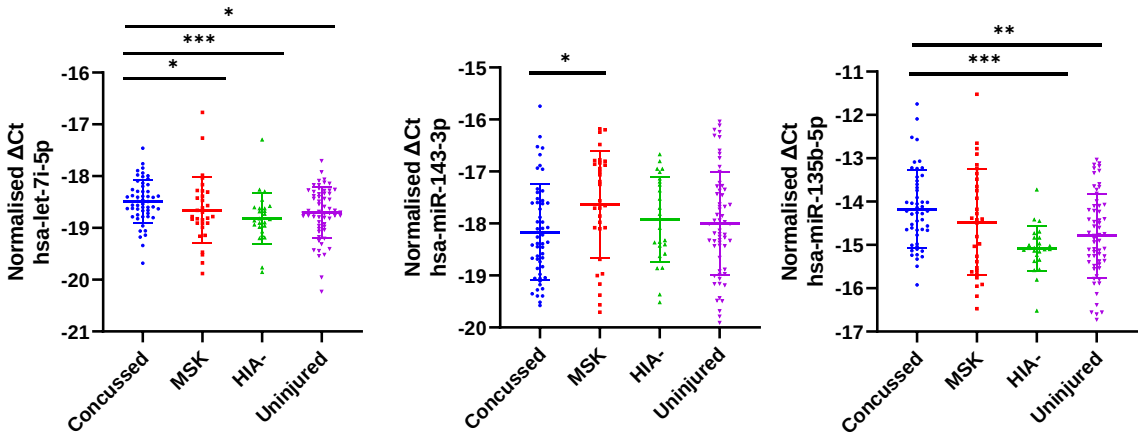

Figure 31 - Showing an interleaved scatter plot of differentially expressed concussion related miRNAs against other groups at time point b. (Left) hsa-let-7i-5p. (Middle) hsa-miR-143-3p. (Right) hsa-miR-135b-5p were used for luciferase analysis. The graph shows mean±SD. Mann-Whitney U test was used to compute statistical analysis between groups of pairs with *p<0.05, **p<0.01 and ***p<0.001.

All data shown was at time point b. Hsa-let-7i-5p was significant against all control groups. Hsa-miR-143-3p was only significant against MSK, which makes it unclear what it is signalling but it is not specifically concussion. Hsa-miR-135b-5p was significant against both HIA- and uninjured but not MSK at time point b and is likely to be a trauma marker, which may be enhanced during concussion.

The miRNA hsa-miR-143-3p was significantly different at the baseline time point (Figure 32). This change may mean individuals are a risk of concussion-based injuries in the future as stated in previous chapters.

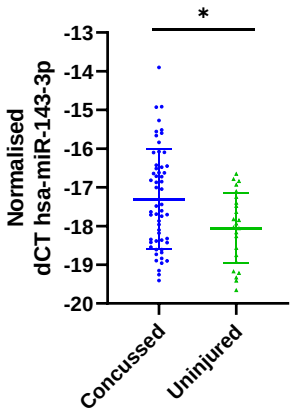

Figure 32 – Showing an interleaved scatter plot the statistically significant difference between hsa-miR-143-3p in baseline concussed against baseline uninjured. Hsa-miR-143-3p was used for in vitro analysis. The graph shows mean±SD. A Mann-Whitney U test was used to compare means between both groups with *p<0.05, **p<0.01 and ***p<0.001.

Target selection

The miRWalk database – most appropriate at the time – was used to select the mRNA targets to be tested for using the luciferase assay [152]. The selection process limits the number of mRNAs down from ~2,500 to around 30. After this, targets were chosen based on strength of potential interaction (maximum), no previous in vitro evidence of an interaction and a perceived biologically relevant pathway from existing concussion-based knowledge.

Table 24 - Selected mRNA targets for each differentially regulated miRNA. These were selected using MiRWalk.

MicroRNA	Selected mRNA targets
hsa-let-7i-5p	IL13, GAN, PPP1R15B and CASP3
hsa-miR-143-3p	PHF6, HTR2A, AP2B1, NRG1, TARDBP and PROSC
hsa-miR-135b-5p	GNG7, CACNA1D and SSR1

hsa-let-7i-5p interaction with mRNAs

This experiment was to establish if hsa-let-7i-5p interacted with IL13

IL13

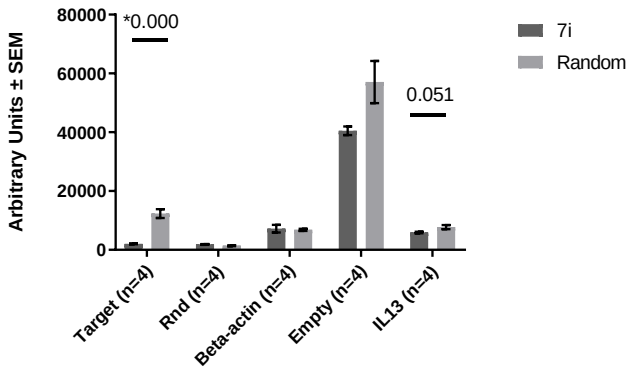

Figure 33 – Boxplot showing relative luminescence results not demonstrating an interaction between hsa-let-7i-5p and target IL13. An independent t-test was used for statistical analysis with a p-value of less than 0.05 considered significant.

The luciferase assay was run on for the interaction of hsa-let-7i-5p and IL13. There was no significant difference found even though there was a clear difference on the Let-7i target vector this was not present with IL13 although it reached close to significance (p=0.051).

GAN, PPP1R15B and CASP3

This experiment was to establish if hsa-let-7i-5p interacted with GAN, PPP1R15B and CASP3.

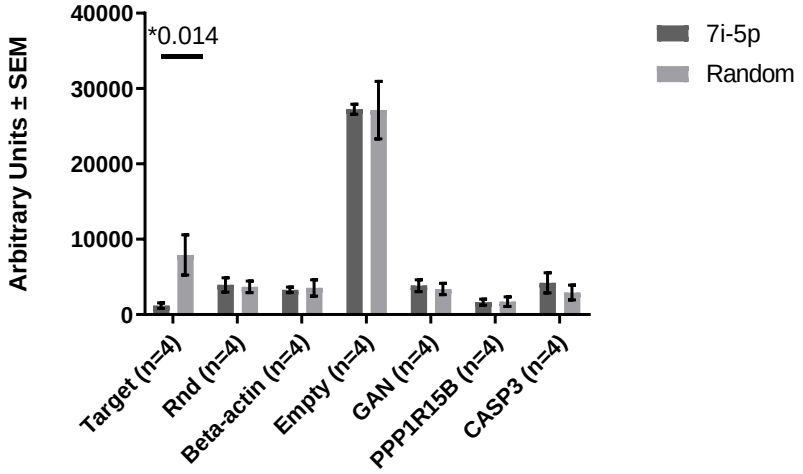

Figure 34 – Boxplot showing relative luminescence results indicating no interaction between hsa-let-7i-5p and potential targets GAN, PPP1R15B and CASP3. An independent t-test was used for statistical analysis with a p-value of less than 0.05 considered significant.

No significant differences were found between the control groups. There was a significant difference between the target reporter gene as expected. There were no significant interactions were found between hsa-let-7i-5p and GAN, PPP1R15B and CASP3, which can be interpreted as no interaction due to the experimental controls working.

hsa-miR-143-3p interaction with mRNAs

PHF6 and HRT2A

This experiment was to establish if hsa-miR-144-3p interacted with HRT2A or PHF6

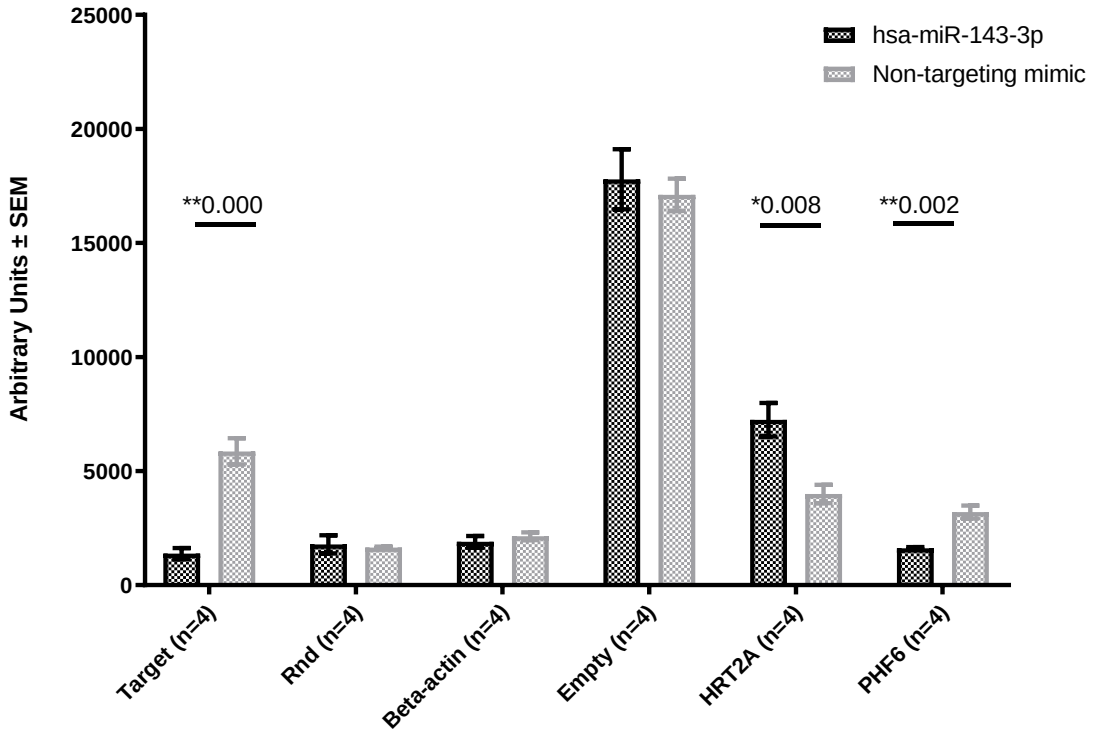

Figure 35 - Boxplot showing the relative luminescence results indicating an interaction of miR-143-3p and PHF6 but not HRT2A. An independent t-test was used for statistical analysis with a p-value of less than 0.05 considered significant.

The luciferase assay showed no difference between control values. There was a significant difference between the target gene, which was expected (p=0.000). This was replicated in the PHF6 gene therefore showing a significant interaction (p=0.002) (Figure 35). PHF6 is likely to be a target of hsa-miR-143-3p. This interaction was not witnessed with HRT2A. The significant value was put down to being an artefact of the normalisation methodology used.

TARDBP, PROSC, AP2B1 and NRG1

This experiment was to establish if hsa-miR-144-3p interacted with TARDBP, PROSC, AP2B1 or NRG1.

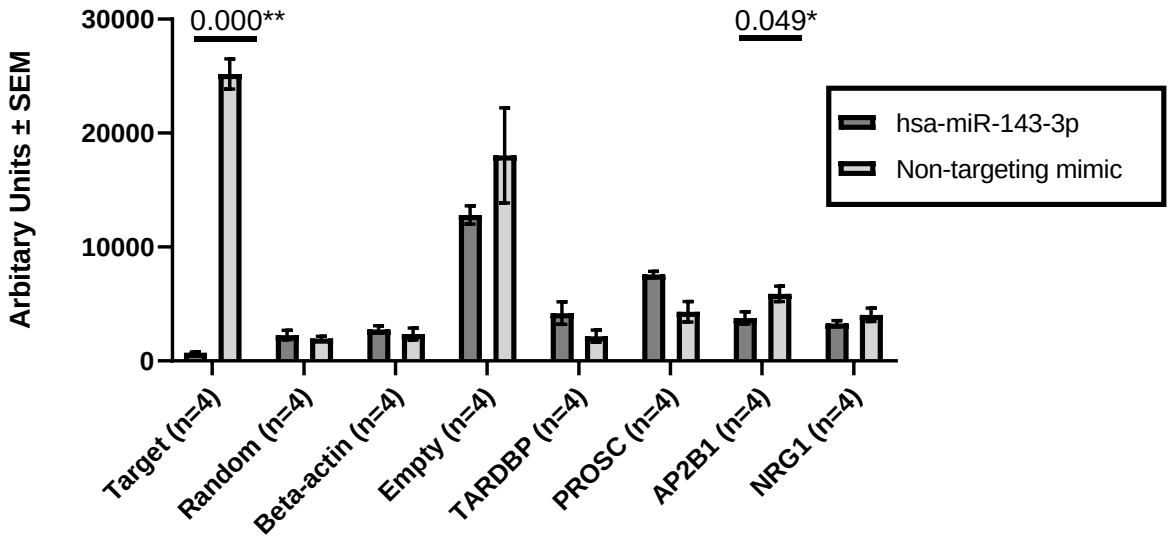

Figure 36 – Boxplot showing the relative luminescence results indicating a potential interaction of hsa-miR-143-3p and AP2B1 but not TARDBP, PROSC and NRG1. An independent t-test was used for statistical analysis with a p-value of less than 0.05 considered significant.

There was no significant difference between the three control groups. There was a significant interaction with the target mRNA as expected. TARDBP, PROSC and NRG1 were not significantly different between the groups. AP2B1 was significantly different between the two groups (p=0.049). As a result, it can be considered a target of hsa-miR-143-3p.

hsa-miR-135b-5p interaction with mRNA targets

GNG7, CACNA1D and SSR1

This experiment was to establish if hsa-miR-144-3p interacted with GNG7, CACNA1D or SSR1.

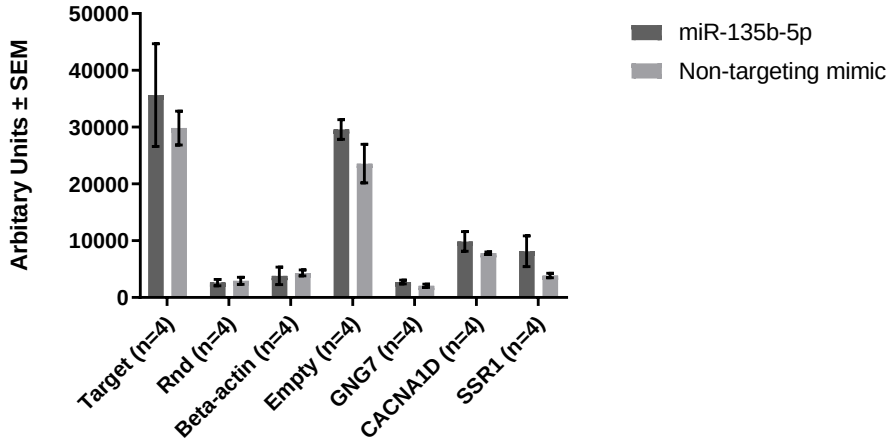

Figure 37 – Boxplot showing the relative luminescence results demonstrating inaccurate controls. No conclusion could be made of an interaction between hsa-miR-135b-5p and GNG7, CACNA1D and SSR1. An independent t-test was used for statistical analysis with a p-value of less than 0.05 considered significant.

No significant difference was found between the interaction of non-targeting miRNA or miR-135b-5p with the miR-135b-5p specific target. This meant that the results are not representative as to what was set out to be achieved so it will be re-run. This could be due to the A549 cells have endogenous levels of miR-135b-5p so this will be repeated followed by a repeat in a different cell line if the results are the same.

Discussion

As previously discussed, the potential in vitro interactions of concussion based salivary miRNAs were investigated. The selection of miRNAs was done prior to conclusion of the study – owing to the timescale of the project – and therefore a mixed selection of miRNAs was chosen. Although not necessarily having a defined role in concussion they are still relevant and may be useful in the development of the scientific field.

Unfulfilled role of hsa-miR-135b-5p

Multiple repeats of this experimentation demonstrated an inadequate experimental setup. So, no conclusions could be drawn on the in vitro interactions of this particular miRNA. In future a new cell line will be utilised to assess whether a different experimental set up with less control variation may produce valid results.

Role of hsa-let-7i-5p

The role of hsa-let-7i-5p is involved in the saliva after concussion-based injury as demonstrated in the first chapter. This study did not reveal any further in vitro involvement of hsa-let-7i-5p and only demonstrated three potential targets that do not have a significant interaction. With more time more targets for hsa-let-7i-5p would have been investigated.

Role of hsa-miR-143-3p

In the saliva of concussed patients' post-injury, there does not seem to be a specific response of hsa-miR-143-3p. However, there was evidence in the baseline analysis that there may be longer-term changes of this miRNA that may pre-dispose concussion-based injuries.

With HRT2A

The change witnessed here was significant however it opposed the expected change. As a result, it was excluded and considered an artefact of the normalisation method due to differences between the control groups. There is some evidence that miRNAs can be positive regulators of gene expression [153], however this assay is not designed for assessment of these parameter so this cannot be concluded.

With PHF6

There was a significant interaction between hsa-miR-143-3p and PHF6 in vitro that demonstrates an increase in hsa-miR-143-3p may cause a decrease in PHF6 expression. The precise function of PHF6 still remains elusive. Its most established role is within Borjeson-Forssman-Lehmann intellectual disability syndrome (BFLS) where a germline mutation causes this neurodevelopment syndrome, which demonstrates its importance as a neurological protein [154].

Other mechanistic studies show a transcriptional function for PHF6 as it interacts with both RNA polymerase II associated factor 1 (PAF1) to impact transcriptional elongation of gene targets and ribosomal proteins that can affect ribosome biosynthesis. These interactions can influence neuronal migration as well as dendritic maintenance, respectively [155, 156]. This shows how hsa-miR-143-3p may influence gene expression in a neuronal setting and through these ribosome defects may demonstrate early stages of neurodegenerative disease in sub-groups of patients [157].

PHF6 has other links to neurodegenerative diseases, as it has a genomic location within the microtubule binding region of both three-repeat (3R) and four-repeat (4R) Tau gene isoforms on chromosome X, exon 10. Within neurodegenerative diseases such as Alzheimer's disease (AD) the tauopathies that exist come from 6 different isoforms of Tau, and PHF6 exists within all [158, 159]. PHF6 has been shown to be a key nucleating sequence in the formation of tau aggregates [160]. So hsa-miR-143-3p, linked with higher ‘risk’ of concussion, can modulate PHF6 activity and could be implicated in the causation or protection in development of tauopathy based neurodegenerative disease such as Alzheimer’s disease (AD) and chronic

traumatic encephalopathy (CTE). Currently, little is known about this link so future studies must focus on establishing whether these links hold truth in a human environment.

With AP2B1

Another interaction was found between hsa-miR-143-3p and AP2B1 in vitro, which demonstrates that hsa-miR-143-3p may modulate AP2B1 expression. AP2B1 is part of the adaptor protein complex 2 (AP-2) that is concentrated at synapses for clathrin-dependent endocytosis, which transports cargo proteins into vesicles surrounded by clathrin [161]. This process is considered important in neuronal synaptic vesicle recycling with AP-2 involved in the formation of clathrin coating [162]. This may indicate synaptic importance however AP2B1 has shown potential involvement in more far-reaching applications.

AP2B1 levels are altered when compared to control in both Parkinson's disease (PD) and AD [163]. Another study an association of ADAM10 and AP2 was increased in the hippocampi of AD patients. With long term potentiation in hippocampal neuronal cultures causing ADAM10 endocytosis through AP2 to decrease the expression of ADAM10. Whereas long term depression cultures promoted synaptic membrane insertion of ADAM10 [164]. This demonstrates one potential impact of AP2, thereby AP2B1, on synaptic membrane function and how hsa-miR-143-3p may be able to modulate this balance and cause long-term depressive states or neurodegenerative disease.

However, the limitations of this technique are it does not take into consideration the dynamics of human homeostasis so within humans these interactions may be prevented in some way.

The bioinformatics tools to find potential targets is the most challenging part to achieving success with this technique. There are numerous tools with varying levels of complexity upon

nearing the end of my PhD I found a new tool MiRDip that combined numerous databases to produce a weighted value based on that. I would suggest future users use a tool such as that if it is up to date.

Specifically, if I were to do this section again, I would choose multiple targets from a defined pathway to give direction to my findings. The scope of this project was so open, giving structure points like this would allow interpretation to become simpler.

Overall

Overall, there have been two targets found for hsa-miR-143-3p in this in vitro environment. The implication of this targets is currently unclear due to the differential expression being present in the saliva of concussed athletes. However, it does raise questions as to whether this signalling could be indicative of concussion-based response or long-term neurodegenerative response in some individuals. This must be investigated further in future.

Future work

Investigation of in vitro targets for differentially expressed miRNAs across all groups. At time point b that would be hsa-let-7a-5p and hsa-let-7i-5p while at time point c that would be hsa-let-7f-5p and hsa-miR-144-3p. Attempt to find in vitro evidence of pathways responding during concussion.

Chapter 5: The potential involvement of concussion injury microRNAs in Alzheimer's disease: implications for future management methods

Rationale

Currently, whether there is a link between head trauma and Neurodegenerative disease is unclear and so there is a requirement for more information. In the previous chapters, differentially regulated miRNAs have been found in the saliva of concussed patients. Understanding whether there were differentially regulated miRNAs in common between both would begin to unpick whether these miRNAs may have neurological consequences.

A miRNA found to be differentially regulated in the saliva of concussed athletes (hsa-miR-143-3p) was found to interact with PHF6. PHF6 is a plant homeodomain-like finger family protein that lies within the tau gene and has a role in tau aggregate formation during AD. This was investigated further to establish if this miRNA opposed the correlation of the PHF6 expression, to implicate its involvement in the disease.

Aims

- To establish if any SCRUM related miRNAs are present in the development of Alzheimer's disease
- Understand the dynamics of miRNA signalling during Alzheimer's disease
- To establish if PHF6 and hsa-miR-143-3p interact during Alzheimer's disease
- Proteomic analysis of AD samples was planned but could not be finished due to COVID-19

Statement of Contribution

Dr Ghazala Begum and I completed all experimentation. I completed all data normalisation and data analysis after statistical guidance from Dr Animesh Acharjee. Dr Valentina Di Pietro supported and guided throughout.

Methods

Samples

Ethics

Samples were obtained from the South West Dementia Brain Bank (SWDBB). We would like to thank the South West Dementia Brain Bank (SWDBB) for providing brain tissue for this study. The SWDBB is part of the Brains for Dementia Research programme, jointly funded by Alzheimer's Research UK and Alzheimer's Society and is supported by BRACE (Bristol Research into Alzheimer's and Care of the Elderly) and the Medical Research Council.

Brain samples comprised of 100mg frozen temporal cortex samples split into groups based on Braak tangle stage to give; no AD (I-II) (BBN_9359, BBN_9422, BBN_24337, BBN_24561 and BBN006.31516), early stage AD (III-IV) (BBN_8871, BBN_9050, BBN_9343, BBN_4215 and BBN006.26344) and late stage AD (V-VI) (BBN006.26447, BBN006.27017, BBN_9293, BBN_9401 and BBN_9421). The demographics of the samples can be seen in Table 25.

Table 25 - Demographics of samples received from South West Dementia Brain Bank

Group	Braak Stage	Average Age ± SD	Average PM delay ± SD
No AD	I-II	85.4±9.2	49.7±11.8
Early stage AD	III-IV	82±4.5	35.8±20.2
Late stage AD	V-VI	84±6.8	43.25±17.68

Storage

Samples sent on dry ice from the SWDBB and upon receipt they were stored at -80^{o}C until use.

Homogenisation

Samples were homogenised for 30 seconds using a TissueRuptor II (Qiagen) in RNase free PBS (ThermoFisher Scientific).

RNA preparation and qPCR reaction

RNA was extracted from the homogenised samples using the miRNeasy Mini Kit (Qiagen) by following the manufacturer's protocol. The RNA concentration was measured on a nanophotometer (IMPLEN). RNA (100ng) was converted to cDNA using the miRCURY LNA kit (Qiagen) in a 50ul reaction.

20ul (40ng) of cDNA was mixed with a SYBR master-mix to a total of 4000ul (Table 26). 10ul (0.1ng of RNA) of this mixture was added to each well of the miRCURY LNA miRNA miRNome Panel I-II using the QIAgility (Qiagen) for the final reaction. These were run using qPCR cycles shown in

Table 27 upon the Quantstudio 5 qPCR machine (ThermoFisher Scientific).

Table 26 - Components of qPCR reaction mix (Qiagen)

Component	Volume of component
miRCURY SYBR Green Master Mix	2000ul
ROX reference dye	20ul
cDNA template	20ul
RNase-free water	1960ul
Total reaction volume	4000ul

Table 27 - Cycling conditions for qPCR reaction using the Quantstudio 5 (ThermoFisher Scientific)

Step	Time	Temperature	Ramp Rate
PCR initial heat activation	2 min	95°C	Maximal/Fast mode
2-step cycling			
Denaturation	10s	95°C	Maximal/Fast mode
Combined annealing/extension	60s	56°C	Maximal/Fast mode
Number of cycles	40		
Melting curve analysis	60-95°C		

Protein preparation

Protein was extracted using the instructions of manufacturer's ELISA kit. These were then frozen with a protease inhibitor before analysis using ELISA kits(PHF6 ELISA, Wuhan Fine Biotech).

A BCA protein assay (Pierce, Thermo Fisher) was used to quantify the protein concentration after extraction with a standard curve. A linear regression line was used to make a standard curve to establish protein concentrations. Measurements were taken using a Tecan Infinite 200 Pro (Tecan).

An equal amount of protein was then added to the ELISA assay through prior dilution using RNase free water (Qiagen) as a diluent. The manufacturer's protocol was followed for ELISAs.

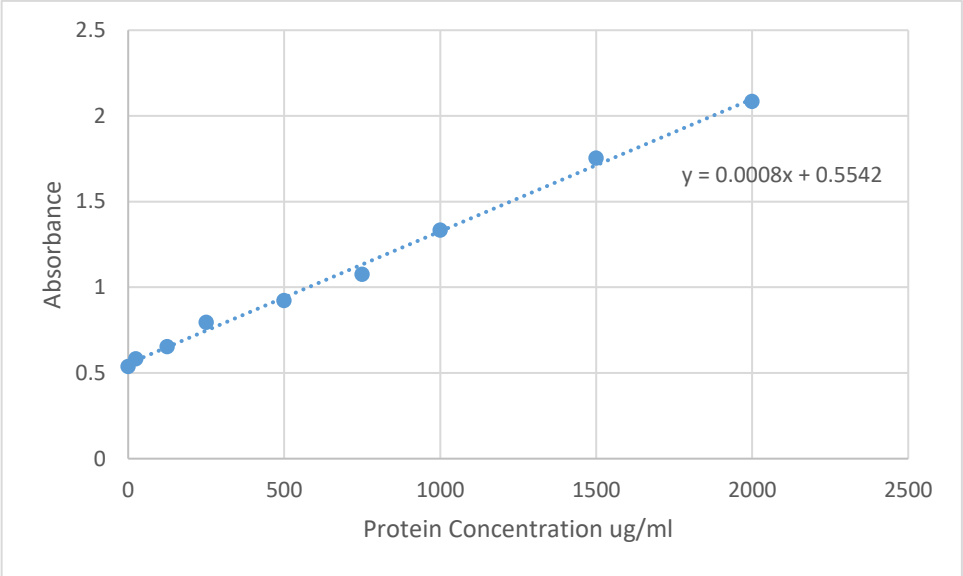

Figure 38 – BCA assay standard curve which was used to calculate the concentration of extracted Alzheimer's disease samples

Data Analysis

RNA

The Ct value was taken for each miRNA. The threshold was set by the Design and Analysis Software V1.5.1 (ThermoFisher).

Normalisation

NormFinder was used to find the most stable pair of miRNAs (Table 28) [165]. The most stable combined miRNA pair was hsa-miR-99a-5p and hsa-miR-361-5p. They were used as housekeeping genes (HK) across all samples.

Table 28 - Ten most stable pairs of miRNA stabilising genes. The more stable a pair of genes the lower the stability value. As a result, hsa-miR-99a-5p and hsa-miR-361-5p were used as housekeeping genes. These were found using NormFinder.

Number	Gene1	Gene2	Stability
4005	hsa-miR-99a-5p	hsa-miR-361-5p	0.05
13907	hsa-miR-361-5p	hsa-miR-30c-1-3	0.05
523	hsa-miR-140-5p	hsa-miR-99a-5p	0.06
568	hsa-miR-140-5p	hsa-miR-361-5p	0.06
4006	hsa-miR-99a-5p	hsa-miR-125b-5p	0.06
4037	hsa-miR-99a-5p	hsa-miR-215-5p	0.06
4051	hsa-miR-99a-5p	hsa-miR-30e-3p	0.06
4068	hsa-miR-99a-5p	hsa-miR-192-5p	0.06
4070	hsa-miR-99a-5p	hsa-miR-197-3p	0.06
4096	hsa-miR-99a-5p	hsa-miR-425-3p	0.06

All miRNAs were normalised to the housekeeping genes (HK) using Equation 3 before further analysis was carried out.

$$Normalised\ \Delta Cq\ value = -\left(\left(\left(\frac{HK1 + HK2}{2}\right) - miRNA\ Ct\ value\ of\ interest\right) + 20\right)$$

Equation 3 – Normalisation methodology to produce normalised ΔCq value.

Data handling

751 miRNAs were tested for analysis using mirnome plates. MiRNAs were not considered if they had one or more missing values across the 15 participant samples as the small sample size could not account for the variation. This left a total of 620 miRNAs for analysis.

Statistical analysis

Normalised ΔCq values were tested for normality and found to not be normally distributed using the Shapiro-Wilk test. Two different analysis were then carried out:

1. Normalised ΔCq were used to perform a Kruskal-Wallis test to compare ranks to establish if there was a difference across all three groups. (Control, Braak III-IV and Braak V-VI)
2. Normalised ΔCq were used to perform Mann-Whitney U tests to compare means of paired groups (Control vs. Braak III-IV, Control vs. Braak V-VI and Braak III-IV vs. Braak V-VI). MiRNAs with a p-value <0.1 using the Kruskal-Wallis test were checked for differences within particular groups using a Mann-Whitney U test.

To check for variability across different groups Principal Component Analysis (PCA) and heat map analysis were both performed.

Protein

A standard curve from ELISA kit was used. A sigmoidal curve was plotted to interpolate the points of the curve and calculate the PHF6 protein concentration.

Statistical analysis

All data was tested for normality using the Shapiro-Wilk test. Following this, two analyses were carried out:

1. Firstly, a Kruskal-Wallis analysis was used to compare across three groups (Control, Braak Stage III-IV and Braak Stage V-VI).
2. Secondly by Mann-Whitney U analysis between paired groups (Control-Braak Stage III-IV, Control-Braak Stage V-VI and Braak Stage III-IV-Braak Stage V-VI).

Simple linear correlation was used to compute correlations.

Downstream analysis

Diana Tools mirPath V.3

Diana tools mirPath v.3 was used for all downstream analysis. The DIANA-microT-CDS algorithm with a set threshold of 0.8 was used to select mRNA targets on the gene union tool. The final p-value was corrected for with FDR. A p-value of less than 0.05 was considered significant

MirDip

This tool was used to establish the viability of an interaction. The unidirectional search tool was used for analysis.

Results

MicroRNA analysis

This experiment was to establish if there were significantly associated miRNAs with Alzheimer's disease progression and whether any of these miRNAs crossed over with those present in concussion.

Differences across all groups

Kruskall-Wallis statistical testing was used to establish the miRNAs that differ across the groups. There were 52 differentially regulated miRNAs found (Table 29). The most significant of these findings was hsa-miR-185-3p (p=0.0045). This demonstrates there are numerous differentially regulated miRNAs that need to be investigated further.

Table 29 – Showing statistically significant microRNAs across Control, Braak Stage III-IV and Braak stage V-VI groups. Kruskall-Wallis analysis was carried out with a value of less than 0.05 considered significant.

MiRNA	Control Average	Control SD	Braak III-IV Average	Braak III-IV SD	Braak V-VI Average	Braak V-VI SD	Chi-squared	Kruskal Wallis P-value
hsa-miR-185-3p	-12.299	0.580	-11.811	0.167	-11.016	0.531	10.82	0.0045
hsa-miR-425-5p	-18.375	0.358	-18.040	0.112	-17.648	0.224	10.64	0.0049
hsa-miR-425-3p	-15.665	0.204	-15.518	0.154	-15.060	0.146	9.5	0.0087
hsa-miR-204-5p	-18.876	0.412	-19.457	0.107	-19.582	0.270	9.42	0.0090
hsa-miR-1539	-9.397	0.679	-8.839	0.594	-7.740	0.754	9.38	0.0092
hsa-miR-212-3p	-14.020	0.494	-13.403	0.242	-12.402	0.582	8.88	0.0118
hsa-miR-1244	-9.548	0.461	-8.968	0.259	-8.450	0.400	8.88	0.0118
hsa-miR-542-5p	-11.918	0.498	-11.050	0.302	-10.390	0.738	8.88	0.0118
hsa-miR-671-5p	-13.965	0.259	-13.338	0.329	-12.948	0.489	8.78	0.0124
hsa-let-7i-5p	-20.460	0.365	-20.297	0.099	-19.745	0.522	8.64	0.0133
hsa-miR-185-5p	-19.132	0.553	-18.829	0.139	-18.490	0.105	8.64	0.0133
hsa-miR-887-3p	-14.129	0.221	-14.435	0.178	-13.804	0.251	8.42	0.0148
hsa-miR-582-3p	-12.900	0.381	-12.427	0.116	-12.192	0.133	8.42	0.0148
hsa-miR-503-5p	-12.614	0.698	-11.962	0.381	-10.940	0.916	8.24	0.0162
hsa-miR-622	-7.989	0.748	-7.591	0.776	-6.352	0.750	8.24	0.0162
hsa-miR-920	-10.512	0.622	-9.377	1.087	-7.930	0.874	8	0.0183
hsa-miR-484	-17.025	0.472	-16.733	0.143	-16.407	0.173	7.98	0.0185
hsa-miR-219a-1-3p	-8.985	0.420	-8.586	0.425	-7.850	0.471	7.98	0.0185
hsa-miR-146b-5p	-18.132	1.377	-17.068	0.259	-16.809	0.277	7.74	0.0209
hsa-miR-636	-9.781	0.398	-8.271	0.562	-7.787	1.250	7.58	0.0226
hsa-miR-93-5p	-18.485	0.707	-18.409	0.194	-18.020	0.063	7.28	0.0263
hsa-miR-877-5p	-13.347	0.242	-13.301	0.171	-12.751	0.237	7.28	0.0263
hsa-miR-431-5p	-12.251	0.245	-11.502	0.491	-11.342	0.321	7.28	0.0263
hsa-miR-148b-3p	-18.173	0.021	-18.024	0.326	-17.743	0.465	7.22	0.0271
hsa-miR-22-5p	-16.141	0.183	-15.806	0.154	-15.166	1.200	7.22	0.0271
hsa-miR-760	-12.714	0.296	-12.940	0.253	-12.253	0.341	6.98	0.0305

hsa-miR-642a-5p	-11.216	0.640	-12.830	0.936	-11.776	0.315	6.98	0.0305
hsa-miR-518a-3p	-7.288	1.729	-6.881	1.703	-9.588	0.860	6.86	0.0324
hsa-miR-132-3p	-19.045	0.444	-18.498	0.098	-17.838	0.541	6.86	0.0324
hsa-miR-34c-3p	-16.999	1.128	-16.105	0.642	-15.517	0.577	6.86	0.0324
hsa-miR-30e-5p	-19.856	0.146	-19.483	0.285	-19.453	0.151	6.74	0.0344
hsa-miR-1237-3p	-13.082	0.643	-12.609	0.558	-11.950	0.372	6.72	0.0347
hsa-miR-30b-3p	-11.423	0.281	-10.763	0.698	-10.660	0.244	6.72	0.0347
hsa-miR-874-3p	-18.493	0.705	-18.691	0.120	-18.089	0.575	6.62	0.0365
hsa-miR-106b-5p	-18.469	0.296	-18.455	0.272	-17.979	0.232	6.62	0.0365
hsa-miR-140-5p	-17.542	0.094	-17.608	0.293	-17.233	0.140	6.62	0.0365
hsa-miR-146b-3p	-12.144	1.351	-10.917	0.436	-10.889	0.248	6.62	0.0365
hsa-miR-132-5p	-15.841	0.784	-15.339	0.195	-14.600	0.476	6.54	0.0380
hsa-miR-98-5p	-18.492	0.695	-18.603	0.067	-18.230	0.232	6.5	0.0388
hsa-let-7a-5p	-22.711	0.488	-22.933	0.076	-22.587	0.087	6.32	0.0424
hsa-miR-30c-1-3p	-11.910	0.263	-11.586	0.217	-11.475	0.162	6.32	0.0424
hsa-let-7e-5p	-20.470	0.481	-20.739	0.230	-20.229	0.134	6.26	0.0437
hsa-miR-665	-15.301	0.609	-14.822	0.757	-13.934	0.336	6.26	0.0437
hsa-miR-450a-5p	-13.389	0.559	-12.484	0.180	-12.182	0.645	6.26	0.0437
hsa-miR-671-3p	-12.919	0.258	-12.585	0.326	-12.334	0.228	6.26	0.0437
hsa-miR-210-3p	-16.256	0.796	-15.884	0.081	-15.325	0.384	6.18	0.0455
hsa-miR-212-5p	-12.437	0.889	-11.907	0.222	-10.931	0.583	6.14	0.0464
hsa-miR-494-3p	-13.956	0.245	-13.291	0.412	-13.628	0.327	6.14	0.0464
hsa-miR-106a-5p	-18.441	0.789	-18.684	0.322	-18.238	0.070	6.02	0.0493
hsa-let-7d-5p	-19.812	0.554	-19.982	0.150	-19.573	0.160	6.02	0.0493
hsa-miR-181a-5p	-21.047	0.295	-21.575	0.457	-20.871	0.227	6.02	0.0493
hsa-miR-602	-10.311	0.468	-10.039	0.399	-9.413	0.512	6.02	0.0493

Cluster differentiation

Principal Component Analysis

Using the 52 statistically significant miRNAs (Kruskall-Wallis p-value of <0.05) PCA analysis was carried out to establish if differences between the group could be visualised using miRNAs. PCA cluster analysis shows a clear separation between Braak stage V-VI and both other groups. There is one sample that crosses over between control and Braak stage III-IV otherwise there is a closer relationship but still a clear change. The samples separate effectively, and they order in the staged groups they were allocated to (Figure 39). This demonstrates that with disease progression the greater miRNA changes are greater with Braak stage V-VI showing the largest alterations from control.

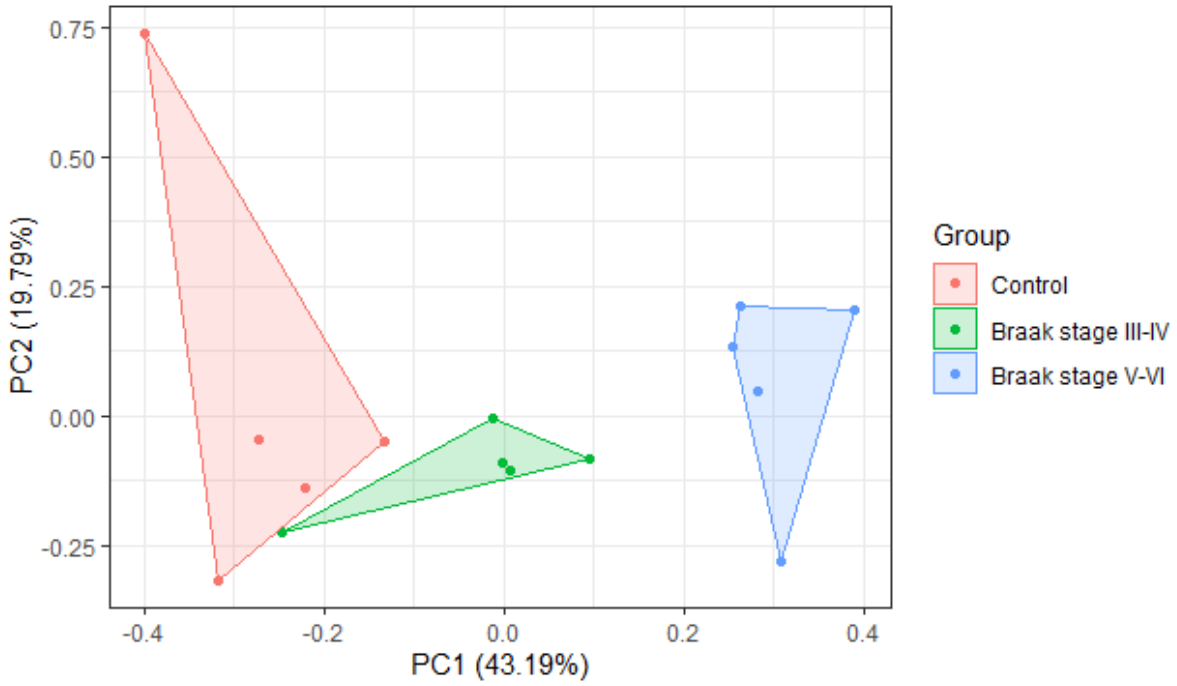

Figure 39 – Principle Component Analysis showing the clustering of Control, Braak III-IV and Braak V-VI. The fifty-two significant microRNAs found using Kruskal-Wallis analysis were used to produce this PCA plot. A p-value of less than 0.05 was considered significant. There was separation between all groups. Produced by ggplot2 in R programming language.

These changes can also be visualised using a hierarchal clustered heatmap (Figure 40). There is a clear shift towards red in the Braak stage V-VI (group labelled blue) whereas the control group is majority blue with the Braak stage III-IV sharing differences with both sides airing closer to the control group. This is a visual representation showing that the majority of differentially expressed miRNAs are upregulated with development of the disease.

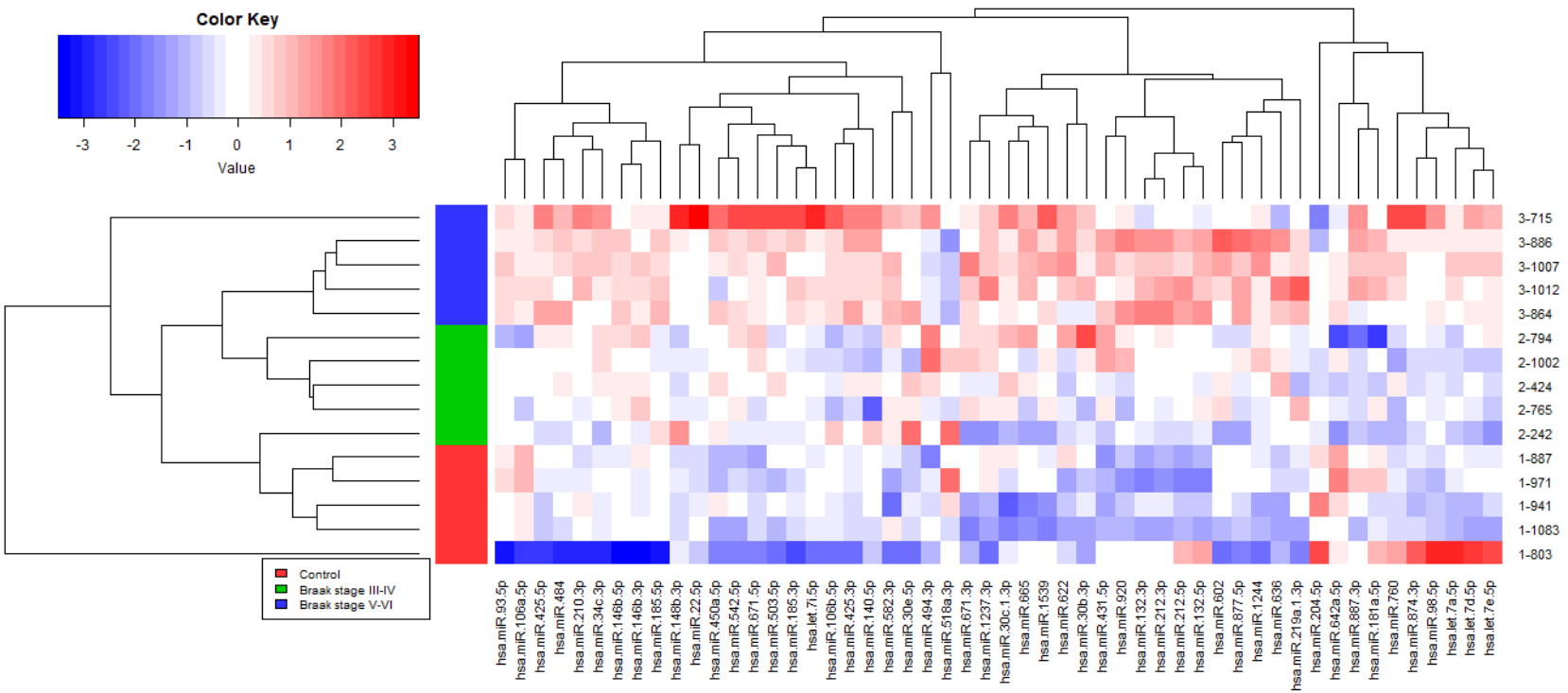

Figure 40- Heatmap showing the expression of 52 differentially regulated microRNAs in Alzheimer's disease. Fifty-two microRNAs were found using Kruskal-Wallis statistical analysis across all groups. A p-value of less than 0.05 was considered significant. Hierarchal clustering is present on the left with colours relevant to their group. This was made using heatmap.2 in the R programming language with complete linkage and Euclidean distance used to compute.

Differences between individual groups

To investigate the impact between individual groups Mann-Whitney testing was used to establish the miRNAs that were differentially expressed. Data for these results can be found in the supplementary materials.

Venn diagram

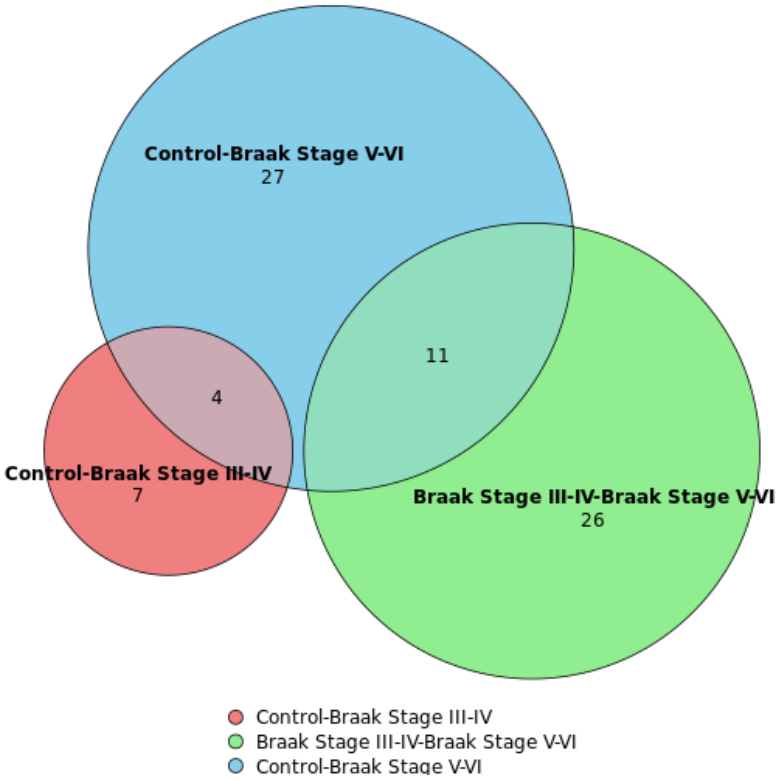

Figure 41 - Venn diagram that shows the crossover of microRNAs between each stage. Significant microRNAs were found using a Mann-Whitney U test to compare means between pairs as stated in the figure. A value was considered significant if $p<0.05$.

Most miRNAs differences were between Control-Braak stage V-VI (43 miRNAs), the two end groups. Cross-over was only seen when an end group was compared e.g. Braak V-VI or Control. There were 11 miRNAs that crossed over between Control-Braak stage V-VI and Control-Braak stage III-IV these miRNAs signal at a later stage in AD disease development. There were 4

miRNAs that could distinguish between control and both Braak stage III-IV and Braak stage V-VI these are earlier disease related markers.

There were no miRNAs that were differentially regulated across all groups, so not miRNA can distinguish all the separate groups. This is likely to be due to variation of Braak stage III-IV and the crossover with other groups. However, with more numbers this may have been achievable.

Potential biomarkers at early stages of AD development

All four of these miRNAs show a statistical change between control group and both groups of AD patients. The strongest response was hsa-miR-204-5p (Table 30). These are strong early-stage markers that may be able to separate stages of AD more effectively with greater numbers in the groups. The impact of the later stage was also assessed and is present in the supplementary materials.

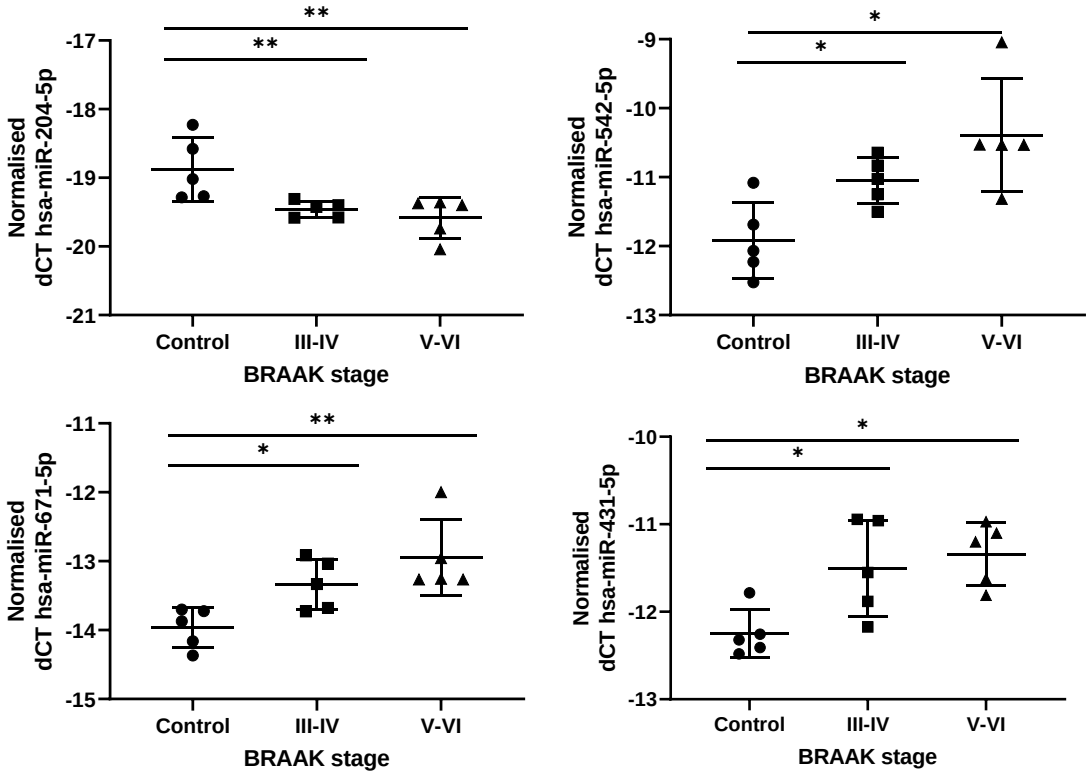

Figure 42 – Showing interleaved scatter plot of differentially expressed microRNAs between control and both Braak Stage III-IV and Braak Stage V-VI. A Mann-Whitney U test was used to compare mean differences between each individual groups e.g. Control vs. Braak stage III-IV, Control vs. Braak stage V-VI and Braak stage III-IV and Braak stage V-VI. P-values are represented using **<0.01, *<0.05. Graph shows Mean±SD.

Table 30 - P-values of microRNAs that were significantly different between control and both groups of Alzheimer's disease patients. These were calculated using a Mann-Whitney U test to compare means between paired groups. A value of less than 0.05 was considered significant.

	Control-Braak stage III-IV	Control-Braak stage V-VI
hsa-miR-204-5p	0.0079	0.0079
hsa-miR-542-5p	0.0317	0.0159
hsa-miR-671-5p	0.0317	0.0079
hsa-miR-431-5p	0.0317	0.0159

Let 7 Family Involvement

The Let-7 family has been routinely involved across the concussion group. There are multiple hsa-let-7 family members found to be differentially expressed (Figure 43) so they could hold an important function.

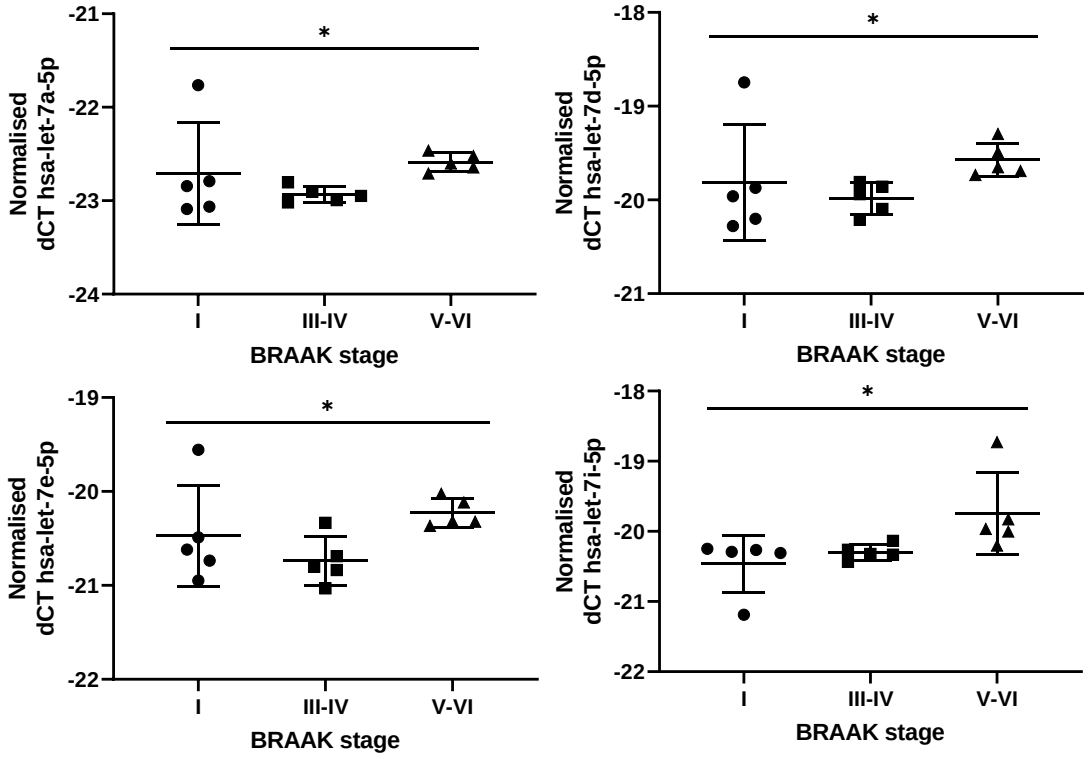

Figure 43 – Showing an interleaved scatter plot of differentially expressed Let 7 microRNA family in response to Alzheimer's disease. A Kruskal-Wallis test was used to compare rank differences across all groups. P-values are represented using **<0.01, *<0.05. Graph shows mean±SD.

Table 31 – Showing p-values of differentially expressed hsa-let-7 family members between individual groups during Alzheimer's disease. Significantly different microRNAs were calculated using a Mann-Whitney U test between individual sample groups. A significant p-value was considered if it was less than 0.05.

	Control-Braak stage III-IV	Control-Braak stage V-VI	Braak stage III-IV-Braak stage V-VI
hsa-let-7a-5p	0.8413	0.1508	0.0079

hsa-let-7d-5p	0.8413	0.1508	0.0079
hsa-let-7e-5p	0.4206	0.1508	0.0159
hsa-let-7i-5p	0.9999	0.0079	0.0159

There was a consistent significant difference between Braak stage III-IV and Braak stage V-VI across all four of these family members (hsa-let-7a-5p, hsa-let-7d-5p, hsa-let-7e-5p and hsa-let-7i-5p) (

Table 31). Both hsa-let-7a-5p and hsa-let-7d-5p show the largest changes between these groups (p=0.0079). Hsa-let-7i-5p was the only one able to distinguish between control and Braak stage V-VI (p=0.0079) however with larger n numbers others may gain significance.

Links to SCRUM study

Two miRNAs (hsa-let-7a-5p and hsa-let-7i-5p) were both upregulated in saliva of concussed patients at time point b of the SCRUM study. Both miRNAs are also upregulated in the brains of Braak stage V-VI patients, which demonstrates their importance to normal brain functioning. It is unclear if these are linked but it certainly needs further investigation as to the role of hsa-let-7a-5p and hsa-let-7i-5p immediately post-concussion to ensure this is a healthy short-term response that does not make patients more at risk of AD.

The miRNA hsa-let-7i-5p does show differential regulation at baseline compared to HIA- group so this should be checked to ensure that this is not differential signalling due to an 'at risk' group.

Downstream signalling

This experiment was to assess the bioinformatics involvement of miRNAs significantly associated with Alzheimer's disease progression.

Significantly associated miRNAs used to assess bioinformatics function

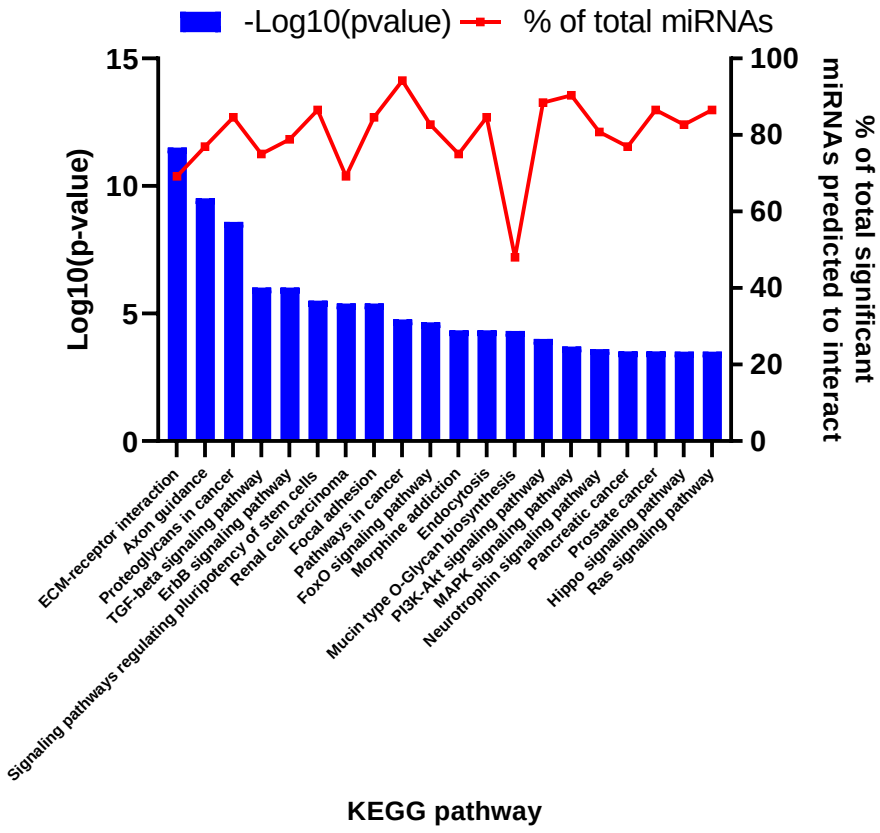

Figure 44 – Showing top 20 most significantly associated KEGG pathways. Using the 52 differentially regulated microRNAs in AD brain samples using Kruskal-Wallis statistical analysis these KEGG pathways were associated with use of the Diana Mirpath V.3 genes union tool with a target selection criteria of microT-CDS.

There were 57 differentially regulated KEGG pathways between control and Braak stage III-IV. The top 20 differentially regulated KEGG pathways are shown in Figure 44 with the strongest association being ECM-receptor interaction. Also, within the top 20 are TGF-beta signalling pathway, FoxO signalling pathway and hippo signalling pathway that all have links to Alzheimer's disease development showing the diverse role that these miRNAs are having.

Differences in signalling across individual groups

MicroRNAs that were differentially expressed between individual groups using the Mann-Whitney U test were used to establish downstream signalling within the different groups. As seen in Table 32 (highlighted in green) a large proportion of the miRNAs work in similar pathways. There are some pathways that may be AD progression dependent.

Owing to their presence in two groups (Control – Braak stage III-IV and Control – Braak stage V-VI) (highlighted in orange) the glutamatergic synapse and thyroid hormone synthesis pathways are the most likely to be involved in early progression of disease, although other pathways may be involved. While the later Braak stages are typified by a much larger representation of pathways with much greater crossover between Control –Braak stage V-VI and Braak Stage III-IV – Braak stage V-VI, shown in purple. A greater proportion have a relation to the brain with the Neurotrophin signalling pathway, Dopaminergic synapse and PI3K-Akt signalling pathway in this group.

Table 32 – Summary of signalling pathways involved in Alzheimer' disease at different stages. MicroRNAs were chosen if they were significant in the Mann-Whitney U test paired analysis. Values were only accepted if $p<0.05$ was found after FDR correction methodology using Diana tools miRPath v.3. Green – present in all groups. Yellow – Present in Control – Braak stage III-IV + Control – Braak stage V-VI. Blue – Present in Control – Braak stage III-IV + Braak stage III-IV – Braak stage V-VI.

Group	KEGG pathway
Control – Braak stage III-IV	Adherens junction, Adrenergic signaling in cardiomyocytes, Axon guidance, Chronic myeloid leukemia, Endocytosis, ErbB signaling pathway, FoxO signaling pathway, Glioma, Hepatitis B, Hippo signaling pathway, Lysine degradation, Pathways in cancer, Prion diseases, Prolactin signaling pathway, Prostate cancer, Proteoglycans in cancer, Signaling pathways regulating pluripotency of stem cells, TGF-beta signaling pathway, Thyroid hormone signaling pathway, Wnt signaling pathway, Glutamatergic synapse, Morphine addiction, Thyroid hormone synthesis, Ubiquitin mediated proteolysis, Mucin type O-Glycan biosynthesis, Thyroid cancer, Transcriptional misregulation in cancer, Adipocytokine signaling pathway, Basal cell carcinoma, cGMP-PKG signaling pathway, Circadian rhythm, Dorso-ventral axis formation, Endocrine and other factor-regulated calcium reabsorption, Estrogen signaling pathway, Glycosaminoglycan biosynthesis - heparan sulfate / heparin, Hedgehog signaling pathway, Oocyte meiosis
Control – Braak Stage V-VI	Adherens junction, Adrenergic signaling in cardiomyocytes, Axon guidance, Chronic myeloid leukemia, Endocytosis, ErbB signaling pathway, FoxO signaling pathway, Glioma, Hepatitis B, Hippo signaling pathway, Lysine degradation, Pathways in cancer, Prion diseases, Prolactin signaling pathway, Prostate cancer, Proteoglycans in cancer, Signaling pathways regulating pluripotency of stem cells, TGF-beta signaling pathway, Thyroid hormone signaling pathway, Wnt signaling pathway, Glutamatergic synapse, Morphine addiction, Thyroid hormone synthesis, Ubiquitin mediated proteolysis, Acute myeloid leukemia, Amphetamine addiction, AMPK signaling pathway, Arrhythmogenic right ventricular cardiomyopathy (ARVC), cAMP signaling pathway, Colorectal cancer, Dopaminergic synapse, Endometrial cancer, Focal adhesion, Insulin signaling pathway, MAPK signaling pathway, Melanoma, mTOR signaling pathway, Neurotrophin signaling pathway, Nicotine addiction, Non-small cell lung cancer, Oxytocin signaling pathway, Pancreatic cancer, PI3K-Akt signaling pathway, Rap1 signaling pathway, Ras signaling pathway, Renal cell carcinoma, Retrograde endocannabinoid signaling, Type II diabetes mellitus, Circadian entrainment, ECM-receptor interaction, Glycosphingolipid biosynthesis - ganglio series, Long-term depression, Aldosterone-regulated sodium reabsorption, Bacterial invasion of epithelial cells, Central carbon metabolism in cancer, Choline metabolism in cancer, Cholinergic synapse, Dilated cardiomyopathy, GABAergic synapse,

	Hypertrophic cardiomyopathy (HCM), Platelet activation, Regulation of actin cytoskeleton, Shigellosis, Small cell lung cancer, T cell receptor signaling pathway
Braak Stage III-IV – Braak Stage V-VI	Adherens junction, Adrenergic signaling in cardiomyocytes, Axon guidance, Chronic myeloid leukemia, Endocytosis, ErbB signaling pathway, FoxO signaling pathway, Glioma, Hepatitis B, Hippo signaling pathway, Lysine degradation, Pathways in cancer, Prion diseases, Prolactin signaling pathway, Prostate cancer, Proteoglycans in cancer, Signaling pathways regulating pluripotency of stem cells, TGF-beta signaling pathway, Thyroid hormone signaling pathway, Wnt signaling pathway, Mucin type O-Glycan biosynthesis, Thyroid cancer, Transcriptional misregulation in cancer, Acute myeloid leukemia, Amphetamine addiction, AMPK signaling pathway, Arrhythmogenic right ventricular cardiomyopathy (ARVC), cAMP signaling pathway, Colorectal cancer, Dopaminergic synapse, Endometrial cancer, Focal adhesion, Insulin signaling pathway, MAPK signaling pathway, Melanoma, mTOR signaling pathway, Neurotrophin signaling pathway, Nicotine addiction, Non-small cell lung cancer, Oxytocin signaling pathway, Pancreatic cancer, PI3K-Akt signaling pathway, Rap1 signaling pathway, Ras signaling pathway, Renal cell carcinoma, Retrograde endocannabinoid signaling, Type II diabetes mellitus, Long-term potentiation, Phosphatidylinositol signaling system, Viral carcinogenesis

Protein Analysis

This experiment was to assess the PHF6 protein concentration in samples.

PHF6

A standard curve was used to identify the absorbance relevant for protein concentration. A sigmodial curve was used to interpolate the points and enable the protein concentration to be calculated. Due to the data being non-normally distributed based on a Shapiro-Wilk test. The Kruskal-Wallis test was used to assess the differences between groups followed by a Mann-Whitney test.

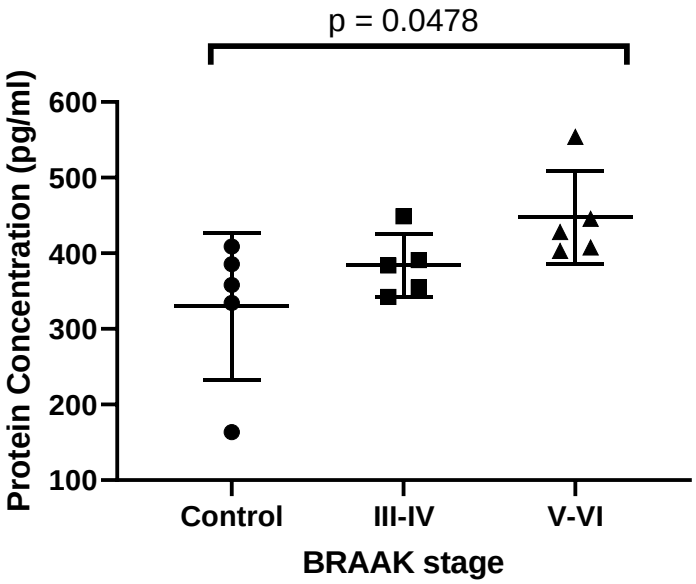

Figure 45 – Showing PHF6 protein concentration after ELISA quantification – There was a significant difference between control and Braak stage V-VI. A Kruskal-Wallis test was used to compare for differences across all groups.

Figure 45 shows how that the protein concentration varies with disease progression (Kruskal-Wallis p-value = 0.0478). There is an increase of PHF6 protein with increasing severity of disease. This increase was not significant between neighbouring groups (Control and Braak Stage III-IV or Braak Stage III-IV and Braak Stage V-VI) although with increasing sample number this may change. However, across the biggest group Control to Braak Stage V-VI there was a significant difference (p=0.0317) (Figure 45), which demonstrates that PHF6 changes are more visible at the later stages of disease.

Does hsa-miR-143-3p interact with PHF6?

This experiment was to address whether hsa-miR-143-3p interacts with PHF6 in this setting. For this, hsa-miR-143-3p was measured against PHF6.

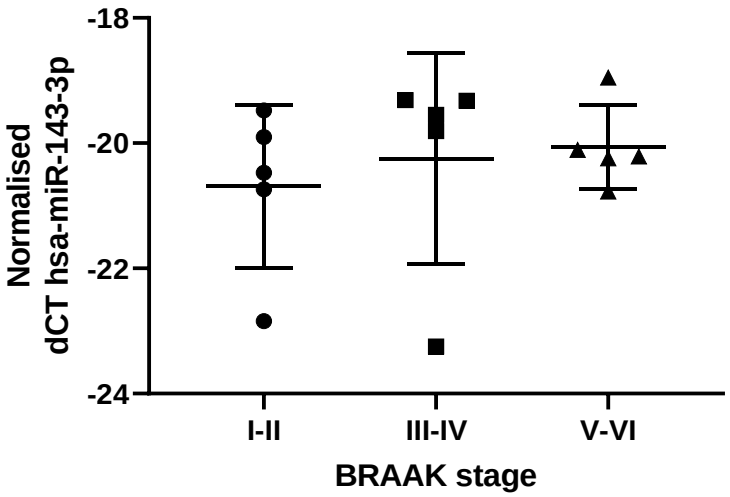

Figure 46 – hsa-miR-143-3p in Alzheimer's disease brain samples – There was no significant difference found here. So although has-miR-143-3p can act on PHF6 it is not having an impact here and something else could be regulating PHF6 expression during AD.

There was no significant trend with hsa-miR-143-3p across any of the groups. In addition, when plotting PHF6 against hsa-miR-143-3p (Figure 47) there was an upward trend demonstrating that they may be co-expressing by they are not interacting, which would be explained by a negative trend. As a result, in this context dysregulation of hsa-miR-143-3p is not causing the increase in PHF6 expression that has been seen.

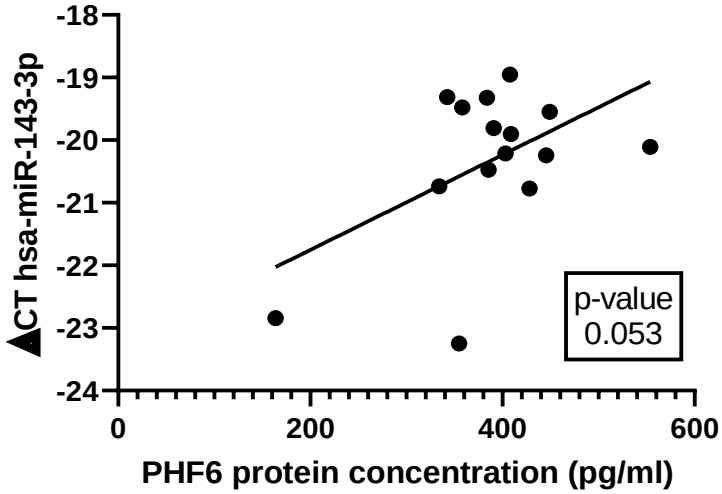

Figure 47 – Showing no correlation between hsa-miR-143-3p and PHF6. A simple linear correlation was used to calculate statistical analysis.

PHF6 interaction with other miRNAs

Although hsa-miR-143-3p did not have a negative correlation with PHF6 other miRNAs may do. The miRNA data already accrued was used to see whether other miRNAs may have a negative correlation with PHF6 to implicate their interaction.

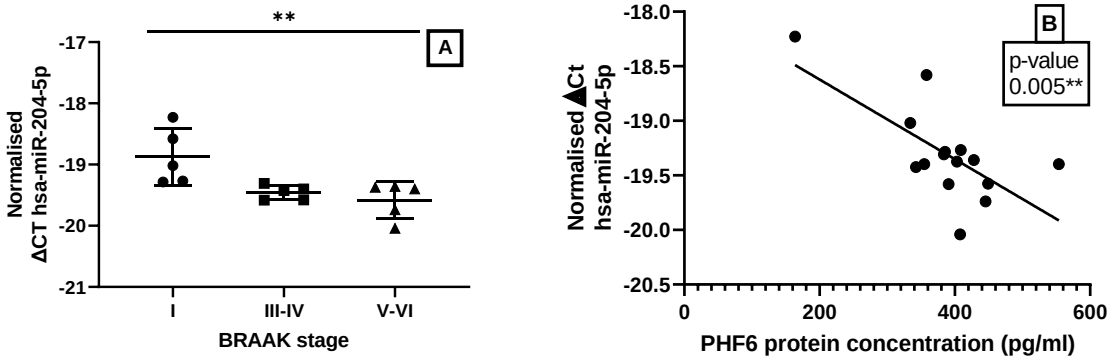

Figure 48 – (A) Showing hsa-miR-204-5p differential expression during Alzheimer's disease. A clear decrease in expression when controls are compared to Early and Late stage AD patients. Kruskal-Wallis test was carried out for statistical analysis. **(B) Showing significant negative correlation when PHF6 is compared to hsa-miR-204-5p.** A simple linear regression was used to compute significance. **p <0.01.

One miRNA found to be significantly differentially regulated in this study with a negative trend was hsa-miR-204-5p (Figure 48A). There were changes between Control to Braak Stage III-IV and Control to Braak Stage V-VI. Normalised ΔCT hsa-miR-204-5p was plotted against PHF6 protein concentration (Figure 48B), which showed a significantly negative correlation. This demonstrates a potential interaction between hsa-miR-204-5p and PHF6 that could implicate a role in the development of AD. This interaction has been predicted on eight different miRNA interaction databases with miRDip rating it as 'high' probability of interaction (Table 33) so should be investigated further [166].

Table 33 - MiRDip entry for interaction between hsa-miR-204-5p and PHF6

Gene Symbol	Uniprot	MicroRNA	Integrated Score	Number of Sources	Score Class	Sources
PHF6	Q8IWS0	hsa-miR-204-5p	0.222914206	8	High	BCmicrO, MBStar, MirAncesTar, MirMAP, miRTar2GO, PITA, RepTar, RNAhybrid

Discussion

Our study investigated the differential regulation of miRNAs in the temporal cortex of patients at pre-defined stages of AD (Control, Braak Stage III-IV and Braak stage V-VI). The purpose was to create a far-reaching miRNA study of the potential miRNAs involved in the different stages of AD to establish if any concussion related miRNAs were involved in AD.

The potential of miRNA differential expression as a biomarker

Our study showed 52 differentially expressed miRNAs. Differences were found between all Braak stage groups and have demonstrated a preliminary capability to distinguish disease progression based on miRNA signature. The strongest separation was between Braak stage V-VI and control. Perhaps an unsurprising finding given these are most differing groups.

Together this shows that in accordance with the literature there is differential expression of miRNAs in the brain during AD [167], and if found in a more accessible bio-fluid it could be an excellent biomarker.

Most promisingly four miRNAs could distinguish between control patients and both Braak III-IV and Braak V-VI patients. If these markers can be found in peripheral bio-fluids, then could be used as a diagnostic marker. In particular hsa-miR-204-5p has been found to be integral in axonal maintenance and the decrease found in the AD patient group may be a finding of use [168, 169].

The most similar study, that looked at miRNA expression in the temporal cortex, in the literature had a crossover of 16 miRNAs showing differential expression between control and AD patients [170]. However, the differences they demonstrated were largely opposing with 15 (94%) decreasing with AD progression in their study, while increasing in our study. Only 1 (6%) showed a comparable change across studies with hsa-miR-146b-3p increasing across both [170]. This was surprising but demonstrates these miRNAs are integral but their directional change may be more varied than previously thought. This could be due to differences in design of the study with housekeeping genes and/or temporal expression likely to be important. Another factor could be RNA degradation that may take place before brains were appropriately frozen that cannot be controlled for.

Out of the 16 shared miRNAs from both studies 10 different miRNAs (hsa-miR-212-3p, hsa-miR-93-5p, hsa-miR-30e-5p, hsa-miR-106b-5p, hsa-let-7a-5p, hsa-let-7e-5p, hsa-miR-106a-5p, hsa-miR-185-5p, hsa-miR-425-5p and hsa-miR-98-5p) have previously been associated with blood based potential in AD patients [170-172]. Although these results have come from varied

preparations of blood products it further demonstrates the potential of circulating biomarkers and their relevance in AD brain related signalling.

The role of hsa-let-7 family in Alzheimer's disease

Another finding was that four hsa-let-7 family members were differentially regulated in the AD disease brains. All have been shown as potential peripheral biomarkers for AD (hsa-let-7a-5p [173], hsa-let-7d-5p [174], hsa-let-7e-5p [173, 175] and hsa-let-7i-5p [176]). This overrepresentation of differential expression of the let-7 family may stem from their similar sequence homology and combined with their high expression in the brain may implicate them in underlying pathogenesis of disease [177, 178].

Potential pathogenesis roles include the ability of hsa-let-7i-5p to mediate neuronal survival. This occurs through inhibition of Pgrmc1 that causes a reduction in brain-derived neurotrophic factor (BDNF) [179]. While hsa-let-7d-5p can impact axonal outgrowth through inhibition of nerve growth factor (NGF) [180]. Other hsa-let-7 family members have been linked to neuronal maintenance with changes having the potential to impact neuronal function [175, 181, 182]. This combination of literature-based data gives the impression the balance of the hsa-let-7 family signalling is essential for neuronal homeostasis.

Furthermore, two hsa-let-7 family miRNAs were shared with concussion related miRNAs. They were hsa-let-7i-5p and hsa-let-7a-5p, which further demonstrates the relevance of the hsa-let-7 family to neurological signalling. Based on this evidence the hsa-let-7 family can be detrimental in the long-term, but the impact of short-term signalling is unknown. So future research is important to assess whether the short-term trauma response that implicates these miRNAs in concussion is temporary and does not cause lasting long-term changes such as AD.

MiRNA involvement in AD progression

As demonstrated in this study the differential miRNA expression may show the underlying signalling that governs AD progression. Largely, based on bioinformatics, the miRNAs are signalling in similar ways with typical AD based pathways such as TGF-β signalling pathway and ECM-receptor interaction involved [183, 184].

However there seems to be greater differential expression with later disease progression, so miRNA changes are likely to be more impactful at this later stage. Although more impactful the balance of miRNAs can be varied and not necessarily consistent response, which may make this later stage more difficult to study. So although they are relevant pathways (e.g. Neurotrophin signalling pathway) like the literature suggests an early intervention is more suitable for diagnostic and treatment options [185].

Earlier disease changes are more specific and can be targeted – based on this study – with the glutamatergic synapse and thyroid hormone synthesis shown to be involved. These pathways have both previously been shown to be involved in AD. However, a NMDAR antagonist (memantine) that targets glutamate signalling is only effective in moderate to severe AD, which conflicts with it being involved at the early stages of AD [186]. Even so a similar drug may be effective in the future. Thyroid hormone levels have been shown to be altered in cognitively impaired and Alzheimer's disease patients [187], which strengthens this finding and may demonstrate associated miRNAs potential as biomarkers. As these pathways are involved in AD disease development they should be investigated further to establish how – if at all – the linked miRNAs could be used as diagnostic tools or to further knowledge and development treatments pathway relevant treatment methods.

Potential role for hsa-miR-204-5p in modulating PHF6 expression

PHF6 is a zinc finger protein that is believed to be involved in the initiation of tau protein aggregation [188]. This study showed PHF6 protein content increases in AD brains with Braak stage severity, which aligns with the literature-based assessment.

The previously found PHF6 interaction with hsa-miR-143-3p was not replicated in this AD. However, hsa-miR-204-5p showed a significant negative correlation with PHF6, which may demonstrate that hsa-miR-204-5p is a regulator of PHF6. In this scenario, a decrease in hsa-miR-204-5p reduces PHF6 inhibition leading to more PHF6 protein and AD development. This could show hsa-miR-204-5p as a potential biomarker directly related to the disease presentation or highlight a novel treatment method to prevent the development of AD disease. Although there is no clear established role in the literature there was a downregulation found in frontotemporal dementia (FTD) patients, which supports a role for hsa-miR-204-5p role in AD development [189]. This is an observation based on the data and would need more assessment to establish if there is a miRNA interaction with PHF6 mRNA.

MicroRNAs are from the literature and this work involved in the development of Alzheimer's disease. Even though this is brain tissue it gave me confidence that early differences can be found in other biofluids that could be early biomarkers and gave me the conceptual idea of risk monitoring in concussion. Prolonged signalling seems to produce a more consistent miRNA signature, which could make them more able to detect risk over immediate response.

The Let-7 family of miRNAs are clearly present across both groups, this could be a coincidence. However, it should be investigated further as this could be an interesting line of work for future scientists to investigate.

Limitations

Sample number was limited and would increase strength of the study with more numbers. This could also be addressed by using a second validation cohort.

Any link with previous SCRUM study is currently tenuous owing to the different source of biological material and is aimed to open scientific understanding.

Overall

Overall, there is further evidence here for a panel of biomarkers for early AD management. In addition, there is likely to be a fundamental role of the hsa-let-7 family in the development of AD. This involvement highlights the hsa-let-7 family response in concussion and establishes that more work is required to understand the molecular basis of these changes and their impact in the long term.

Future work

Understand role of let 7 in the context of concussion and whether it is a key linking factor between concussion/head trauma and AD or other neurodegenerative diseases.

Assess some of the miRNAs in this study to see if they can distinguish AD in saliva and/or blood products.

Further establish if hsa-miR-204-5p is a regulator of PHF6 in AD.

Chapter 6: The differential expression of Small Extracellular Vesicles in concussion injury using the novel Exoview platform

Rationale

Differential regulation of microRNAs in concussion has been shown throughout this study. The reason for its presence in biofluids is still unknown so as extracellular vesicles are widely known to be associated with miRNAs investigating if there are vesicle changes could be of use.

Exoview is a new technology – produced by Nanoview biosciences – that uses an antibody capture technology to purify your sample. This is unique and removes a lot of pre-analytic variables that exist in the field so was the best instrument available to address this question.

Aims

To establish if there are small extracellular vesicle changes in response to concussion in biological fluids using the Exoview technology.

Statement of Contribution

I completed all work associated with this chapter.

Methods

Study approval

Study participants were recruited through the Surgical Reconstruction and Microbiology Research Centre (SRMRC), based at Queen Elizabeth Hospital of Birmingham (United Kingdom), as part of the ReCoS (The REpetitive COncussion in Sport). This study was carried out in accordance with the recommendations of the University of Birmingham Research Ethics Committee. The protocol was approved by that same ethical committee together with peer review by the National Institute of Health Research Centre for Surgical, Reconstruction and

Microbiological Research Centre (NIHR SRMRC – Ethics Ref. 11-0429AP28). All subjects gave written informed consent in accordance with the Declaration of Helsinki.

Sample collection

Saliva

Saliva (5ml) was collected in a 50ml sterile plastic universal container tube kept on ice for no more than 30 minutes. Samples were then centrifuged at 2600 × *g* for 10 minutes at 4°C and the supernatant was collected. Followed by 10,000 x *g* for 1 minute at 4°C where the supernatant was collected again before adding RNase inhibitor (500 Units/ml) (Qiagen) for storage at -80°C.

Urine

Urine (30ml) was collected in a 50ml sterile plastic universal container tube kept on ice for no more than 30 minutes. Samples were then centrifuged at 2600 × *g* for 10 minutes at 4°C and the supernatant was collected for storage at -80°C.

Exoview

A new technology (Exoview R100. Nanoview Biosciences) in the development stage that uses a silicon microarray chip to categorise extracellular vesicles from original bio-fluid. More details can be found on their website (https://www.nanoviewbio.com/exoview-r100).

Tetraspanin chips

Nanoview provided silicon chips that have specific primary antibodies printed in triplicate onto the chip surface, with each replicate referred to as a 'spot'. The Tetraspanin kit that was used

throughout has CD9, CD63, CD81 and mouse IgG antibodies printed onto the surface making a total of twelve spots.

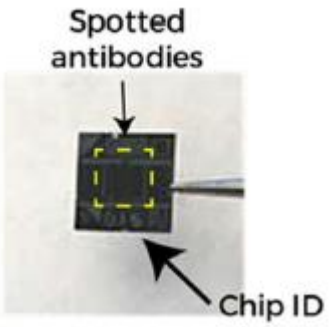

Figure 49 - Example of a chip. Spotted antibodies are in the middle.

Procedure

Pre-scan

Upon receipt of the tetraspanin chips they were pre-scanned to account for any pre-existing particles on the surface of the chip. This measurement was taken away from the final post-scan lightscatter measurement.

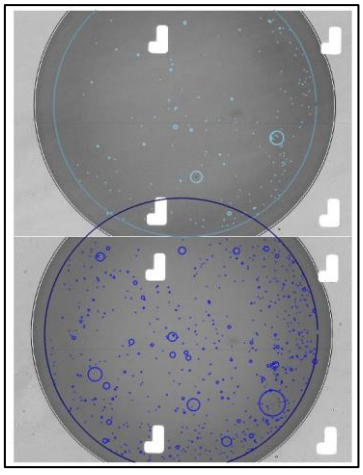

Figure 50 –Example of a pre- and post-scan in lightscatter mode. Showing the pre-scan that is taken away from the final image of the post-scan.

Incubation

They were incubated at room temperature with 35ul of pre-diluted sample. This isolated a specific tetraspanin population of vesicles on each spotted antibody. Three primary conjugated antibodies were added to this isolated sample to specify co-localised markers (Table 34). The manufacturer's protocol was used for all experimentation.

Table 34 - Formation of conjugated antibodies used in this study. All antibodies were received from Nanoview biosciences except CD24 that was received from (**https://www.biolegend.com/en-us/products/alexa-fluor-647-anti-human-cd24-antibody-3364**, Biolegend)

Excitation wavelength (nm)	Protein of interest	Fluorophore
488	CD9	Alexa 488
555	CD81, Syntenin	Alexa 555
640	CD63, CD24	Alexa 647

Post-scan

After incubation, the Exoview instrument using the NScan (Measuring software) and Nanoviewer (Analysis software) software was used for visualisation of the vesicle population. It has two different measurement methods to accrue data:

1. Interferometric imaging using 410nm excitation wavelength (Lightscatter). This allows visualisation and sizing of particles >50nm that are present on the surface of the chip. They are specific for the marker on the surface.

2. Fluorescence imaging (three fluorescent channels shown in Table 34). Allows for assessment of co-localised vesicle markers with more specific visualisation. Two direct capture antibodies (surface and conjugated antibody) are required for positive signal. This technique has no sizing but with also can capture sizes <50nm.

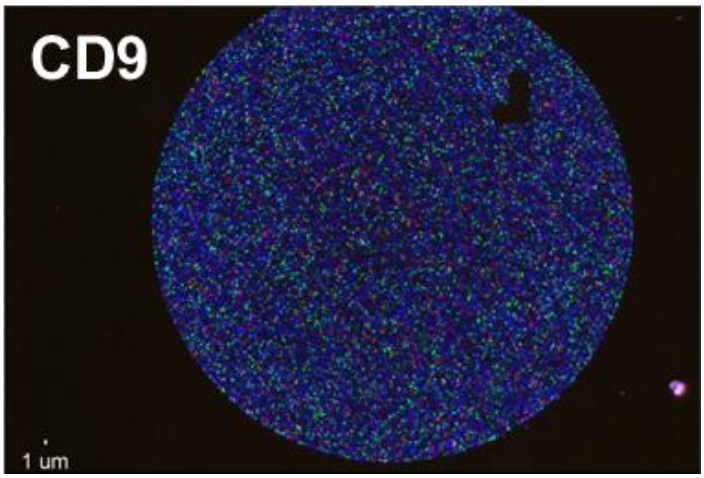

Figure 51 - Example fluorescent image of a CD9 spot. Individual small round "dots" are vesicles with that specific marker on. This was a urine sample at a 1:5 dilution incubated with three fluorescent antibodies (CD9 blue, CD63 red and CD81 green).

Post data collection normalisation

Data points that are referred to as 'normalised particles' means they have been refined through the process stated below.

Lightscatter

After accounting for the pre-scan measurement, lightscatter measurements were further controlled by taking away the mouse IgG to account for non-specific binding to the silicon chips.

Fluorescence

To control for background in fluorescence the gating was set using a mouse IgG spot value of no more than 10 normalised particles on the spot with the highest count. This was to ensure there was no non-specific binding to the chip.

Osmolality

Osmolality measurements were taken using a freezing point osmometer using 50ul of urine (Gonotec).

Statistical analysis

All analysis was carried out using GraphPad Prism.

Shapiro-Wilk normality testing was used followed by an unpaired t-test or Mann-Whitney U test. A p-value of less than 0.05 was considered significant.

Results

The Exoview platform (Nanoview) was purchased at the University of Birmingham – a novel technology to measure sEV's – and was considered the ideal platform to evaluate the potential of sEV's quantification in concussion. This was due to the unique antibody capture technology that allowed high quality purification with ease, which causes a lot of pre-analytical variation with sEV preparation using other technology.

Saliva

This experiment was to establish if salivary small extracellular vesicles could be measured using this technology on the samples that had been collected.

Oragene tubes

The oragene collection tubes – that were used for collection in the SCRUM study – were tested and there was found to be no presence of vesicles. Subsequently it was found there was a lysis buffer in the preservation solution. This deemed the SCRUM samples unusable and therefore a move to RECOS samples instead.

RECOS protocol

All spots were under the saturation of the instrument (<5000 normalised particles) and were considered linear measurements. This showed that salivary vesicles can be visualised using RECOS samples and 1:600 dilution would be adequate to ensure enough variability for all samples to be within the linear range Figure 52.

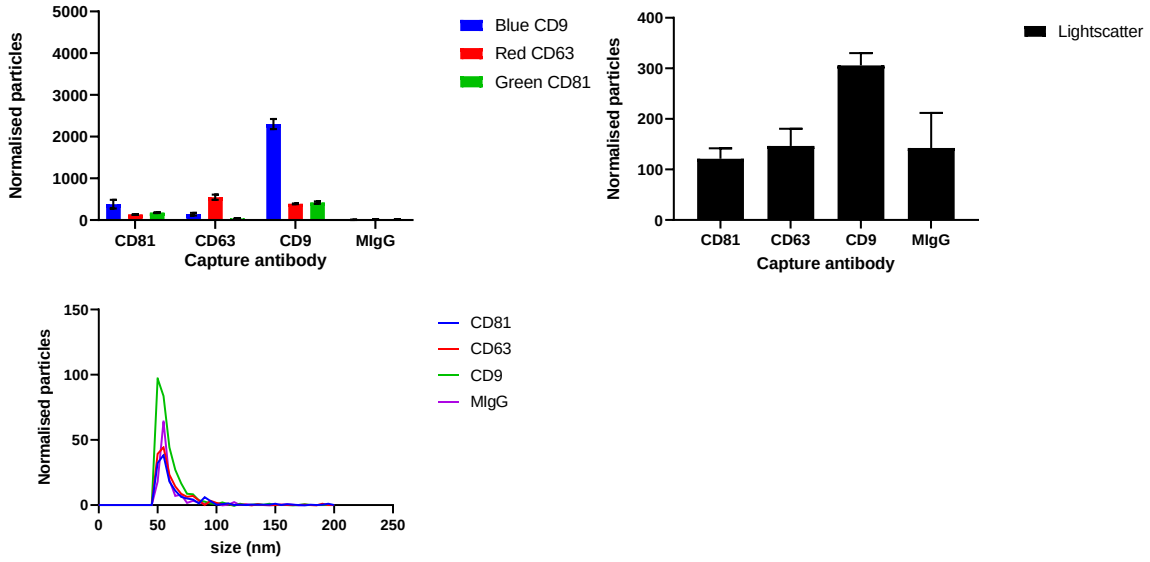

Figure 52 - RECOS saliva sample (RCA02) analysed at 1:600 dilution. (A - Top left) Fluorescence measurement shows a variety of different vesicles phenotypes with the most prevalent being CD9-CD9, all capture spots were below the saturation point of 5,000. (B – Top Right) Lightscatter measurement has a clear population of CD9+ vesicles. (C – Bottom Left) Size graph has a clear population of CD9+ vesicles.

The graphs displayed in Figure 52 are representative of all patient measurements that are largely similar. On the lightscatter (Figure 52A) there was a clear population of CD9 vesicles above the background level (MIgG). This was not the same for CD81 and CD63 that were no different from background. The numbers are low across all spots, which is due to the high dilution of the sample to ensure the fluorescence counts are in range. This may limit the sensitivity of lightscatter measurements. The size graph is based on the lightscatter measurement and can be seen as similar. There was a clear CD9 population above mIgG that

is not the same for both CD63 and CD81. This size trace with a peak at 55nm is typical (Figure 52B).

Fluorescence measurements demonstrate that the main population of vesicles was CD9-CD9. There was also a clear population of CD63-CD63 positive vesicles. The co-localisation of vesicle markers was less present with the CD9 spot showing the most co-localisation between markers (Figure 52C).

RECOS samples across patients

This experiment was to establish if there were differences in small extracellular vesicle content between concussed and non-concussed patients.

To establish if there were differences in the saliva of concussed patients compared to controls samples were taken from RECOS athletes (RCA) and RECOS patients (RCP). They were measured at a dilution of 1:600 using the Exoview, which was considered optimal for fluorescence measurements.

Demographics

Table 35 - Demographics of RECOS participants for saliva measurements on Exoview

					Impact Score					
Group	Sex	Concussion	Age	Age SD	Verbal memory	SD	Visual memory	SD	Symptom	SD
RCA (n=6)	M	None	25.7	3.8	78.6	10.8	75.8	12.6	8.0	11.5
RCP (n=6)	M	Day 2	25.1	2.6	86.3	10.6	81.7	6.3	25.7	29.4

Samples from all male patients who played professional or semi-professional rugby union were obtained. RCA were athlete samples taken pre-season. RCP samples in this case were

patients who gave a sample two days after their concussion. The ages were similar between groups (Table 35).

Lightscatter

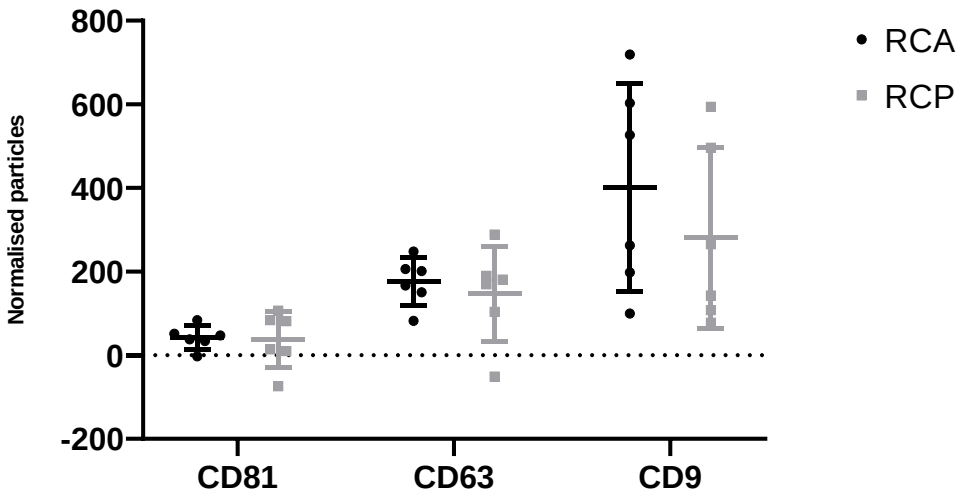

Figure 53 – Showing light scatter results of saliva samples compared between healthy and concussed patients (Day 2) after normalisation. To normalise the mouse IgG was taken away from the normalised particle value. Graph shows mean±SD.

There were small extracellular vesicles (sEV) present on CD9 and CD63 spots but the CD81 spot was not consistently above background. The highest EV counts were seen on the CD9 capture antibody, which was closely followed by CD63. The sEV numbers were low due to dilution, which was optimal for fluorescence. This was unlikely to be optimum concentration for light scatter measurements, which may explain some of the variability at the low number range. There were no significant differences across any of the tetraspanin spots.

Size

Size was considered based on the capture spot. The size measurement is based on the lightscatter data so due to the consistently low value of CD81 it was not considered for analysis.

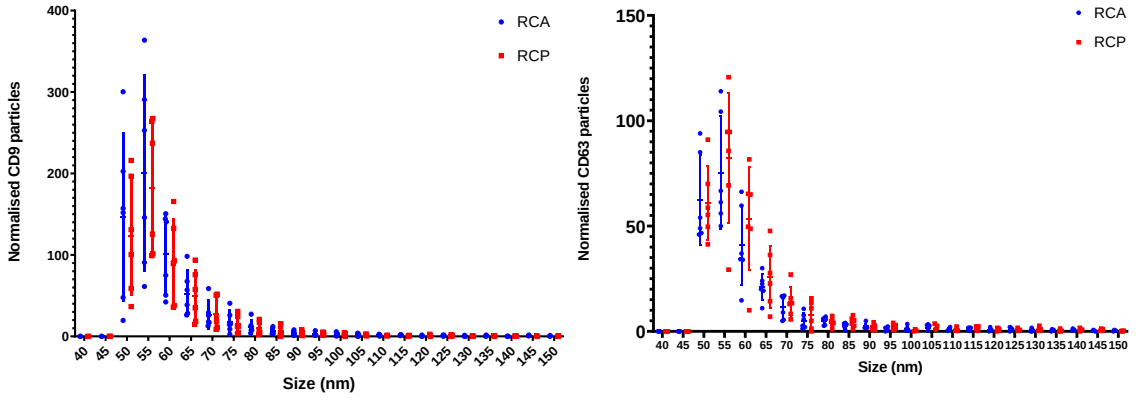

Figure 54 – Showing a size comparison between RCA and RCP across CD9 and CD63. They look similar in format. Graph shows mean±SD.

There were no differences between the groups found. There was a consistent trend of vesicles with individual patient peaks lying around 55nm in both CD63 and CD9 demonstrating these are small extracellular vesicles (sEVs). There was very little larger than 100nm, which could demonstrate a very specific type of vesicle.

Fluorescence

This experiment was optimised so all fluorescent values would be within the linear range of the instrument. Primary conjugated antibodies of CD81, CD63 and CD9 were used to accompany the capture spots.

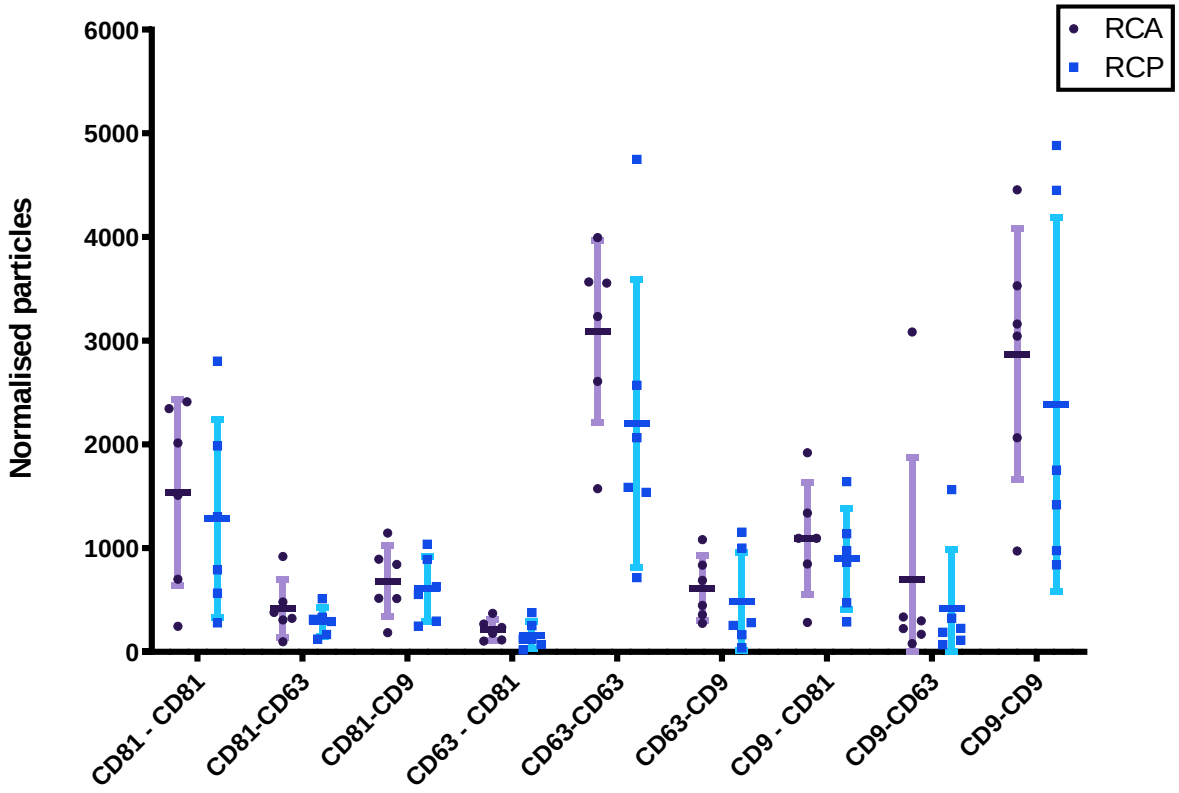

Figure 55 – Showing interleaved scatter plot for normalised particles compared between RCA and RCP patients (n=6). There was no significant differences between any spot and fluorescent antibody combinations. An independent t-test was used to compare spots. Graph shows Mean±SD.

Across all fluorescent locations there was no significant difference between groups. The highest populations are those of dual positivity with the highest being CD63-CD63 (RCA: 3088±874, RCP: 2204±1391). There was evidence of co-localised populations with a population of CD81-CD9 vesicles (RCA: 683±343, RCP: 609±314) that can also be visualised on CD9-CD81 combination as well. Although these were not significantly different it demonstrates that a co-localised population of interest can be captured effectively.

There was a large variability across all combinations between patient samples, which can be shown through the large standard deviations. To improve salivary based work using this technology either a normalisation method or more standardised collection method would be

required to gain more consistency. Using this setup there are unlikely to be significant differences between groups.

Urine

This experiment was to establish if urinary small extracellular vesicles could be measured using this technology on the samples that had been collected.

Norgen Preservative

Due to a combination of storage method and preservative the urine samples stored with Norgen – the collection method for SCRUM – were degraded on the Exoview. As a result RECOS samples were focussed on for analysis.

RECOS

Establishing a protocol

RECOS samples were tested to establish the optimum concentration for analysis.

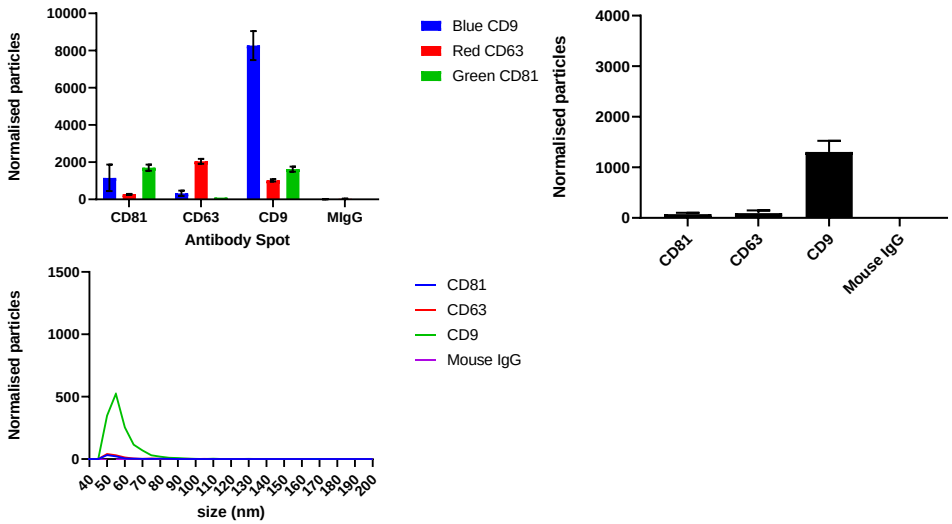

Figure 56 – Showing RECOS urine sample (RCA01) results from Exoview at 1:5 dilution. (A - Top Left) Fluorescence measurement showing nine different antibody combinations with very little background on MIgG. (B - Top Right) Lightscatter measurement shows a large population of CD9 vesicles above

background with CD81 and CD63 being small populations above background. (C – Bottom left) Size measurement shows a clear population of CD9+ vesicles that peak at around 55nm.

Lightscatter measurements (Figure 56B) show a population of CD9+ vesicles in the sample with both CD81 and CD63 being small populations that are close to background level. CD9 is a marker present in the urine and this was an expected result. Size measurements (Figure 56C) show a similar representation of lightscatter with a large population of CD9+ vesicles above the background level. These vesicles peak at 55nm and there are very few larger than 100nm.

Fluorescence measurements show the largest population to be CD9-CD9 (Figure 56A), which at this dilution was saturated (Normalised particles: 7492). There was a large difference between CD9-CD9 and any other combination with the next largest CD63-CD63 (Normalised particles: 2201). There was some co-localisation with CD81-CD9 and CD9-CD63 showing reasonable population sizes. From this a 1:5 dilution was used going forward, the CD9-CD9 fluorescence channel was saturated, but there would be little to no information about the other vesicle populations if it was to be diluted further.

RECOS samples across patients

This experiment was to establish if there were differences in small extracellular vesicle content between concussed and non-concussed patients.

After a protocol was devised the next stage was to establish if there were urinary EV changes in response to concussion and for this – like with saliva – RCA and RCP samples were compared. The graphs in Figure 56 were similar across all patients and therefore they were combined for ease of understanding going forward.

Demographics

Table 36 -Demographics of samples used for urinary small extracellular vesicle measurments on Exoview

							Impact Score					
Group	Sex	Concussion	Age	SD	Osmolality	SD	Verbal memory	SD	Visual memory	SD	Symptoms	SD
RCA (n=7)	M	None	27.3	4.9	679.9	259.9	81.4	9.5	79.1	7.6	2.3	1.8
RCP (n=7)	M	Day 2	22.9	3.4	781.3	252.4	88.4	8.8	76.9	12.3	15.3	25.6

RCA and RCP samples were compared. There was a slight difference in age and osmolality although neither was significantly different. The impact scores were similar and could not distinguish except the symptoms that was higher in the RCP group.

Lightscatter

In Figure 56 there was a clear population of CD9+ vesicles while there was little to no CD63+ or CD81+ populations when compared against the control. This trend transpired across all samples and as a result CD9 was the only antibody spot considered for analysis between groups.

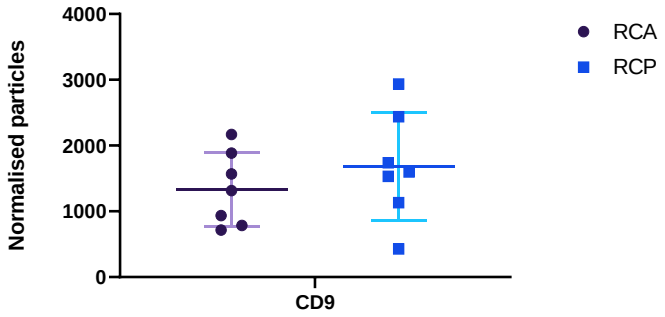

Figure 57 – Showing interleaved scatter plot comparing the CD9 normalised particle values between RCA and RCP groups (n=7). For this analysis, the mouse IgG was removed to equilibrate the results for background activity. There was no significant difference between the groups. An independent t-test

was used to compare between groups and a p-value of less than 0.05 was considered significant. The graph shows mean±SD.

Figure 57 shows no significant difference between groups. There was variability across samples but in general the trend across all samples was similar and demonstrates lightscatter with CD9, CD63 and CD81 was not a sensitive enough measurement to distinguish between groups with this number of samples.

Size

Due to the small numbers on lightscatter for CD63 and CD81 these spots were not considered for size analysis.

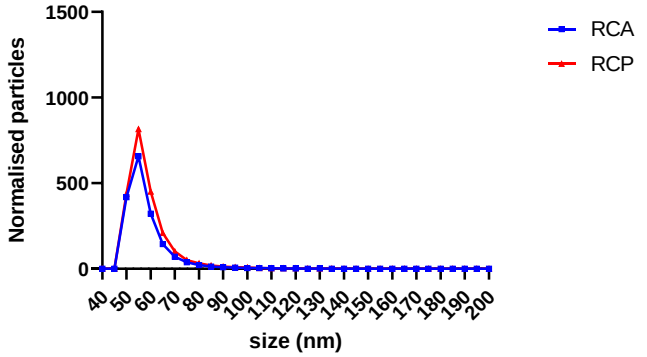

Figure 58 – Showing size distribution comparisons for RCA vs. RCP samples (n=7). Average traces across both groups showing a very similar trace across both groups.

All graphs show a similar trend with a lower peak at 50nm, which generally peaks at 55nm before dropping gradually in the CD9 spots (Figure 58). There are no peaks higher than 100nm showing there no larger vesicles. Figure 58B shows an average curve for each group, which is largely similar. This consistency indicates that the CD9 population of vesicles is consistent in size distribution in urine samples.

Fluorescence

There was little background so the signal is clear and should not have interruption from the machine as a result any variablity was pre-analytical (Figure 56). Urine was shown to be a consistent bio-fluid that using this platform has the potential to diagnose not only concussion but other diseases with the correct protocol in the first place.

As shown in Figure 59, there was a significant difference between RCA and RCP when CD81 was the capture spot and fluorescent antibody (CD81-CD81) (RCA: 2435±479, RCP: 3711±935). This increase was also present on CD9-CD81 spot (RCA: 2474±606, RCP: 3631±755), which could show some form of CD81 involvement. Although there was a significant difference between CD9-CD9 this was discounted due to the unknown impact of saturation. All other spots showed no significant differences with relative consistency between groups. This demonstrates the potential to find significant differences between concussed urinary EV's and those of controls. However, the effect of other factors such as osmolality is unknown and more investigation should be considered.

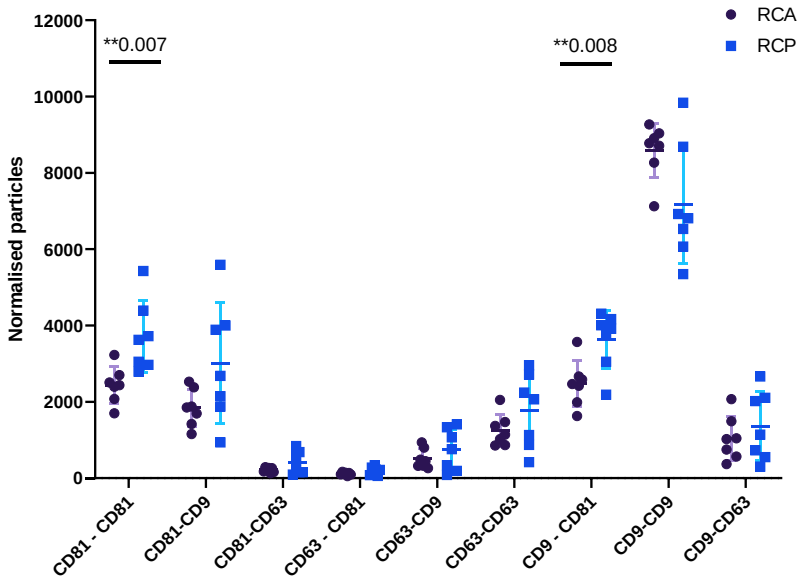

Figure 59 – Showing an interleaved scatter plot for fluorescence data comparing RCA against RCP (n=7). There were significant increases in the RCP group on CD81-CD81 as well as CD9-CD81. CD9-CD9 was saturated and therefore not considered for statistical analysis. An independent t-test was used for statistical analysis with a p value of less than 0.05 considered significant. **p<0.01. The graph shows mean±SD.

When three populations related to CD81 and CD81 colocalised with CD9 are combined there was a significance, which may demonstrate that there is an overall increase in EV population related to this CD81 subgroup. Furthermore, if a >8,000 normalised particles was used to measure differences between groups then it would be possible to achieve a 93% correct diagnosis rate. This is premature and purely demonstrative but could show its potential uses if ratified with a larger sample population.

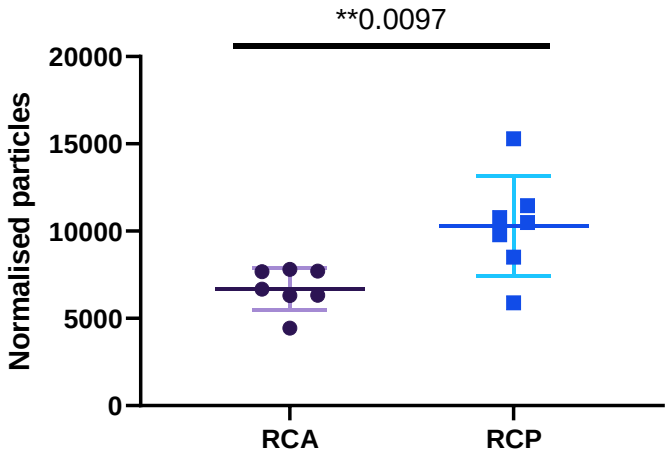

Figure 60- Showing the sum total of three spot locations in urine between RCA and RCP patients. The spot locations were CD81-81+CD81-9+CD9-81. An unpaired t test was used for statistical analysis with a p value of less than 0.05 considered significant. **p<0.01. The graph shows mean±SD.

Other measureable proteins in urine

The aim of this was to establish the origin of vesicles and whether other proteins could be found. Not only that but to establish if we could understand the CD81 population further.

Exosomal population of vesicles

Syntenin is an intracellular protein that is involved in the production of exosomes. CD9-CD9 levels were similar to CD9-Syntenin EV's (Figure 61), which means that the CD9 population of vesicles is likely to be an exosome population.

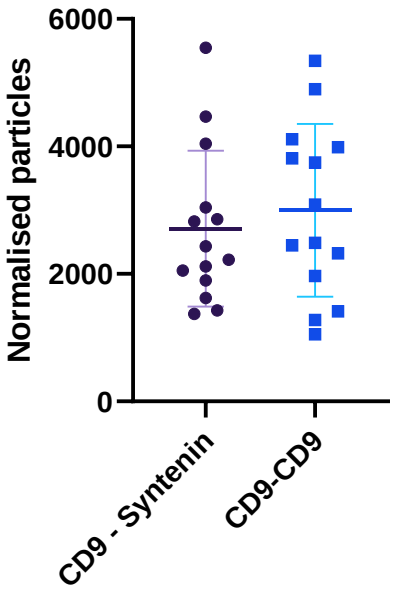

Figure 61 – Showing an interleaved scatter plot of CD9-CD9 compared with CD9-Syntenin. These populations show similar amounts.

CD24

CD24 is a urinary vesicle marker. To understand the prevalence of other markers and how they appear on this technology CD24 was used to establish what could be found. A clear population was found to be co-localised with CD9 demonstrating that other extracellular markers can be found (Figure 62).

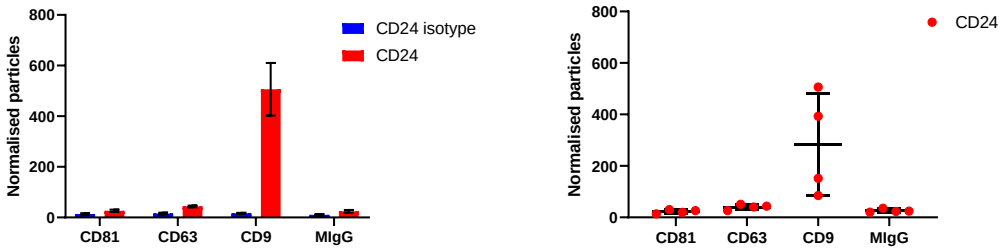

Figure 62 – (Left) Showing CD24 compared to its isotype within a RECOS urine sample at 1:75. There was a clear population of CD9-CD24 positive vesicles. **(Right) CD24 content across four participants.** This population exists across more participants although in varies quantities.

Discussion

The Exoview R100 is a novel tool for assessing small extracellular vesicles (sEVs). In this study we have utilised this technology to establish a protocol for use in our bio-fluid samples. Further to that have begun to highlight the capabilities of the technology by showing a statistically significant CD81-CD81 vesicle change in urinary samples of concussed patients when compared to controls.

Potential of small extracellular vesicles as biomarker using Exoview

We have highlighted the capability to capture and quantify both salivary and urinary small extracellular vesicles that have tetraspanin proteins on the surface (CD9, CD63 and CD81). There were different dilutions required for each bio-fluid – saliva 1:600 and urine 1:15 – that proves the concentration differences between bio-fluids. This matches the literature and may be a reason why saliva may make a better biomarker fluid for sEV research.

Both bio-fluids showed populations across all tetraspanins including co-localised versions to different quantities. Saliva showed a predominant population of CD63 and CD9, while urine showed a predominant population of CD9 with a secondary population of CD81 vesicles. These results were not surprising given the undefined location and high enrichment of CD63, CD9 and CD81 on sEV's [190, 191]. The presence of CD9 in urine is also supported by the literature showing CD9 may derive from the thick ascending limb of the loop of Henle [192]. Other protein markers were shown to be present in CD9 urinary vesicles with syntenin – a protein involved in production of exosomes – present [193]. Likewise, this study showed CD24 a urinary marker to be co-localised to CD9 [194], which demonstrates the potential to find more specific markers of interest using this technology under optimal conditions.

Together this shows an ability to ably quantify sEV's and with optimisation a protocol could be developed for sensitive analysis.

Potential of small extracellular vesicles as biomarker in concussion using Exoview

Saliva showed no significant difference across all groups. This is likely due to the variability of collection, which a normalisation strategy would reduce the difference and may show a more specific marker may be required. However, in adapted, more optimised conditions salivary sEV changes will be visible if present.

Urine showed a statistically significant difference between concussed patients at day 2 and controls using the fluorescence measurement of CD81-CD81. This implies there is a vesicle-based change in the immediate response to injury. CD81 is a sEV marker so its presence is likely to be in co-ordination with a co-localisation protein factor essential for the signalling change. However if CD81 is a key signalling factor its role may be in cell migration in a neuronal environment [195] and this may be mediated by the PI3K-Akt pathway that was associated – using bioinformatics tools – with the differentially expressed miRNAs found in concussed patients saliva. The findings cannot truly be attributed to concussion as there are no MSK or uninjured control with similar exertion. However, it is a proof of principle that vesicle changes are present, measureable and could harbour concussion related miRNA changes.

Key challenges for Exoview technology for biomarkers-based research

Finding an optimum dilution is a key challenge in maximising the potential of this machine. As many as fifteen measures can be in place at any one time, which is excellent to capture a heterogeneous population of vesicles. However as found in this study the variation in quantity of tetraspanin vesicle subtype leads to two compromises: (1) between the most effective

capture method (e.g. lightscatter or fluorescence) as numbers vary between the two techniques and (2) prioritisation of vesicle subtype of interest because the upper limit of saturation (5000 normalised particles) may mean not all vesicle subtypes can be effectively measured at the same dilution.

The other thing to consider is the tetraspanin proteins are highly prevalent on small extracellular vesicles so if your co-localisation factor is rarely present its prevalence may not be recognisable due to the clouding affect (looking for needle in a haystack. Look in needle box instead). As a result, you may need to capture on your target specifically, which is expensive due to lack of established capture markers currently and requires expertise to choose correctly.

Currently there are no normalisation strategies for biomarker based sEV studies using this technology. In this study saliva was variable across vesicles subtypes this may have due to differences in production of sample – as it was whole saliva – but still highlights the need for a normalisation strategy. In urine the variability corresponded to the osmolality of samples highlighting the importance and a potential normalisation strategy if employed correctly. The development of a normalisation strategy, which works in a similar way to miRNA biomarker normalisation would be advantageous and may be essential when working on less prevalent protein markers.

The design of this methodology as it is direct quantification of the bio-fluid suits a diagnostic test format. There would still be limitations of analysis time and whether a suitable membrane associated protein could be found upon sEVs. However, there is certainly a lot of potential with this technique and if I had time, I would certainly take this further.

The things to consider for future users would be sample storage and designing an appropriate study where access to samples for vesicle use was routinely available. If sEVs are as important as the literature thinks they are then I would expect this technology to be used widely in the future.

Overall

Overall, it is an excellent tool for finding a specific co-localised signal using the fluorescence tool. The accuracy of the machine and the ability to isolate those specific groups make it an ideal tool for biomarker analysis. However, the key take away message is that you need to have found your specific target before utilising the machine, focus on that target when choosing a dilution and you may need a specific antibody spot to truly maximise the potential of the machine. Using this knowledge together with preliminary data showing differential expression of CD81 sEVs in urine proves the potential for finding a specific concussion related sEV signal using this instrument.

Future

Create another appropriate study with more controls to understand impact of MSK and uninjured response to establish if this response is specific.

Size exclusion chromatography-based experiment and would choose a selection of protein targets and miRNA targets to see if they co-localise in the same fraction as CD81, which could likely mean they are present on the same vesicles. Then analysis on Evoview would be done if a target were found.

Chapter 7: Overall Discussion

Concussion management is emerging, with novel techniques to recognise the complexity of presentation that are key challenges for diagnosis. While the fast resumption of symptoms means long term consequences are difficult to monitor. Biomarkers have shown potential in this study to be the answer to both challenges with two methodologies demonstrating an ability to quantify easily obtainable biological samples, using sncRNAs and sEV's, that give a biological representation of aberrant concussion signalling.

Biomarkers for concussion diagnosis: are sncRNAs the future?

This study has shown several potential candidate markers that have definable, measurable changes when compared against applicable control groups. Their fast-acting nature (more differential expression at time point b over time point c), accompanied with their stability make sncRNAs an ideal candidate for diagnostic biomarkers, based on a combination of previous literature and this study [79, 120].

Any diagnostic biomarker would clinically be used alongside current measures to best evaluate patients. This biologically relevant representation, would give a different perspective on the injury-based response compared to current quantification methods, and most importantly would be objective.

Other key advantages of salivary based biomarker are their ease of collection without any specialist training, room temperature, opposed to frozen, storage conditions for travel and they are cheap to analyse using qPCR that is routinely available in all diagnostic laboratories [196]. This makes them accessible to the general population as unlike other novel methods, such as fMRI, there is little inconvenience to the injured patient as no additional time-sensitive travel arrangements to a specialist clinic are necessarily required, and once established are

likely to be affordable. Once biomarker use in a clinical setting becomes routine, the knowledge of their underlying pathophysiological function combined with their accessibility could be some of their key advantages, and may enable them to become a gold-standard measurement for diagnosis.

Still challenges of cost, impact of normalisation genes and applicability to general population apply. These must be considered alongside accuracy of diagnosis. This must be highly accurate to become a routinely accepted measure, a difficult challenge that may or may not be surmountable when the gold-standard method is not completely accurate. To achieve the required accuracy with miRNAs a large, complex set of miRNAs will likely be required to account for the complexity of concussion, so other avenues must continue to be pursued in future research.

One option evaluated in this study was sEVs that showed promise in easily obtainable bio-fluids. They could be used to accompany sncRNA biomarkers as they can encapsulate sncRNAs to allow them to elicit their function. If the sncRNA differential concussion signal travels in this way, which is highly possible, sEVs may offer a more effective way to measure the differential signalling [87]. Specific protein markers on the surface of sEVs could indicate the essential signalling response to concussion, enabling them to act as a biomarker. Then, as demonstrated by the differential CD81 response in this study the Exoview technology could be used to capture and quantify the differential expression. Limitations currently exist due to the novel nature of the technology, emerging sEV field and a need for more specific protein marker than CD81 that would be challenging to find. However, in the future this may accompany or enable quantification of the snRNA content within sEVs to enhance the sensitivity of diagnosis so should be seen as benefit to the sncRNA biomarker.

To fully utilise any future biomarker the underlying pathophysiology is a key component to maximise its use clinically. In concussion this is no different as individual sncRNA molecules or families could be signalling independently and could account for individual symptomology profiles. Understanding the pathophysiological role of individual signalling molecules should be a key component of new research as it may allow for future tailored treatments and this study has highlighted two potential families of interest.

Pathophysiology of concussion based on sncRNAs differential signalling

Two sncRNA families have shown to be involved in concussion during this study: (1) the snRNA family of RNU-6 (time point b), (2) the hsa-let-7 miRNA family (baseline, time point b and time point c).

The differential expression of seven RNU-6 family members, a novel finding that highlights the potential of snRNAs as biomarkers, shows that they are likely to be an integral signalling molecule in the immediate aftermath of injury. The role of these snRNAs is currently unclear but their upregulation could derive from their transcription via RNA polymerase III, which differs from the other snRNA members [197]. U6 snRNAs are also a core component of the spliceosome so any change is likely to alter RNA splicing via the spliceosome. This may explain the differential miRNA signalling that is witnessed and demonstrates a requirement for more understanding of their function and their role in concussion development.

Differential expression can also be seen of hsa-let-7 family members at time point b (hsa-let-7a-5p and hsa-let-7i-5p) and time point c (hsa-let-7f-5p). This time dependent family-based response is perhaps unsurprising given their high prevalence in the brain. The families similar sequence homolog means they have similar mRNA targets and thereby potential pathway

interactions [175]. The hsa-let-7 family continually demonstrate an interaction with the extracellular matrix (ECM). This role in regulation of the ECM may be of importance in the immediate aftermath of injury and could be an important target for treatment or further pathophysiological knowledge.

Long term consequences: could miRNAs demonstrate neurological changes?

This pathophysiological knowledge may help with diagnosis further and enable preventative treatment methods. Like previous management methods this is post-injury management for recuperation in the short-term, which by all accounts has improved immeasurably, still has some improvement to go, in the last few years. Schemes such as 'Recognise and Remove' employed by World Rugby have increased understanding, which has reduced prevalence of repetitive concussions [53]. However, these methods will only ever have a minimal ability to reduce incidence of concussion after full recovery.

A methodology that could predict those individuals at higher 'risk' of concussion-based injury to orchestrate rest patterns to prevent injury. This may be the most effective way of managing incidence of concussion after full recovery as other tested preventative measures such as helmets have shown little effectiveness in contact sports [198]. This study has demonstrated the capability to distinguish differences at baseline in the sncRNA expression of athletes who went onto to receive a concussion. These differences could indicate early signs of neurological trauma, often termed sub concussive blows, or previous trauma that may increase 'risk' of future injury. These sncRNA differences could be utilised as biomarkers to assess risk of injury to prevent future injury through rest at appropriate junctures. Although there are clear limitations of a large proportion of concussions will be inevitable in contact sports a pre-

disposable element through environmental and potentially genetic factors could potentially be of importance. This demonstrates a novel method to identify at risk individuals and its potential may be able to be harnessed to identify individuals, if any, at risk of neurodegenerative diseases.

Whether a link between head trauma and neurodegenerative diseases exists is still to be fully revealed. Numerous studies suggest a link with CTE and Alzheimer's disease among diseases demonstrated to have a potential link generally in repetitive concussion. However full clarification of any potential link requires some form of pathophysiological mechanism behind it.

The role of the hsa-let-7 family and potential link between concussion and AD

This study has demonstrated two hsa-let-7 family members (hsa-let-7a-5p and hsa-let-7i-5p) involved in the post-injury response of concussed patients to be differentially expressed in the brains of AD patients. The finding of differential expression of hsa-let-7 family in AD is consistent with the literature and highlights a potential disruptive role for this family [175]. Although the concussion change is in a less invasive bio-fluid it may indicate that this miRNA family may be a pathophysiological linking factor between head trauma and neurodegenerative disease.

The role of hsa-let-7 family should be investigated further to understand the implication of these changes, whether it is a short term neurological protective mechanism that when dysregulated can cause neurodegenerative disease or demonstration.

Overall

Concussion is a problem that affects a large population. This study has demonstrated that the management of concussion has some way to go to improve and has given, in my opinion, three mechanisms of improving management over a wider population; (1) to establish an effective and accessible diagnostic biomarker, (2) to find ways to prevent concussion in patients with the aim of reducing concussion incidence and downstream consequences and (3) establish mechanistic understanding of concussion pathophysiology to enable novel treatment methods and elucidation of any potential link between concussion and to future Neurodegenerative diseases.

Small non-coding RNAs have demonstrated in this study they can help in all three areas and could underpin the complexities that we are currently struggling to comprehend. They are unlikely to be the answer to all the issues, but they could address a proportion that could aid management and our understanding, so my belief is they warrant further study in a concussion environment.

List of References

1. Kamins, J. and C.C. Giza, *Concussion-Mild Traumatic Brain Injury: Recoverable Injury with Potential for Serious Sequelae.* Neurosurg Clin N Am, 2016. **27**(4): p. 441-52.
2. Maroon, J.C., C. Mathyssek, and J. Bost, *Cerebral concussion: a historical perspective.* Prog Neurol Surg, 2014. **28**: p. 1-13.
3. Di Pietro, V., et al., *Antioxidant Therapies in Traumatic Brain Injury.* Antioxidants (Basel), 2020. **9**(3).
4. Vagnozzi, R., et al., *Temporal window of metabolic brain vulnerability to concussion: a pilot 1H-magnetic resonance spectroscopic study in concussed athletes--part III.* Neurosurgery, 2008. **62**(6): p. 1286-95; discussion 1295-6.
5. Bey, T. and B. Ostick, *Second impact syndrome.* West J Emerg Med, 2009. **10**(1): p. 6-10.
6. Vos, B.C., K. Nieuwenhuijsen, and J.K. Sluiter, *Consequences of Traumatic Brain Injury in Professional American Football Players: A Systematic Review of the Literature.* Clin J Sport Med, 2018. **28**(2): p. 91-99.
7. Omalu, B., *Chronic traumatic encephalopathy.* Prog Neurol Surg, 2014. **28**: p. 38-49.
8. McCrory, P., et al., *What is the definition of sports-related concussion: a systematic review.* Br J Sports Med, 2017. **51**(11): p. 877-887.
9. Katayama, Y., et al., *Massive increases in extracellular potassium and the indiscriminate release of glutamate following concussive brain injury.* J Neurosurg, 1990. **73**(6): p. 889-900.
10. Farkas, O., J. Lifshitz, and J.T. Povlishock, *Mechanoporation induced by diffuse traumatic brain injury: an irreversible or reversible response to injury?* J Neurosci, 2006. **26**(12): p. 3130-40.
11. Cheng, G., et al., *Mitochondria in traumatic brain injury and mitochondrial-targeted multipotential therapeutic strategies.* Br J Pharmacol, 2012. **167**(4): p. 699-719.
12. Yi, J.H. and A.S. Hazell, *Excitotoxic mechanisms and the role of astrocytic glutamate transporters in traumatic brain injury.* Neurochem Int, 2006. **48**(5): p. 394-403.
13. Giza, C.C. and D.A. Hovda, *The new neurometabolic cascade of concussion.* Neurosurgery, 2014. **75 Suppl 4**(0 4): p. S24-33.
14. Kawamata, T., et al., *Administration of excitatory amino acid antagonists via microdialysis attenuates the increase in glucose utilization seen following concussive brain injury.* J Cereb Blood Flow Metab, 1992. **12**(1): p. 12-24.
15. Hovda, D.A., et al., *The increase in local cerebral glucose utilization following fluid percussion brain injury is prevented with kynurenic acid and is associated with an increase in calcium.* Acta Neurochir Suppl (Wien), 1990. **51**: p. 331-3.
16. Kawamata, T., et al., *Lactate accumulation following concussive brain injury: the role of ionic fluxes induced by excitatory amino acids.* Brain Res, 1995. **674**(2): p. 196-204.
17. Yoshino, A., et al., *Dynamic changes in local cerebral glucose utilization following cerebral conclusion in rats: evidence of a hyper- and subsequent hypometabolic state.* Brain Res, 1991. **561**(1): p. 106-19.
18. Grossman, E.J., M. Inglese, and R. Bammer, *Mild traumatic brain injury: is diffusion imaging ready for primetime in forensic medicine?* Top Magn Reson Imaging, 2010. **21**(6): p. 379-86.
19. Adams, J.H., et al., *Diffuse axonal injury due to nonmissile head injury in humans: an analysis of 45 cases.* Ann Neurol, 1982. **12**(6): p. 557-63.
20. Adams, J.H., et al., *Diffuse axonal injury in head injury: definition, diagnosis and grading.* Histopathology, 1989. **15**(1): p. 49-59.
21. Johnson, V.E., W. Stewart, and D.H. Smith, *Axonal pathology in traumatic brain injury.* Exp Neurol, 2013. **246**: p. 35-43.
22. Tang-Schomer, M.D., et al., *Partial interruption of axonal transport due to microtubule breakage accounts for the formation of periodic varicosities after traumatic axonal injury.* Exp Neurol, 2012. **233**(1): p. 364-72.
23. Pettus, E.H., et al., *Traumatically induced altered membrane permeability: its relationship to traumatically induced reactive axonal change.* J Neurotrauma, 1994. **11**(5): p. 507-22.
24. Greer, J.E., M.J. McGinn, and J.T. Povlishock, *Diffuse traumatic axonal injury in the mouse induces atrophy, c-Jun activation, and axonal outgrowth in the axotomized neuronal population.* J Neurosci, 2011. **31**(13): p. 5089-105.

25. Wang, J., R.J. Hamm, and J.T. Povlishock, *Traumatic axonal injury in the optic nerve: evidence for axonal swelling, disconnection, dieback, and reorganization.* J Neurotrauma, 2011. **28**(7): p. 1185-98.
26. Junger, E.C., et al., *Cerebral autoregulation following minor head injury.* J Neurosurg, 1997. **86**(3): p. 425-32.
27. Yamakami, I. and T.K. McIntosh, *Alterations in regional cerebral blood flow following brain injury in the rat.* J Cereb Blood Flow Metab, 1991. **11**(4): p. 655-60.
28. DeWitt, D.S. and D.S. Prough, *Traumatic cerebral vascular injury: the effects of concussive brain injury on the cerebral vasculature.* J Neurotrauma, 2003. **20**(9): p. 795-825.
29. Gardner, A.J., et al., *Cerebrovascular reactivity assessed by transcranial Doppler ultrasound in sport-related concussion: a systematic review.* Br J Sports Med, 2015. **49**(16): p. 1050-5.
30. Mucha, A., et al., *A Brief Vestibular/Ocular Motor Screening (VOMS) assessment to evaluate concussions: preliminary findings.* Am J Sports Med, 2014. **42**(10): p. 2479-86.
31. Kontos, A.P., M. Collins, and S.A. Russo, *An Introduction to Sports Concussion for the Sport Psychology Consultant.* Journal of Applied Sport Psychology, 2004. **16**(3): p. 220-235.
32. Elbin, R.J., et al., *Removal From Play After Concussion and Recovery Time.* Pediatrics, 2016. **138**(3).
33. Yue, J.K., et al., *Pre-injury Comorbidities Are Associated With Functional Impairment and Post-concussive Symptoms at 3- and 6-Months After Mild Traumatic Brain Injury: A TRACK-TBI Study.* Front Neurol, 2019. **10**: p. 343.
34. McCrory, P., et al., *Consensus statement on concussion in sport: the 4th International Conference on Concussion in Sport, Zurich, November 2012.* J Athl Train, 2013. **48**(4): p. 554-75.
35. McCrea, M., et al., *Incidence, clinical course, and predictors of prolonged recovery time following sport-related concussion in high school and college athletes.* J Int Neuropsychol Soc, 2013. **19**(1): p. 22-33.
36. Broglio, S.P. and T.W. Puetz, *The effect of sport concussion on neurocognitive function, self-report symptoms and postural control : a meta-analysis.* Sports Med, 2008. **38**(1): p. 53-67.
37. Broglio, S.P., et al., *National Athletic Trainers' Association position statement: management of sport concussion.* J Athl Train, 2014. **49**(2): p. 245-65.
38. McCrory, P., et al., *Consensus statement on concussion in sport-the 5(th) international conference on concussion in sport held in Berlin, October 2016.* Br J Sports Med, 2017. **51**(11): p. 838-847.
39. Iverson, G., *Predicting slow recovery from sport-related concussion: the new simple-complex distinction.* Clin J Sport Med, 2007. **17**(1): p. 31-7.
40. Broglio, S.P., S.N. Macciocchi, and M.S. Ferrara, *Neurocognitive performance of concussed athletes when symptom free.* J Athl Train, 2007. **42**(4): p. 504-8.
41. Iverson, G.L., M.R. Lovell, and M.W. Collins, *Interpreting change on ImPACT following sport concussion.* Clin Neuropsychol, 2003. **17**(4): p. 460-7.
42. Resch, J.E., M.A. McCrea, and C.M. Cullum, *Computerized neurocognitive testing in the management of sport-related concussion: an update.* Neuropsychol Rev, 2013. **23**(4): p. 335-49.
43. Farnsworth, J.L., 2nd, et al., *Reliability of Computerized Neurocognitive Tests for Concussion Assessment: A Meta-Analysis.* J Athl Train, 2017. **52**(9): p. 826-833.
44. Nelson, L.D., et al., *Prospective, Head-to-Head Study of Three Computerized Neurocognitive Assessment Tools (CNTs): Reliability and Validity for the Assessment of Sport-Related Concussion.* J Int Neuropsychol Soc, 2016. **22**(1): p. 24-37.
45. Kirkwood, M.W., K.O. Yeates, and P.E. Wilson, *Pediatric Sport-Related Concussion: A Review of the Clinical Management of an Oft-Neglected Population.* Pediatrics, 2006. **117**(4): p. 1359-1371.
46. Halstead, M.E. and K.D. Walter, *Sport-Related Concussion in Children and Adolescents.* Pediatrics, 2010. **126**(3): p. 597-615.
47. Lee, B. and A. Newberg, *Neuroimaging in traumatic brain imaging.* NeuroRx, 2005. **2**(2): p. 372-83.
48. Coles, J.P., *Imaging after brain injury.* BJA: British Journal of Anaesthesia, 2007. **99**(1): p. 49-60.
49. Toledo, E., et al., *The young brain and concussion: imaging as a biomarker for diagnosis and prognosis.* Neurosci Biobehav Rev, 2012. **36**(6): p. 1510-31.
50. Shenton, M.E., et al., *A review of magnetic resonance imaging and diffusion tensor imaging findings in mild traumatic brain injury.* Brain Imaging Behav, 2012. **6**(2): p. 137-92.
51. Fuller, C.W., et al., *Evaluation of World Rugby's concussion management process: results from Rugby World Cup 2015.* British Journal of Sports Medicine, 2017. **51**(1): p. 64-69.
52. Schneider, K.J., et al., *Rest and treatment/rehabilitation following sport-related concussion: a systematic review.* British Journal of Sports Medicine, 2017. **51**(12): p. 930-934.

53. McCrory, P., et al., *Consensus statement on concussion in sport—the 5th international conference on concussion in sport held in Berlin, October 2016.* British Journal of Sports Medicine, 2017. **51**(11): p. 838-847.
54. Papa, L., *Potential Blood-based Biomarkers for Concussion.* Sports Med Arthrosc Rev, 2016. **24**(3): p. 108-15.
55. Jones, A. and P. Jarvis, *Review of the potential use of blood neuro-biomarkers in the diagnosis of mild traumatic brain injury.* Clin Exp Emerg Med, 2017. **4**(3): p. 121-127.
56. Papa, L., et al., *Elevated levels of serum glial fibrillary acidic protein breakdown products in mild and moderate traumatic brain injury are associated with intracranial lesions and neurosurgical intervention.* Ann Emerg Med, 2012. **59**(6): p. 471-83.
57. Rodríguez-Rodríguez, A., et al., *Role of S100B protein in urine and serum as an early predictor of mortality after severe traumatic brain injury in adults.* Clin Chim Acta, 2012. **414**: p. 228-33.
58. Müller, K., et al., *S100B serum level predicts computed tomography findings after minor head injury.* J Trauma, 2007. **62**(6): p. 1452-6.
59. Ingebrigtsen, T. and B. Romner, *Management of minor head injuries in hospitals in Norway.* Acta Neurol Scand, 1997. **95**(1): p. 51-5.
60. Nygren De Boussard, C., et al., *S100 in mild traumatic brain injury.* Brain Inj, 2004. **18**(7): p. 671-83.
61. Zemlan, F.P., et al., *C-tau biomarker of neuronal damage in severe brain injured patients: association with elevated intracranial pressure and clinical outcome.* Brain Res, 2002. **947**(1): p. 131-9.
62. Bazarian, J.J., et al., *Serum S-100B and cleaved-tau are poor predictors of long-term outcome after mild traumatic brain injury.* Brain Inj, 2006. **20**(7): p. 759-65.
63. Ost, M., et al., *Initial CSF total tau correlates with 1-year outcome in patients with traumatic brain injury.* Neurology, 2006. **67**(9): p. 1600-4.
64. Büki, A. and J.T. Povlishock, *All roads lead to disconnection?--Traumatic axonal injury revisited.* Acta Neurochir (Wien), 2006. **148**(2): p. 181-93; discussion 193-4.
65. Siman, R., et al., *A panel of neuron-enriched proteins as markers for traumatic brain injury in humans.* J Neurotrauma, 2009. **26**(11): p. 1867-77.
66. Gatson, J.W., et al., *Detection of neurofilament-H in serum as a diagnostic tool to predict injury severity in patients who have suffered mild traumatic brain injury.* J Neurosurg, 2014. **121**(5): p. 1232-8.
67. Jackson, P. and R.J. Thompson, *The demonstration of new human brain-specific proteins by high-resolution two-dimensional polyacrylamide gel electrophoresis.* J Neurol Sci, 1981. **49**(3): p. 429-38.
68. Tongaonkar, P., et al., *Evidence for an interaction between ubiquitin-conjugating enzymes and the 26S proteasome.* Mol Cell Biol, 2000. **20**(13): p. 4691-8.
69. Papa, L., et al., *Time Course and Diagnostic Accuracy of Glial and Neuronal Blood Biomarkers GFAP and UCH-L1 in a Large Cohort of Trauma Patients With and Without Mild Traumatic Brain Injury.* JAMA Neurol, 2016. **73**(5): p. 551-60.
70. Fire, A., et al., *Potent and specific genetic interference by double-stranded RNA in Caenorhabditis elegans.* Nature, 1998. **391**(6669): p. 806-11.
71. Di Pietro, V., et al., *MicroRNAs as Novel Biomarkers for the Diagnosis and Prognosis of Mild and Severe Traumatic Brain Injury.* J Neurotrauma, 2017. **34**(11): p. 1948-1956.
72. Pasquinelli, A.E., *MicroRNAs and their targets: recognition, regulation and an emerging reciprocal relationship.* Nat Rev Genet, 2012. **13**(4): p. 271-82.
73. Davis, B.N. and A. Hata, *Regulation of MicroRNA Biogenesis: A miRiad of mechanisms.* Cell Communication and Signaling, 2009. **7**(1): p. 18.
74. Bartel, D.P., *MicroRNAs: target recognition and regulatory functions.* Cell, 2009. **136**(2): p. 215-33.
75. Lytle, J.R., T.A. Yario, and J.A. Steitz, *Target mRNAs are repressed as efficiently by microRNA-binding sites in the 5' UTR as in the 3' UTR.* Proc Natl Acad Sci U S A, 2007. **104**(23): p. 9667-72.
76. Thomas, K.T., C. Gross, and G.J. Bassell, *microRNAs Sculpt Neuronal Communication in a Tight Balance That Is Lost in Neurological Disease.* Frontiers in Molecular Neuroscience, 2018. **11**(455).
77. Patz, S., et al., *More than cell dust: microparticles isolated from cerebrospinal fluid of brain injured patients are messengers carrying mRNAs, miRNAs, and proteins.* J Neurotrauma, 2013. **30**(14): p. 1232-42.
78. Yang, T., et al., *Elevated serum miR-93, miR-191, and miR-499 are noninvasive biomarkers for the presence and progression of traumatic brain injury.* J Neurochem, 2016. **137**(1): p. 122-9.

79. Di Pietro, V., et al., *Salivary MicroRNAs: Diagnostic Markers of Mild Traumatic Brain Injury in Contact-Sport.* Front Mol Neurosci, 2018. **11**: p. 290.
80. Redell, J.B., et al., *Human traumatic brain injury alters plasma microRNA levels.* J Neurotrauma, 2010. **27**(12): p. 2147-56.
81. Bhomia, M., et al., *A Panel of Serum MiRNA Biomarkers for the Diagnosis of Severe to Mild Traumatic Brain Injury in Humans.* Sci Rep, 2016. **6**: p. 28148.
82. Papa, L., et al., *Elevations in MicroRNA Biomarkers in Serum Are Associated with Measures of Concussion, Neurocognitive Function, and Subconcussive Trauma over a Single National Collegiate Athletic Association Division I Season in Collegiate Football Players.* J Neurotrauma, 2019. **36**(8): p. 1343-1351.
83. Hicks, S.D., et al., *Overlapping MicroRNA Expression in Saliva and Cerebrospinal Fluid Accurately Identifies Pediatric Traumatic Brain Injury.* J Neurotrauma, 2018. **35**(1): p. 64-72.
84. Johnson, J.J., et al., *Association of Salivary MicroRNA Changes With Prolonged Concussion Symptoms.* JAMA Pediatr, 2018. **172**(1): p. 65-73.
85. Atif, H. and S.D. Hicks, *A Review of MicroRNA Biomarkers in Traumatic Brain Injury.* J Exp Neurosci, 2019. **13**: p. 1179069519832286.
86. Mitchell, P.S., et al., *Circulating microRNAs as stable blood-based markers for cancer detection.* Proc Natl Acad Sci U S A, 2008. **105**(30): p. 10513-8.
87. Zhao, C., X. Sun, and L. Li, *Biogenesis and function of extracellular miRNAs.* ExRNA, 2019. **1**(1): p. 38.
88. Valadi, H., et al., *Exosome-mediated transfer of mRNAs and microRNAs is a novel mechanism of genetic exchange between cells.* Nat Cell Biol, 2007. **9**(6): p. 654-9.
89. Prud'homme, G.J., et al., *Neuropilin-1 is a receptor for extracellular miRNA and AGO2/miRNA complexes and mediates the internalization of miRNAs that modulate cell function.* Oncotarget, 2016. **7**(42): p. 68057-68071.
90. Laterza, O.F., et al., *Plasma MicroRNAs as sensitive and specific biomarkers of tissue injury.* Clin Chem, 2009. **55**(11): p. 1977-83.
91. Kalsotra, A., et al., *Brain trauma leads to enhanced lung inflammation and injury: evidence for role of P4504Fs in resolution.* J Cereb Blood Flow Metab, 2007. **27**(5): p. 963-74.
92. Espinosa-Parrilla, Y., et al., *Decoding the Role of Platelets and Related MicroRNAs in Aging and Neurodegenerative Disorders.* Front Aging Neurosci, 2019. **11**: p. 151.
93. Rapado-González, Ó., et al., *Human salivary microRNAs in Cancer.* J Cancer, 2018. **9**(4): p. 638-649.
94. Zhang, D., et al., *Post-transcriptional Regulation is the Major Driver of microRNA Expression Variation.* bioRxiv, 2020: p. 2020.01.07.897975.
95. Watson, C.N., A. Belli, and V. Di Pietro, *Small Non-coding RNAs: New Class of Biomarkers and Potential Therapeutic Targets in Neurodegenerative Disease.* Front Genet, 2019. **10**: p. 364.
96. Aryani, A. and B. Denecke, *Exosomes as a Nanodelivery System: a Key to the Future of Neuromedicine?* Mol Neurobiol, 2016. **53**(2): p. 818-34.
97. Pfeffer, S.R., *Two Rabs for exosome release.* Nat Cell Biol, 2010. **12**(1): p. 3-4.
98. Wolfers, J., et al., *Tumor-derived exosomes are a source of shared tumor rejection antigens for CTL cross-priming.* Nat Med, 2001. **7**(3): p. 297-303.
99. Yamada, T., et al., *Comparison of methods for isolating exosomes from bovine milk.* J Vet Med Sci, 2012. **74**(11): p. 1523-5.
100. van den Boorn, J.G., et al., *Exosomes as nucleic acid nanocarriers.* Adv Drug Deliv Rev, 2013. **65**(3): p. 331-5.
101. Hartjes, T.A., et al., *Extracellular Vesicle Quantification and Characterization: Common Methods and Emerging Approaches.* Bioengineering (Basel), 2019. **6**(1).
102. Konoshenko, M.Y., et al., *Isolation of Extracellular Vesicles: General Methodologies and Latest Trends.* Biomed Res Int, 2018. **2018**: p. 8545347.
103. Buczko, P., A. Zalewska, and I. Szarmach, *Saliva and oxidative stress in oral cavity and in some systemic disorders.* J Physiol Pharmacol, 2015. **66**(1): p. 3-9.
104. Mikkonen, J.J., et al., *Salivary metabolomics in the diagnosis of oral cancer and periodontal diseases.* J Periodontal Res, 2016. **51**(4): p. 431-7.
105. Fleminger, S., et al., *Head injury as a risk factor for Alzheimer's disease: the evidence 10 years on; a partial replication.* J Neurol Neurosurg Psychiatry, 2003. **74**(7): p. 857-62.

106. Manley, G., et al., *A systematic review of potential long-term effects of sport-related concussion.* Br J Sports Med, 2017. **51**(12): p. 969-977.
107. Omalu, B.I., et al., *Chronic traumatic encephalopathy in a National Football League player.* Neurosurgery, 2005. **57**(1): p. 128-34; discussion 128-34.
108. Hayes, J.P., et al., *Mild traumatic brain injury is associated with reduced cortical thickness in those at risk for Alzheimer's disease.* Brain, 2017. **140**(3): p. 813-825.
109. Marjanovic, S., et al., *A Review of the Dementia Research Landscape and Workforce Capacity in the United Kingdom*. 2015: RAND Corporation.
110. Braak, H. and E. Braak, *Neuropathological stageing of Alzheimer-related changes.* Acta Neuropathol, 1991. **82**(4): p. 239-59.
111. Swarbrick, S., et al., *Systematic Review of miRNA as Biomarkers in Alzheimer's Disease.* Molecular Neurobiology, 2019. **56**(9): p. 6156-6167.
112. Wang, M., L. Qin, and B. Tang, *MicroRNAs in Alzheimer's Disease.* Front Genet, 2019. **10**: p. 153.
113. Swarbrick, S., et al., *Systematic Review of miRNA as Biomarkers in Alzheimer's Disease.* Mol Neurobiol, 2019. **56**(9): p. 6156-6167.
114. Rafferty, J., et al., *On average, a professional rugby union player is more likely than not to sustain a concussion after 25 matches.* British Journal of Sports Medicine, 2019. **53**(15): p. 969-973.
115. Yakoub, K.M., et al., *Investigation into repetitive concussion in sport (RECOS): study protocol of a prospective, exploratory, observational cohort study.* BMJ Open, 2019. **9**(7): p. e029883.
116. Yakoub, K.M., et al., *Study of Concussion in Rugby Union through MicroRNAs (SCRUM): a study protocol of a prospective, observational cohort study.* BMJ Open, 2018. **8**(11): p. e024245.
117. Fuller, C.W., et al., *Evaluation of World Rugby's concussion management process: results from Rugby World Cup 2015.* Br J Sports Med, 2017. **51**(1): p. 64-69.
118. Wu, Y., et al., *MiRPara: a SVM-based software tool for prediction of most probable microRNA coding regions in genome scale sequences.* BMC Bioinformatics, 2011. **12**(1): p. 107.
119. Andersen, C.L., J.L. Jensen, and T.F. Ørntoft, *Normalization of real-time quantitative reverse transcription-PCR data: a model-based variance estimation approach to identify genes suited for normalization, applied to bladder and colon cancer data sets.* Cancer Res, 2004. **64**(15): p. 5245-50.
120. LaRocca, D., et al., *Comparison of serum and saliva miRNAs for identification and characterization of mTBI in adult mixed martial arts fighters.* PLoS One, 2019. **14**(1): p. e0207785.
121. Sun, L., et al., *MiR-144 promotes β-amyloid accumulation-induced cognitive impairments by targeting ADAM10 following traumatic brain injury.* Oncotarget, 2017. **8**(35): p. 59181-59203.
122. Xiang, M., et al., *U6 is not a suitable endogenous control for the quantification of circulating microRNAs.* Biochem Biophys Res Commun, 2014. **454**(1): p. 210-4.
123. Jackson, T.C., et al., *The nuclear splicing factor RNA binding motif 5 promotes caspase activation in human neuronal cells, and increases after traumatic brain injury in mice.* J Cereb Blood Flow Metab, 2015. **35**(4): p. 655-66.
124. Yashiro, Y. and K. Tomita, *Function and Regulation of Human Terminal Uridylyltransferases.* Front Genet, 2018. **9**: p. 538.
125. Repetto, E., et al., *RNY-derived small RNAs as a signature of coronary artery disease.* BMC Medicine, 2015. **13**(1): p. 259.
126. Scheckel, C., et al., *Regulatory consequences of neuronal ELAV-like protein binding to coding and non-coding RNAs in human brain.* Elife, 2016. **5**.
127. Bohnsack, M.T. and K.E. Sloan, *Modifications in small nuclear RNAs and their roles in spliceosome assembly and function.* Biol Chem, 2018. **399**(11): p. 1265-1276.
128. Leidinger, P., et al., *A blood based 12-miRNA signature of Alzheimer disease patients.* Genome Biology, 2013. **14**(7): p. R78.
129. Chang, W.S., et al., *Genome-Wide Profiling of miRNA and mRNA Expression in Alzheimer's Disease.* Med Sci Monit, 2017. **23**: p. 2721-2731.
130. Stern, R.A., et al., *Long-term consequences of repetitive brain trauma: chronic traumatic encephalopathy.* Pm r, 2011. **3**(10 Suppl 2): p. S460-7.
131. Yi, J., et al., *Chronic traumatic encephalopathy.* Curr Sports Med Rep, 2013. **12**(1): p. 28-32.
132. Nemetz, P.N., et al., *Traumatic Brain Injury and Time to Onset of Alzheimer's Disease: A Population-based Study.* American Journal of Epidemiology, 1999. **149**(1): p. 32-40.

133. Das, M., S. Mohapatra, and S.S. Mohapatra, *New perspectives on central and peripheral immune responses to acute traumatic brain injury.* Journal of Neuroinflammation, 2012. **9**(1): p. 236.
134. Hemphill, M.A., et al., *Traumatic brain injury and the neuronal microenvironment: a potential role for neuropathological mechanotransduction.* Neuron, 2015. **85**(6): p. 1177-92.
135. Sordillo, P.P., L.A. Sordillo, and L. Helson, *Bifunctional role of pro-inflammatory cytokines after traumatic brain injury.* Brain Inj, 2016. **30**(9): p. 1043-53.
136. Wu, Y., et al., *Implantation of Brain-Derived Extracellular Matrix Enhances Neurological Recovery after Traumatic Brain Injury.* Cell Transplant, 2017. **26**(7): p. 1224-1234.
137. George, N. and H.M. Geller, *Extracellular matrix and traumatic brain injury.* J Neurosci Res, 2018. **96**(4): p. 573-588.
138. Weisová, P., et al., *Regulation of glucose transporter 3 surface expression by the AMP-activated protein kinase mediates tolerance to glutamate excitation in neurons.* J Neurosci, 2009. **29**(9): p. 2997-3008.
139. Briones, T.L., J. Woods, and M. Rogozinska, *Decreased neuroinflammation and increased brain energy homeostasis following environmental enrichment after mild traumatic brain injury is associated with improvement in cognitive function.* Acta Neuropathol Commun, 2013. **1**: p. 57.
140. Hill, J.L., et al., *Traumatic brain injury decreases AMP-activated protein kinase activity and pharmacological enhancement of its activity improves cognitive outcome.* J Neurochem, 2016. **139**(1): p. 106-19.
141. Huang, T., et al., *Long noncoding RNAs in the mTOR signaling network: biomarkers and therapeutic targets.* Apoptosis, 2018. **23**(5-6): p. 255-264.
142. Shen, M., et al., *Dexmedetomidine exerts neuroprotective effect via the activation of the PI3K/Akt/mTOR signaling pathway in rats with traumatic brain injury.* Biomed Pharmacother, 2017. **95**: p. 885-893.
143. Chen, S., et al., *Alterations in mammalian target of rapamycin signaling pathways after traumatic brain injury.* J Cereb Blood Flow Metab, 2007. **27**(5): p. 939-49.
144. Erlich, S., et al., *Rapamycin is a neuroprotective treatment for traumatic brain injury.* Neurobiol Dis, 2007. **26**(1): p. 86-93.
145. Wu, H., et al., *Simvastatin-mediated upregulation of VEGF and BDNF, activation of the PI3K/Akt pathway, and increase of neurogenesis are associated with therapeutic improvement after traumatic brain injury.* J Neurotrauma, 2008. **25**(2): p. 130-9.
146. Zhang, L. and H. Wang, *Autophagy in Traumatic Brain Injury: A New Target for Therapeutic Intervention.* Front Mol Neurosci, 2018. **11**: p. 190.
147. Di Battista, A.P., et al., *Peripheral blood neuroendocrine hormones are associated with clinical indices of sport-related concussion.* Scientific Reports, 2019. **9**(1): p. 18605.
148. Arneson, D., et al., *Single cell molecular alterations reveal target cells and pathways of concussive brain injury.* Nat Commun, 2018. **9**(1): p. 3894.
149. Shutov, A.A. and A.A. Chudinov, *[Thyroid function in brain concussion].* Zh Nevrol Psikhiatr Im S S Korsakova, 1993. **93**(2): p. 39-42.
150. Henry, L.C., et al., *Neurometabolic changes in the acute phase after sports concussions correlate with symptom severity.* J Neurotrauma, 2010. **27**(1): p. 65-76.
151. Qin, K., et al., *"Dual Disease" TgAD/GSS mice exhibit enhanced Alzheimer's disease pathology and reveal PrP(C)-dependent secretion of Aβ.* Sci Rep, 2019. **9**(1): p. 8524.
152. Sticht, C., et al., *miRWalk: An online resource for prediction of microRNA binding sites.* PLoS One, 2018. **13**(10): p. e0206239.
153. Liu, H., et al., *Nuclear functions of mammalian MicroRNAs in gene regulation, immunity and cancer.* Molecular Cancer, 2018. **17**(1): p. 64.
154. Todd, M.A., D. Ivanochko, and D.J. Picketts, *PHF6 Degrees of Separation: The Multifaceted Roles of a Chromatin Adaptor Protein.* Genes (Basel), 2015. **6**(2): p. 325-52.
155. Slomnicki, L.P., et al., *Requirement of Neuronal Ribosome Synthesis for Growth and Maintenance of the Dendritic Tree.* J Biol Chem, 2016. **291**(11): p. 5721-39.
156. Zhang, C., et al., *The X-linked intellectual disability protein PHF6 associates with the PAF1 complex and regulates neuronal migration in the mammalian brain.* Neuron, 2013. **78**(6): p. 986-93.
157. Ding, Q., et al., *Ribosome Dysfunction Is an Early Event in Alzheimer's Disease.* The Journal of Neuroscience, 2005. **25**(40): p. 9171-9175.
158. Park, S.A., S.I. Ahn, and J.M. Gallo, *Tau mis-splicing in the pathogenesis of neurodegenerative disorders.* BMB Rep, 2016. **49**(8): p. 405-13.

159. Fitzpatrick, A.W.P., et al., *Cryo-EM structures of tau filaments from Alzheimer's disease.* Nature, 2017. **547**(7662): p. 185-190.
160. Ganguly, P., et al., *Tau assembly: the dominant role of PHF6 (VQIVYK) in microtubule binding region repeat R3.* J Phys Chem B, 2015. **119**(13): p. 4582-93.
161. Gu, M., et al., *Mu2 adaptin facilitates but is not essential for synaptic vesicle recycling in Caenorhabditis elegans.* J Cell Biol, 2008. **183**(5): p. 881-92.
162. Milosevic, I., *Revisiting the Role of Clathrin-Mediated Endoytosis in Synaptic Vesicle Recycling.* Front Cell Neurosci, 2018. **12**: p. 27.
163. Sjödin, S., et al., *Endo-lysosomal proteins and ubiquitin CSF concentrations in Alzheimer's and Parkinson's disease.* Alzheimers Res Ther, 2019. **11**(1): p. 82.
164. Marcello, E., et al., *Endocytosis of synaptic ADAM10 in neuronal plasticity and Alzheimer's disease.* J Clin Invest, 2013. **123**(6): p. 2523-38.
165. Andersen, C.L., J.L. Jensen, and T.F. Orntoft, *Normalization of real-time quantitative reverse transcription-PCR data: a model-based variance estimation approach to identify genes suited for normalization, applied to bladder and colon cancer data sets.* Cancer Res, 2004. **64**(15): p. 5245-50.
166. Tokar, T., et al., *mirDIP 4.1-integrative database of human microRNA target predictions.* Nucleic Acids Res, 2018. **46**(D1): p. D360-d370.
167. Takousis, P., et al., *Differential expression of microRNAs in Alzheimer's disease brain, blood, and cerebrospinal fluid.* Alzheimers Dement, 2019. **15**(11): p. 1468-1477.
168. Natera-Naranjo, O., et al., *Identification and quantitative analyses of microRNAs located in the distal axons of sympathetic neurons.* Rna, 2010. **16**(8): p. 1516-29.
169. Su, L.N., et al., *Network analysis of microRNAs, transcription factors, and target genes involved in axon regeneration.* J Zhejiang Univ Sci B, 2018. **19**(4): p. 293-304.
170. Wang, W.X., et al., *Patterns of microRNA expression in normal and early Alzheimer's disease human temporal cortex: white matter versus gray matter.* Acta Neuropathol, 2011. **121**(2): p. 193-205.
171. Kumar, S. and P.H. Reddy, *Are circulating microRNAs peripheral biomarkers for Alzheimer's disease?* Biochim Biophys Acta, 2016. **1862**(9): p. 1617-27.
172. Cha, D.J., et al., *miR-212 and miR-132 Are Downregulated in Neurally Derived Plasma Exosomes of Alzheimer's Patients.* Frontiers in Neuroscience, 2019. **13**(1208).
173. Satoh, J., Y. Kino, and S. Niida, *MicroRNA-Seq Data Analysis Pipeline to Identify Blood Biomarkers for Alzheimer's Disease from Public Data.* Biomark Insights, 2015. **10**: p. 21-31.
174. Kumar, P., et al., *Circulating miRNA biomarkers for Alzheimer's disease.* PLoS One, 2013. **8**(7): p. e69807.
175. Derkow, K., et al., *Distinct expression of the neurotoxic microRNA family let-7 in the cerebrospinal fluid of patients with Alzheimer's disease.* PLoS One, 2018. **13**(7): p. e0200602.
176. Gámez-Valero, A., et al., *Exploratory study on microRNA profiles from plasma-derived extracellular vesicles in Alzheimer's disease and dementia with Lewy bodies.* Translational Neurodegeneration, 2019. **8**(1): p. 31.
177. Pena, J.T., et al., *miRNA in situ hybridization in formaldehyde and EDC-fixed tissues.* Nat Methods, 2009. **6**(2): p. 139-41.
178. Roush, S. and F.J. Slack, *The let-7 family of microRNAs.* Trends Cell Biol, 2008. **18**(10): p. 505-16.
179. Nguyen, T., C. Su, and M. Singh, *Let-7i inhibition enhances progesterone-induced functional recovery in a mouse model of ischemia.* Proceedings of the National Academy of Sciences, 2018. **115**(41): p. E9668-E9677.
180. Li, S., et al., *Let-7 microRNAs regenerate peripheral nerve regeneration by targeting nerve growth factor.* Mol Ther, 2015. **23**(3): p. 423-33.
181. Lehmann, S.M., et al., *An unconventional role for miRNA: let-7 activates Toll-like receptor 7 and causes neurodegeneration.* Nature Neuroscience, 2012. **15**(6): p. 827-835.
182. McGowan, H., et al., *hsa-let-7c miRNA Regulates Synaptic and Neuronal Function in Human Neurons.* Front Synaptic Neurosci, 2018. **10**: p. 19.
183. von Bernhardi, R., et al., *Role of TGFβ signaling in the pathogenesis of Alzheimer's disease.* Front Cell Neurosci, 2015. **9**: p. 426.
184. Lepelletier, F.X., et al., *Early changes in extracellular matrix in Alzheimer's disease.* Neuropathol Appl Neurobiol, 2017. **43**(2): p. 167-182.
185. Barnett, J.H., et al., *Early intervention in Alzheimer's disease: a health economic study of the effects of diagnostic timing.* BMC Neurol, 2014. **14**: p. 101.

186. Wang, R. and P.H. Reddy, *Role of Glutamate and NMDA Receptors in Alzheimer's Disease.* J Alzheimers Dis, 2017. **57**(4): p. 1041-1048.
187. Nomoto, S., et al., *The relationship between thyroid function and cerebral blood flow in mild cognitive impairment and Alzheimer's disease.* PLOS ONE, 2019. **14**(4): p. e0214676.
188. KrishnaKumar, V.G., et al., *Mechanistic insights into remodeled Tau-derived PHF6 peptide fibrils by Naphthoquinone-Tryptophan hybrids.* Scientific Reports, 2018. **8**(1): p. 71.
189. Schneider, R., et al., *Downregulation of exosomal miR-204-5p and miR-632 as a biomarker for FTD: a GENFI study.* Journal of Neurology, Neurosurgery & Psychiatry, 2018. **89**(8): p. 851-858.
190. Andreu, Z. and M. Yáñez-Mó, *Tetraspanins in extracellular vesicle formation and function.* Front Immunol, 2014. **5**: p. 442.
191. Campos-Silva, C., et al., *High sensitivity detection of extracellular vesicles immune-captured from urine by conventional flow cytometry.* Scientific Reports, 2019. **9**(1): p. 2042.
192. Ranghino, A., et al., *Extracellular vesicles in the urine: markers and mediators of tissue damage and regeneration.* Clin Kidney J, 2015. **8**(1): p. 23-30.
193. Hessvik, N.P. and A. Llorente, *Current knowledge on exosome biogenesis and release.* Cell Mol Life Sci, 2018. **75**(2): p. 193-208.
194. Keller, S., et al., *CD24 is a marker of exosomes secreted into urine and amniotic fluid.* Kidney Int, 2007. **72**(9): p. 1095-102.
195. Martins, S.A., et al., *CD81 Promotes a Migratory Phenotype in Neuronal-Like Cells.* Microscopy and Microanalysis, 2019. **25**(1): p. 229-235.
196. Yoshizawa, J.M., et al., *Salivary biomarkers: toward future clinical and diagnostic utilities.* Clin Microbiol Rev, 2013. **26**(4): p. 781-91.
197. Lou, G., et al., *Differential distribution of U6 (RNU6-1) expression in human carcinoma tissues demonstrates the requirement for caution in the internal control gene selection for microRNA quantification.* Int J Mol Med, 2015. **36**(5): p. 1400-8.
198. Daneshvar, D.H., et al., *Helmets and mouth guards: the role of personal equipment in preventing sport-related concussions.* Clin Sports Med, 2011. **30**(1): p. 145-63, x.

Supplementary materials

Chapter 2

Supplementary Table 37 - All small non-coding RNAs found to be significantly differentially regulated during the NGS and selected for further qPCR validation.

Form of RNA	Name	Number
MicroRNA	hsa-miR-1180-3p, hsa-miR-1246, hsa-miR-125b-2-3p, hsa-miR-126-3p, hsa-miR-126-5p, hsa-miR-1273h-3p, hsa-miR-1290, hsa-miR-133a-3p, hsa-miR-133a-5p, hsa-miR-133b, hsa-miR-16-1-3p, hsa-miR-193b-5p, hsa-miR-199a-5p, hsa-miR-206, hsa-miR-2277-5p, hsa-miR-3122, hsa-miR-339-5p, hsa-miR-33a-3p, hsa-miR-34b-3p, hsa-miR-34c-3p, hsa-miR-34c-5p, hsa-miR-4449, hsa-miR-449a, hsa-miR-449b-3p, hsa-miR-449c-5p, hsa-miR-484, hsa-miR-5087, hsa-miR-5096, hsa-miR-5195-5p, hsa-miR-548h-5p, hsa-miR-551a, hsa-miR-561-5p, hsa-miR-5699-3p, hsa-miR-619-5p, hsa-miR-671-3p, hsa-miR-6748-3p, hsa-miR-6813-3p, hsa-miR-6824-3p, hsa-miR-885-5p, hsa-miR-92a-3p, hsa-let-7a-5p, hsa-let-7f-5p, hsa-let-7i-5p, hsa-miR-101-3p, hsa-miR-103a-3p, hsa-miR-148a-3p, hsa-miR-21-5p, hsa-miR-223-3p, hsa-miR-23a-3p, hsa-miR-26a-5p, hsa-miR-26b-5p, hsa-miR-29a-3p, hsa-miR-29c-3p, hsa-miR-30e-5p, hsa-let-7b-5p, hsa-miR-107, hsa-miR-1271-5p, hsa-miR-135b-5p, hsa-miR-142-3p, hsa-miR-142-5p, hsa-miR-143-3p, hsa-miR-144-3p, hsa-miR-144-5p, hsa-miR-23b-3p, hsa-miR-27b-3p, hsa-miR-31-5p, hsa-miR-4454, hsa-miR-455-5p, hsa-miR-5100, hsa-miR-548w, hsa-miR-934, hsa-miR-99a-5p	76
SnRNA	RNU4-4P-201, RNU4-6P, RNU4-9P, RNU5E-4P, RNU5F-4P-201, RNU6-1, RNU6-10, RNU6-11, RNU6-14, RNU6-26, RNU6-27-201, RNU6-29, RNU6-31, RNU6-32-201, RNU6-33, RNU6-36, RNU6-39, RNU6-41-201, RNU6-4-201, RNU6-45-201, RNU6-48, RNU6-5, RNU6-6, RNU6-7, RNU6-73-201, RNU6-9, U1.10, U1.105, U1.116, U1.28, U2.3-201, U3.13, U3.2, U3.20-201, U3.24, U3.3, U3.39, U3.4, U3.42, U4.57, U4.64-201, U4.79, U6.1249-201, U6.168, U6.254, U6.266, U6.375, U6.422-201, U6.428, U6.601, U6.97, U6atac.20-201, U6atac.25-201, U6atac.29, U6atac.4	55
SnoRNA or ScaRNA	SCARNA1-201, SCARNA4, SNORA25, SNORA57-201, SNORA65-201, SNORA7.4-201, SNORA70.5, SNORA79.1-201, SNORD114-2, SNORD116-19-201, SNORD116-21-201, SNORD116-25-201, SNORD36A, SNORD3B-2-201, snoU13.120-201, snoU13.160-201, snoU13.318-201, snoU13.328-201, snoU13.348, snoU13.63, snoU13.86	21
tRNAs	tRNA100-PseudoGAA, tRNA105-PseudoTTC, tRNA10-AlaCGC, tRNA10-PseudoTGA, tRNA119-AlaCGC, tRNA11-ArgACG, tRNA11-AsnGTT, tRNA11-IleAAT, tRNA120-AlaAGC, tRNA125-ThrCGT, tRNA12-ArgCCT, tRNA12-SerAGA, tRNA130-ValCAC, tRNA131-GlnCTG, tRNA132-PseudoCAC, tRNA134-GluTTC, tRNA136-AsnGTT, tRNA138-ArgACG, tRNA13-AlaCGC, tRNA13-AlaTGC, tRNA144-AspGTC, tRNA156-ArgACG, tRNA15-ThrCGT, tRNA162-MetCAT, tRNA164-MetCAT, tRNA165-IleAAT, tRNA175-SerGCT, tRNA18-ArgCCT, tRNA19-ArgTCG, tRNA1-ArgCCG, tRNA1-AsnGTT, tRNA1-LeuAAG, tRNA20-MetCAT, tRNA21-ArgCCT, tRNA23-ArgCCG, tRNA26-AsnGTT, tRNA27-MetCAT, tRNA28-IleAAT, tRNA2-ArgCCT, tRNA2-LeuTAA, tRNA31-AsnGTT, tRNA32-MetCAT, tRNA36-ArgACG, tRNA36-ThrAGT, tRNA3-ArgCCT, tRNA3-ProTGG, tRNA40-ThrAGT, tRNA4-ArgTCG, tRNA4-AsnGTT, tRNA4-GluCTC, tRNA4-HisGTG, tRNA4-ThrAGT, tRNA56-ThrTGT, tRNA5-IleTAT, tRNA66-AlaTGC, tRNA6-TrpCCA, tRNA73-ArgCCG, tRNA7-AsnGTT, tRNA7-LeuAAG, tRNA7-SerGCT, tRNA83-AsnGTT, tRNA84-GluTTC, tRNA85-PseudoTTC, tRNA88-PseudoCCT, tRNA8-AlaTGC, tRNA8-SerGCT, tRNA8-ThrAGT, tRNA8-Undet, tRNA95-AlaAGC, tRNA95-AsnGTT, tRNA9-AlaAGC, tRNA9-IleAAT, tRNA9-TyrGTA	73
piRNAs	uc001myu.3, uc002tgp.1, uc003oif.3, uc011ley.2, uc021qtn.1, uc021ybm.1, uc031qaf.1, uc031qpu.1, uc031qtw.1	9
YRNAs	Y_RNA.245, Y_RNA.428-201, Y_RNA.522-201, Y_RNA.597-201, Y_RNA.633-201, Y_RNA.661, Y_RNA.684, Y_RNA.719, Y_RNA.727-201, Y_RNA.75	10
Put-miRs (Sequence)	put-miR-718 (TTCAGGTTACCGCAGG), put-miR-594 (TGATTTTTTTTGGCGAA), put-miR-703 (GACTGCTCGAGCTGCTT), put-miR-477 (TGGGCAGCAAGAATGG), put-miR-727 (GGAGGATTTCAATTGG), put-miR-646 (TCTGTCATGGCTGAGC), put-miR-675 (TACCTCAATTCTCTAGG), put-miR-319 (TGTCGGCGGGGGCCCCGGAC), put-miR-327 (CATTCTCTGAAACTACA), put-miR-338 (GACTTGTGATTAGCGG), put-miR-1187 (GAGCATGTTGACTGGAGA), put-miR-6 (GCGGACCTTGCTCAAGG), put-miR-341	233

	(TGAGAAAACATTTGAGG), put-miR-750 (CAAGAGATGAGGAATG), put-miR-183 (CCAGGCTGGTCGTGATGA), put-miR-980 (TCGGAAGAAGAAGCTGACCCA), put-miR-798 (TAACTCTTGGAAATCTTGG), put-miR-765 (AAAAAAGAGGGACAGAAATG), put-miR-71 (GACCTTGGGTTGGGTCGTGGT), put-miR-1327 (GAAAAGCAATCGTCACAG), put-miR-371 (AATATTCAGCAGTCAGACTGG), put-miR-354 (CAGGGTGATGACTTCTG), put-miR-688 (GTGATGTCGGCTCATCGCAACCT), put-miR-756 (TGAGGGATGTTTGGATGCTCGCTTTGA), put-miR-1146 (CAACTGTAAGTCCATT), put-miR-1333 (TAATTGTCCTCTTGGGG), put-miR-511 (AAGCAGGCGTTACAATG), put-miR-1199 (TGAACTCGGGAGAAGGAAGT), put-miR-705 (CCTGTCTGACTGGGTCTCC), put-miR-1275 (AAGAAGTAGACTGGATTGG), put-miR-1204 (AGGGCTGGGCACGGGGG), put-miR-857 (TAAGTGGGAGTGCTCATG), put-miR-806 (CACGAGAGAACGCACACC), put-miR-680 (GTTAAGTATGCACAGG), put-miR-576 (TGGCATCCTGTCTCTTGC), put-miR-444 (CTGAAAAGGGGACGGATTGGGAA), put-miR-1132 (CACGCTGTCTTTTGTTTCTCT), put-miR-1025 (TGGAAGAGGGGAAAGGAGA), put-miR-496 (CTAAGAGTATGAGTAGC), put-miR-657 (TCAGGACATTGGACTCT), put-miR-625 (GAGAAGACTGAATGCTCTTCTC), put-miR-40 (GCTGGAATAGCTCAGTTGC), put-miR-666 (CAGCATCATGATCATTATGG), put-miR-1098 (AAGGCGAAGGATATGTTG), put-miR-538 (CATTGTGCTTCGTGGGAGAGTAGGGCA), put-miR-952 (GCCGACAGGTCCGGGTAA), put-miR-572 (TAGATTCAGGAACTGCCA), put-miR-972 (TTTAGTAGAATTGTGTTGGGT), put-miR-650 (AAAAGCAAGGCGAAGAGG), put-miR-134 (CAGACTGCTCGAGCTGCTGC), put-miR-975 (TTTGCAGACTGGAAACT), put-miR-161 (TGTCTGTAGCAATGTGCT), put-miR-1265 (TGGGGATAAAGTTAGGT), put-miR-968 (TGGCTGTTGCACTTCT), put-miR-1125 (TTGAAGACTGGCTCTCA), put-miR-892 (CAACGGTCTTGAAAACA), put-miR-1306 (ATAACGTCATCTAGTGTG), put-miR-948 (TGGAAGAAAACGAGGAG), put-miR-925 (ATTTTGGTCTGTTGGTT), put-miR-259 (ATGTAACCGGGCTTTTGTGCT), put-miR-209 (GGTCCTCGGATCGGCC), put-miR-773 (CAGGCAGAAGGGAGCTTGT), put-miR-910 (CACGTTCTTCTCATGGT), put-miR-664 (AAAGTTGTGTTAGCTGA), put-miR-1068 (TATGATTGTAAACTCTGA), put-miR-265 (CACATGGGGGTAGAGCACTGACTGGG), put-miR-490 (CTGCAGGAGTGTTTGAGA), put-miR-1155 (CAAATGATCAAAGCAGG), put-miR-893 (ACCATCCTCTGCTACCA), put-miR-1342 (ATCGGAAAATGTGGGAA), put-miR-967 (AAATGCATTGGATATGG), put-miR-811 (GTTGTAAAGCTCTGTTG), put-miR-812 (GTTCTGAGTTCTTTGGTTGGA), put-miR-1084 (AGGACCATTGCGTTGCC), put-miR-626 (TTCACTACTTTATCTCTTTT), put-miR-127 (AGACTGTGATGACTGGGAGAGCGGGCT), put-miR-219 (GAGGCTCGAGAGCAATGGC), put-miR-863 (AAGTTGGAGTATGTTTTAGG), put-miR-33 (CCATGACTGCAGATGG), put-miR-1246 (CTGGAGATCTGTTTGGGC), put-miR-126 (GTGGGGCTTAGTGCTGA), put-miR-459 (GGGATCAACCTGACAA), put-miR-907 (CCAACAGCTTCTGAGTTG), put-miR-171 (GTCCTGTGTCTTGTACGG), put-miR-1163 (AGAGGACAGGGAAGCTT), put-miR-204 (AGAAGTCAGAACCTCTAT), put-miR-498 (GACAGATTTTAGCTTGTCC), put-miR-286 (TAACAGGCGTTGAAATTGT), put-miR-223 (GATGGGGGTAGAGCACTGC), put-miR-75 (TGGGGATTGTGGGTTCTC), put-miR-548 (AGAGGACAGGGAAGCT), put-miR-1118 (AGAGGGTTCCTGTAGACCTAGGGAGGA), put-miR-943 (AGCCAGAGTTCTGATTGTGAGTG), put-miR-313 (TGAGTTCTTTGGTCAGAA), put-miR-659 (AGTAGCTGGTCGATTTGGC), put-miR-210 (CTTCAGACTGTGAAACTGA), put-miR-144 (TAGAGATAGAGCTTATG), put-miR-563 (TGGAGACATTAACTATGA), put-miR-1140 (TGGGAAGGGCTGCCGG), put-miR-497 (TTGGTAGACTCTCACTT), put-miR-573 (TGGATAACTCTTTTTGTA), put-miR-906 (TATGGGAAGAATCTGGG), put-miR-231 (TATGTCATGGTGGCTTTGG), put-miR-85 (GAATCCCACTTCTGACACCA), put-miR-884 (ATGGTCTAGAGCTACAGGT), put-miR-918 (CAGCTTCTTCCGCTTCTT), put-miR-985 (GTACTGCATCTCTGCA), put-miR-320 (ACTGGATCCAAGAAAAG), put-miR-67 (AGGACGTTGGTCAGAGC), put-miR-221 (TCTCTCAATCCTCTTGG), put-miR-471 (AGAAGCAGAGAACGAGG), put-miR-1352 (TGGATTGTGGGGGAACC), put-miR-610 (AGGAGATATAGCTCTTGT), put-miR-48 (AAAATGGATTCGAACCA), put-miR-529 (TGACCTTTTGCCTTCTGC), put-miR-424 (TAAAAAGTTCTCTGTTTTTC), put-miR-24 (TTGGTGCATCTGTAGTCCAAC), put-miR-164 (TGAAATTCTAAATATTGCA), put-miR-229 (TGGGATTTAGCTCAGC), put-miR-525 (AAGTGGGAAGGCCCAGA), put-miR-325 (TTCAAATCCCACTTCTGACACCA), put-miR-188 (AAATGGCGATACTCAGG), put-miR-1066 (TGCTTTGATCGTAGCCC), put-miR-1295 (GAGGTTAGGATATCTGGCT), put-miR-588 (TTTTGAACGTTCTTTCTT), put-miR-1273 (AAGGGGAGGAATTTCACGTG), put-miR-783 (AAGGAAAAAGCGGATA), put-miR-37 (TGGTGGAGTGAAGACG), put-miR-1317 (TGGAGTGTGGATTGGGG), put-miR-97 (CTGCGTGGCTCTGACAC), put-miR-1016 (AGGTAAAGCTCATGAGG), put-miR-546 (CCAAGGGGTTGTAGGGCCACT), put-miR-1099 (AGACTCCTTTATCGTA), put-miR-874 (ATGAGCATTGATTTAGG), put-miR-701	

	(TTGAGATTTGAGGGGGCCT), put-miR-279 (CTGTGAAGCCTGTTGGTTTGCTGCTG), put-miR-184 (TGCTGAACCTCTGTATGT), put-miR-495 (CAGGGAGTGAAAGAGAATT), put-miR-90 (GAAGTTAAATCCTTGGG), put-miR-468 (ATAAGGAACTGCTCTCTC), put-miR-469 (GCGGGGGATTAGCTCAGCTGGG), put-miR-1195 (ATTCTTTGACATGCAGAT), put-miR-250 (CTGGTGTAGAATTGAGG), put-miR-1264 (CAGGTTTCAGACTTTAGG), put-miR-465 (CCAGTTGTCGTGGGTTTTT), put-miR-1243 (TGTGGATTTTTGTCATGT), put-miR-771 (CCTTGATCTGACTGGGGGCC), put-miR-534 (CTGTTGGAGAATTTGGAATATTAGGT), put-miR-80 (GAAGAGGGAGTGGTCTGTAAATGCG), put-miR-347 (AAAGGGAAACAAGAATTCTT), put-miR-410 (GGAGAATAGAACATGCTGATT), put-miR-891 (TAAATGTTGGTTTGTTTGT), put-miR-189 (GAGCGAAACGGCAGGAT), put-miR-842 (ACCCGGAGAACTGAACT), put-miR-81 (ATTTGAAAGAATGCTTG), put-miR-824 (CTAGCTGAACCTCTGTAT), put-miR-958 (ACAGGGCTGTGCAAAAA), put-miR-742 (CAGGGCTGTGCTAACT), put-miR-605 (TGAGCTTTGGAAGAAGGACCA), put-miR-374 (TGTGAGGATGTTCTGTAAGGAGTGTT), put-miR-135 (TGAATTACGGAAGTGTTGGTTAAT), put-miR-323 (ATAAAATGGGCGTTGAGG), put-miR-506 (AAGAGGGGCTTTTAGAACC), put-miR-293 (GGGTAAAACTGCAGTGGGCGTTGGTAG), put-miR-524 (CGTGGTGATGCTCTGACA), put-miR-517 (TTGGGAAGGGCTGCCGGA), put-miR-391 (ATCTCGATCCAGTAGTC), put-miR-92 (AGAGACTGACTTTGAGTA), put-miR-435 (TTTAGACCGTTTTTATGTC), put-miR-1080 (TGTGGATTGATGCTCT), put-miR-587 (TTTGTAGAAGAGGAAGCG), put-miR-1220 (TAGAATGGGGCTTGTTGC), put-miR-1134 (AAAGAATGAAGTTGGTCTGG), put-miR-352 (TAATGAATGACTGTTTG), put-miR-1162 (AAAGAACGTTCAAAGG), put-miR-377 (AAAGGGCTTTGACTATTT), put-miR-294 (TGCTTCCTCAATCGGT), put-miR-1229 (ACAGTAGCAATGTTCTGC), put-miR-1091 (GATTATGATTGTGATTGTAGC), put-miR-419 (AAAAAGTTAGACTTAGG), put-miR-249 (GCCAGGATGTTGGCTTA), put-miR-122 (GGAACTCATGATTGTTGACTTTGG), put-miR-1320 (TTAGAGGCCACTCAAT), put-miR-335 (TATTTAAATGAGAACTTTGAAGC), put-miR-166 (CGTTTTGGTGTTGGTTG), put-miR-1172 (AGAACCAAGAAGCTCTGG), put-miR-1207 (GTGAAAAGACATAGGGGG), put-miR-1130 (TAGAAGAGGGAGCTTCTTT), put-miR-247 (AGAGCTAGAATCCAGG), put-miR-246 (TTTATTAGAGACGGGACTTT), put-miR-870 (AAAGGATGTAGACAAGGGA), put-miR-704 (CAAATGAATATCTGGGA), put-miR-266 (TTTAGGTACTCTGAACAA), put-miR-928 (CACAGAAGGAACGTTTAGA), put-miR-959 (GAAAGAGAGTGAGACTCA), put-miR-676 (TGGTGGTTGGTTTTGGG), put-miR-1095 (ATTGTGAATGATCTGG), put-miR-550 (GCACTCTGGACTCTGAATCC), put-miR-835 (TTAGGAGTAGGTTACT), put-miR-686 (TGACTGTTTTATATGAGTAA), put-miR-32 (ATCCCGGACGAGCCCCCATTA), put-miR-151 (TTGAAACTGATATACTGTCTTAGG), put-miR-726 (GATGGGCTGATTGAGGGAT), put-miR-256 (ATGAGGCTGAGATTGTCC), put-miR-368 (AATGAGAACTTTGAAGGCCGAAG), put-miR-1232 (ACAGACTGTCTTTGGG), put-miR-1219 (GAAATTATTGATCCAGTCACGA), put-miR-1276 (GAAGAGTTGATCCATG), put-miR-1119 (GTTTTGGGTTGAGTGAGGA), put-miR-901 (GTCTATTTGGATTATCGTC), put-miR-356 (GTTTGAATTGGGAAGCTGGGGG), put-miR-856 (AAGGATAGGGAGGTATTT), put-miR-1244 (CAGTTGGTAGAGCACCTGAC), put-miR-476 (GTGGTCAGGTAGAGAA), put-miR-142 (CAGTATAATTAGGGGTTAATTGTGGGA), put-miR-639 (TGGAGTGTGGATTGGG), put-miR-622 (TGAGTGGTCAATGGGGG), put-miR-337 (TGGGCTCAAGCTTTCTCT), put-miR-422 (TTTAGGGTTTTAAGGTGTTA), put-miR-1339 (GGACTGAGAGCTCTTTCTG), put-miR-1356 (GTGCTGCATGGCTGTCA), put-miR-29 (GAGATTTACGACCTAGG), put-miR-128 (TGGCTCTGACACTAGTA), put-miR-359 (GAAGTGGAAGGACTATGAA), put-miR-1003 (TGGACTTCAGAACAGC), put-miR-238 (AGAGACAGGAACTTTGATTTT), put-miR-961 (TAGCTTGATCCAGTTG), put-miR-751 (AGGCTGAGACTGGACAGAAAGACCT), put-miR-1184 (GCCTGCCCGGTGCTGGT), put-miR-379 (GCGTGTGCGCGGGAGG), put-miR-361 (CAGGTGAAATCGTGGATGT), put-miR-1111 (TGATGCGTTGGGATGTAGC), put-miR-938 (TTAGGAAGCTGCTGATT)	

Control vs. Braak stage III-IV

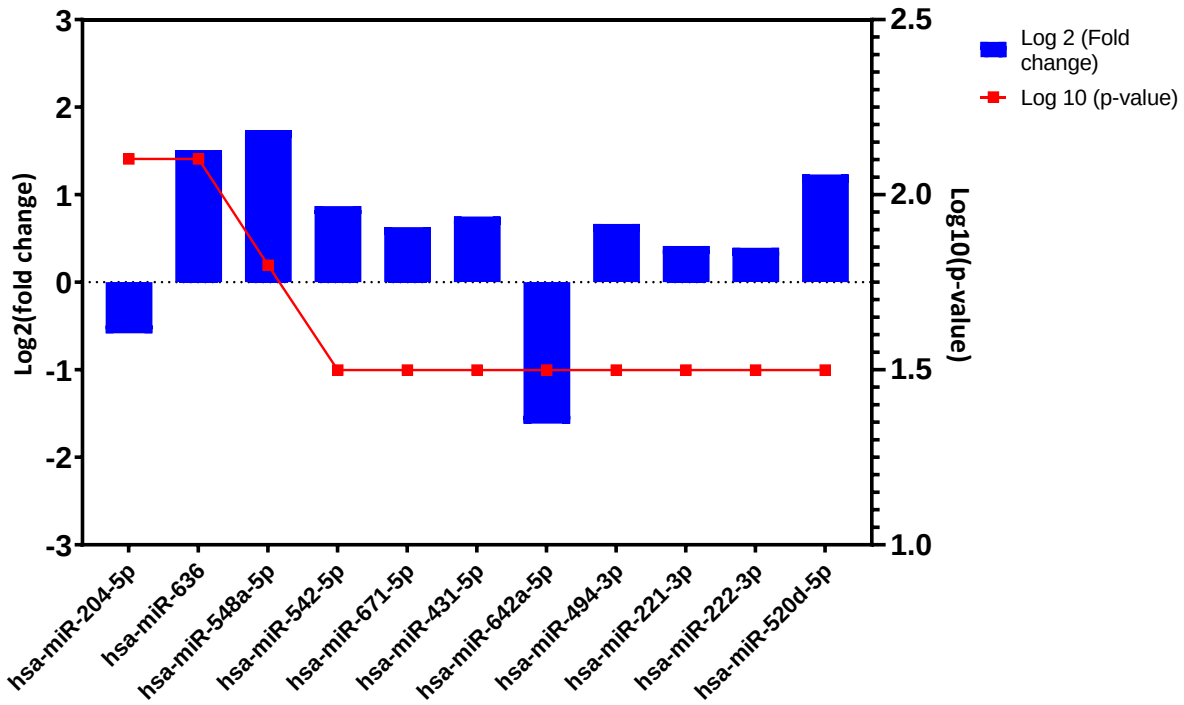

Supplementary Figure 63 – Log fold change and p-values of differentially expressed miRNAs between Control and Braak stage III-IV. A Mann-Whitney U test was used to establish statistical differences between groups. A p-value of less than 0.05 was considered significant.

Supplementary Table 38 – Statistically significant differences of microRNAs between control and Braak stage III-IV. A Mann-Whitney U test was used to establish statistical differences between groups. A p-value of less than 0.05 was considered significant.

MiRNA	Control Average	Control SD	Braak III-IV Average	Braak III-IV SD	Difference	Fold Change	Mann Whitney p-value
hsa-miR-204-5p	-18.876	0.412	-19.457	0.107	-0.5813	1.4962	0.0079
hsa-miR-636	-9.781	0.398	-8.271	0.562	1.5096	0.3512	0.0079
hsa-miR-548a-5p	-9.698	0.354	-7.959	1.265	1.7385	0.2997	0.0159
hsa-miR-542-5p	-11.918	0.498	-11.050	0.302	0.8677	0.5480	0.0317

hsa-miR-671-5p	-13.965	0.259	-13.338	0.329	0.6274	0.6473	0.0317
hsa-miR-431-5p	-12.251	0.245	-11.502	0.491	0.7490	0.5950	0.0317
hsa-miR-642a-5p	-11.216	0.640	-12.830	0.936	-1.6138	3.0606	0.0317
hsa-miR-494-3p	-13.956	0.245	-13.291	0.412	0.6656	0.6304	0.0317
hsa-miR-221-3p	-20.586	0.211	-20.174	0.194	0.4119	0.7516	0.0317
hsa-miR-222-3p	-20.028	0.203	-19.636	0.129	0.3918	0.7622	0.0317
hsa-miR-520d-5p	-7.315	0.922	-6.086	0.437	1.2292	0.4266	0.0317

Control vs. Braak Stage V-VI

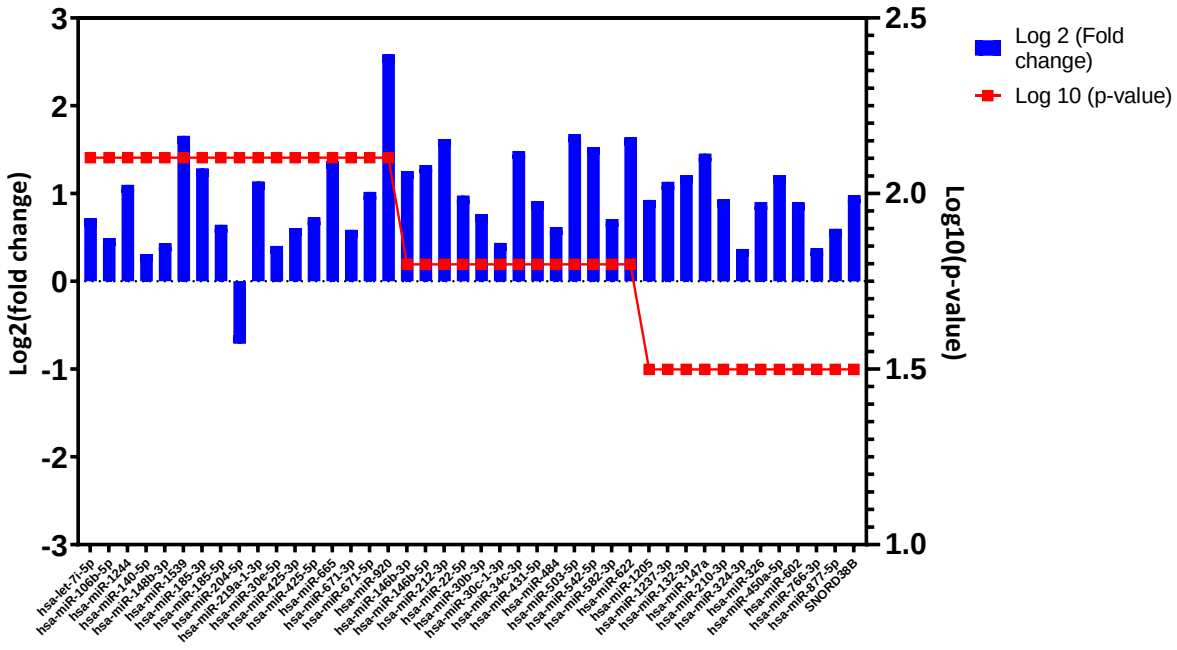

Supplementary Figure 64 - Log fold changes and p-values of statistically significant microRNAs between control and Braak stage V-VI groups. A Mann-Whitney U test was used to establish statistical differences between groups. A p-value of less than 0.05 was considered significant.

Supplementary Table 39 - All statistically significant microRNAs between control and Braak V-VI groups. A Mann-Whitney U test was used to establish statistical differences between groups. A p-value of less than 0.05 was considered significant.

MiRNA	Control Average	Control SD	Braak V-VI Average	Braak V-VI SD	Difference	Fold Change	Mann-Whitney p-value
hsa-let-7i-5p	-20.4596	0.3646	-19.7446	0.5221	0.7149	0.6092	0.0079
hsa-miR-106b-5p	-18.4692	0.2960	-17.9793	0.2324	0.4899	0.7121	0.0079
hsa-miR-1244	-9.5482	0.4605	-8.4498	0.4000	1.0983	0.4671	0.0079
hsa-miR-140-5p	-17.5421	0.0945	-17.2331	0.1403	0.3090	0.8072	0.0079
hsa-miR-148b-3p	-18.1734	0.0209	-17.7427	0.4647	0.4307	0.7419	0.0079
hsa-miR-1539	-9.3968	0.6792	-7.7404	0.7540	1.6565	0.3172	0.0079
hsa-miR-185-3p	-12.2987	0.5802	-11.0157	0.5313	1.2830	0.4109	0.0079
hsa-miR-185-5p	-19.1325	0.5533	-18.4904	0.1050	0.6421	0.6408	0.0079
hsa-miR-204-5p	-18.8759	0.4121	-19.5821	0.2695	-0.7062	1.6315	0.0079
hsa-miR-219a-1-3p	-8.9852	0.4202	-7.8502	0.4709	1.1350	0.4553	0.0079
hsa-miR-30e-5p	-19.8560	0.1460	-19.4533	0.1514	0.4027	0.7564	0.0079
hsa-miR-425-3p	-15.6648	0.2043	-15.0596	0.1459	0.6052	0.6574	0.0079
hsa-miR-425-5p	-18.3754	0.3580	-17.6482	0.2238	0.7272	0.6041	0.0079
hsa-miR-665	-15.3013	0.6087	-13.9344	0.3364	1.3669	0.3877	0.0079
hsa-miR-671-3p	-12.9190	0.2582	-12.3340	0.2281	0.5850	0.6667	0.0079
hsa-miR-671-5p	-13.9649	0.2594	-12.9479	0.4892	1.0171	0.4941	0.0079
hsa-miR-920	-10.5123	0.6218	-7.9298	0.8739	2.5825	0.1670	0.0079
hsa-miR-146b-3p	-12.1436	1.3514	-10.8895	0.2477	1.2542	0.4192	0.0159
hsa-miR-146b-5p	-18.1322	1.3774	-16.8087	0.2772	1.3235	0.3996	0.0159
hsa-miR-212-3p	-14.0197	0.4936	-12.4015	0.5821	1.6182	0.3257	0.0159
hsa-miR-22-5p	-16.1406	0.1825	-15.1659	1.2001	0.9747	0.5088	0.0159
hsa-miR-30b-3p	-11.4234	0.2808	-10.6605	0.2438	0.7629	0.5893	0.0159
hsa-miR-30c-1-3p	-11.9102	0.2631	-11.4750	0.1619	0.4352	0.7396	0.0159
hsa-miR-34c-3p	-16.9990	1.1277	-15.5171	0.5770	1.4819	0.3580	0.0159

hsa-miR-431-5p	-12.2506	0.2450	-11.3420	0.3210	0.9086	0.5327	0.0159
hsa-miR-484	-17.0246	0.4722	-16.4074	0.1734	0.6172	0.6519	0.0159
hsa-miR-503-5p	-12.6135	0.6980	-10.9401	0.9160	1.6734	0.3135	0.0159
hsa-miR-542-5p	-11.9179	0.4975	-10.3903	0.7382	1.5276	0.3468	0.0159
hsa-miR-582-3p	-12.8998	0.3811	-12.1919	0.1333	0.7080	0.6122	0.0159
hsa-miR-622	-7.9891	0.7482	-6.3519	0.7497	1.6372	0.3215	0.0159
hsa-miR-1205	-8.3431	0.4347	-7.4172	0.7768	0.9259	0.5264	0.0317
hsa-miR-1237-3p	-13.0815	0.6428	-11.9496	0.3722	1.1319	0.4563	0.0317
hsa-miR-132-3p	-19.0451	0.4436	-17.8378	0.5411	1.2074	0.4331	0.0317
hsa-miR-147a	-9.5830	0.4449	-8.1312	1.0028	1.4518	0.3656	0.0317
hsa-miR-210-3p	-16.2561	0.7957	-15.3247	0.3844	0.9314	0.5243	0.0317
hsa-miR-324-3p	-17.3016	0.0911	-16.9341	0.4786	0.3675	0.7751	0.0317
hsa-miR-326	-16.3186	0.2605	-15.4172	0.9976	0.9014	0.5354	0.0317
hsa-miR-450a-5p	-13.3885	0.5590	-12.1825	0.6448	1.2061	0.4335	0.0317
hsa-miR-602	-10.3112	0.4681	-9.4128	0.5116	0.8984	0.5365	0.0317
hsa-miR-766-3p	-14.9252	0.1579	-14.5480	0.2062	0.3772	0.7699	0.0317
hsa-miR-877-5p	-13.3469	0.2423	-12.7508	0.2374	0.5961	0.6615	0.0317
SNORD38B	-20.4796	0.4482	-19.5024	0.6619	0.9772	0.5080	0.0317

Braak stage III-IV vs. Braak Stage V-VI

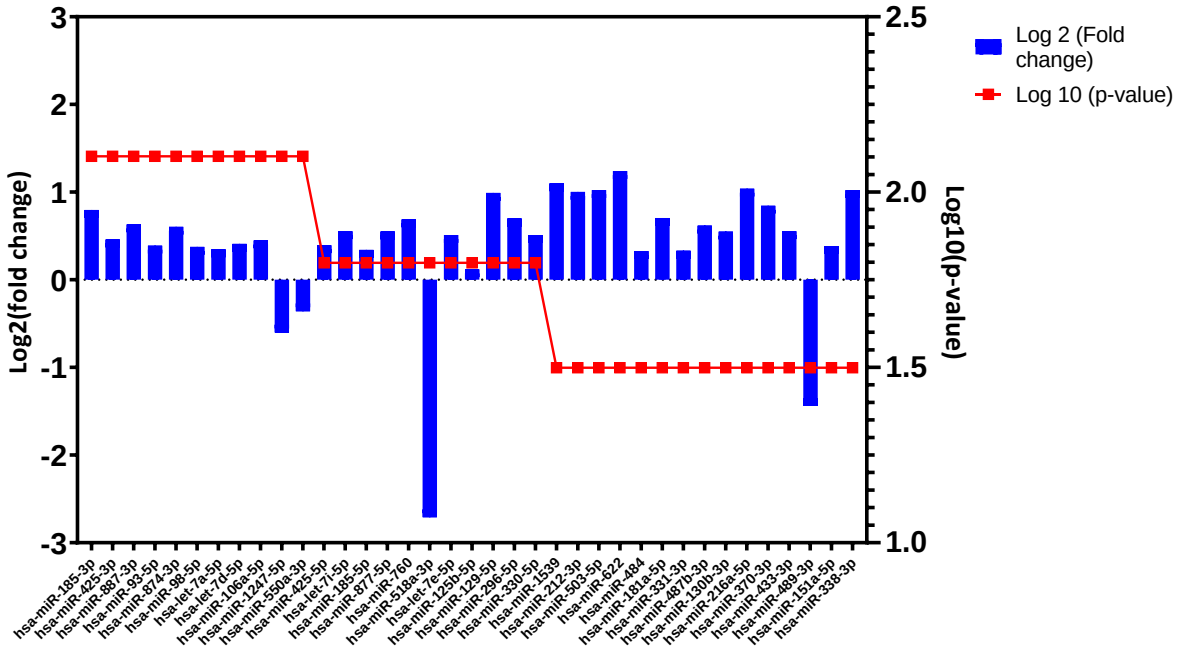

Supplementary Figure 65 – Log fold changes and p-values from differentially expressed microRNAs between Braak stage III-IV and Braak stage V-VI. A Mann-Whitney U test was used to establish statistical differences between groups. A p-value of less than 0.05 was considered significant.

Supplementary Table 40 – Differentially expressed microRNAs between Braak Stage III-IV and Braak stage V-VI. A Mann-Whitney U test was used to establish statistical differences between groups. A p-value of less than 0.05 was considered significant.

MiRNA	Braak III-IV Average	Braak III-IV SD	Braak V-VI Average	Braak V-VI SD	Difference	Fold Change	Mann-Whitney p-value
hsa-miR-185-3p	-11.8113	0.1674	-11.0157	0.5313	0.7956	0.5761	0.0079
hsa-miR-425-3p	-15.5181	0.1543	-15.0596	0.1459	0.4586	0.7277	0.0079
hsa-miR-887-3p	-14.4347	0.1780	-13.8044	0.2510	0.6302	0.6461	0.0079
hsa-miR-93-5p	-18.4087	0.1945	-18.0198	0.0630	0.3889	0.7637	0.0079
hsa-miR-874-3p	-18.6910	0.1198	-18.0888	0.5745	0.6022	0.6587	0.0079
hsa-miR-98-5p	-18.6035	0.0672	-18.2305	0.2318	0.3730	0.7722	0.0079
hsa-let-7a-5p	-22.9334	0.0757	-22.5872	0.0873	0.3462	0.7867	0.0079
hsa-let-7d-5p	-19.9823	0.1501	-19.5729	0.1604	0.4094	0.7529	0.0079
hsa-miR-106a-5p	-18.6845	0.3216	-18.2378	0.0700	0.4467	0.7337	0.0079

hsa-miR-1247-5p	-13.3634	0.1868	-13.9646	0.3507	-0.6012	1.5170	0.0079
hsa-miR-550a-3p	-12.6116	0.0762	-12.9704	0.2522	-0.3589	1.2824	0.0079
hsa-miR-425-5p	-18.0397	0.1116	-17.6482	0.2238	0.3915	0.7623	0.0159
hsa-let-7i-5p	-20.2974	0.0987	-19.7446	0.5221	0.5527	0.6817	0.0159
hsa-miR-185-5p	-18.8293	0.1390	-18.4904	0.1050	0.3389	0.7906	0.0159
hsa-miR-877-5p	-13.3014	0.1710	-12.7508	0.2374	0.5506	0.6827	0.0159
hsa-miR-760	-12.9400	0.2530	-12.2535	0.3414	0.6865	0.6213	0.0159
hsa-miR-518a-3p	-6.8809	1.7025	-9.5882	0.8597	-2.7073	6.5310	0.0159
hsa-let-7e-5p	-20.7386	0.2302	-20.2287	0.1342	0.5099	0.7023	0.0159
hsa-miR-125b-5p	-24.3976	0.0362	-24.2800	0.0660	0.1176	0.9217	0.0159
hsa-miR-129-5p	-17.1260	0.3955	-16.1373	0.3711	0.9888	0.5039	0.0159
hsa-miR-296-5p	-13.8725	0.2705	-13.1737	0.5419	0.6988	0.6161	0.0159
hsa-miR-330-5p	-15.4395	0.1878	-14.9296	0.1918	0.5100	0.7022	0.0159
hsa-miR-1539	-8.8390	0.5937	-7.7404	0.7540	1.0987	0.4669	0.0317
hsa-miR-212-3p	-13.4034	0.2418	-12.4015	0.5821	1.0019	0.4993	0.0317
hsa-miR-503-5p	-11.9619	0.3810	-10.9401	0.9160	1.0217	0.4925	0.0317
hsa-miR-622	-7.5910	0.7764	-6.3519	0.7497	1.2391	0.4236	0.0317
hsa-miR-484	-16.7329	0.1428	-16.4074	0.1734	0.3255	0.7980	0.0317
hsa-miR-181a-5p	-21.5751	0.4574	-20.8706	0.2268	0.7045	0.6137	0.0317
hsa-miR-331-3p	-18.9645	0.1603	-18.6341	0.3707	0.3305	0.7953	0.0317
hsa-miR-487b-3p	-18.4564	0.1902	-17.8405	0.6278	0.6159	0.6525	0.0317
hsa-miR-130b-3p	-14.9886	0.1343	-14.4396	0.4767	0.5490	0.6835	0.0317
hsa-miR-216a-5p	-10.8343	0.3394	-9.7958	0.7391	1.0385	0.4868	0.0317
hsa-miR-370-3p	-15.8825	0.2138	-15.0389	0.6999	0.8436	0.5572	0.0317
hsa-miR-433-3p	-17.3094	0.2868	-16.7569	0.2702	0.5525	0.6819	0.0317
hsa-miR-489-3p	-8.7936	0.7419	-10.2319	0.5984	-1.4383	2.7100	0.0317

hsa-miR-151a-5p	-20.2107	0.3474	-19.8268	0.1121	0.3839	0.7664	0.0317
hsa-miR-338-3p	-22.4151	0.7172	-21.3937	0.6455	1.0215	0.4926	0.0317

MicroRNA differences between Braak stage V-VI and both Control and Braak stage III-IV

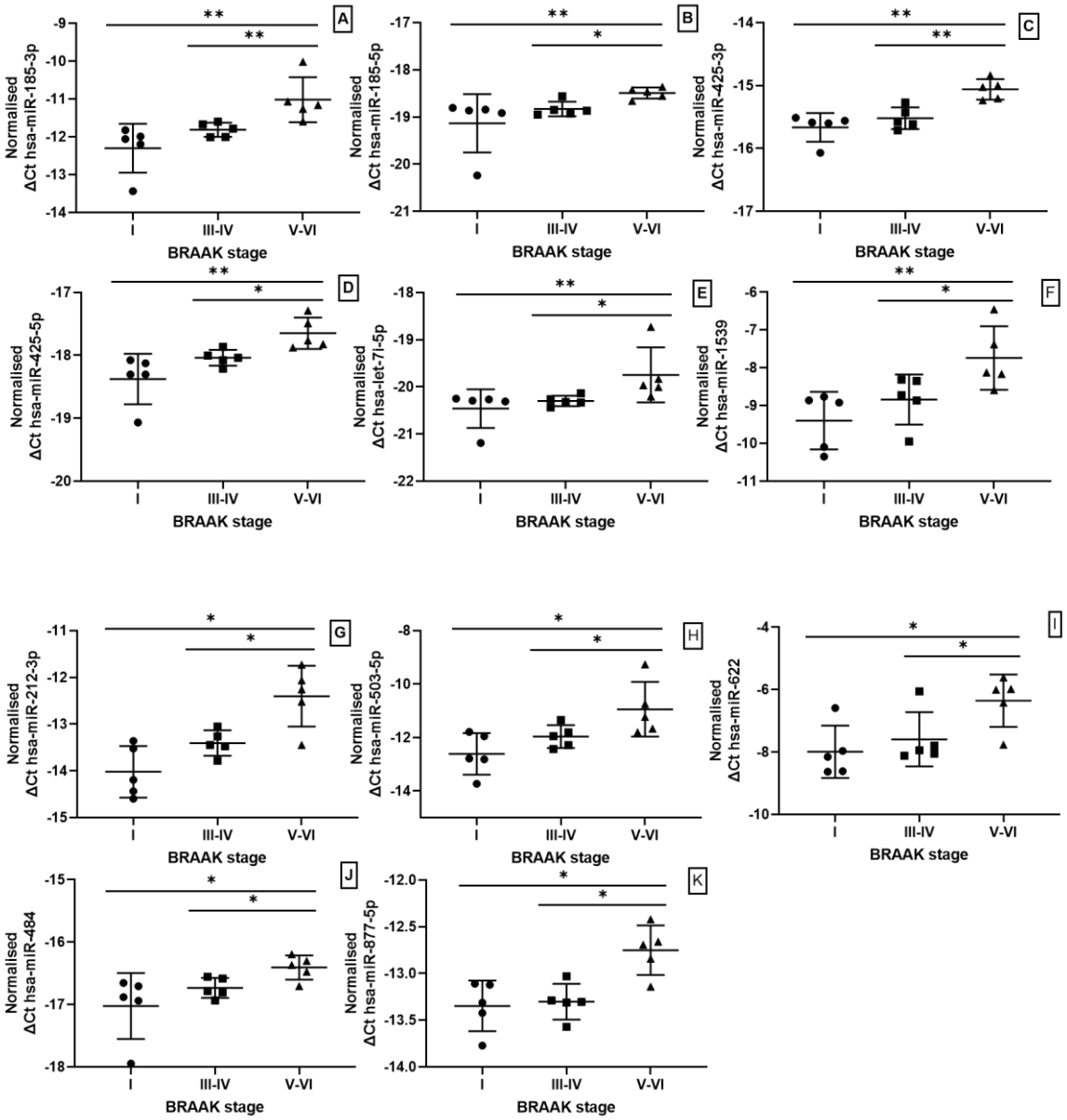

Figure 66 – Differentially expressed microRNAs between Braak stage V-VI and both control and Braak stage III-IV. A Mann-Whitney U test was used to compare for differences between individual groups (e.g. Control – Braak stage III-IV). P-values are represented using **<0.01, *<0.05.

Table 41 - P-values of differentially expressed microRNAs between Braak stage V-VI and both control and Braak stage III-IV. A Mann-Whitney U test was used to establish statistical differences between individual groups. A p-value of less than 0.05 was considered significant.

MicroRNA	Control-Braak stage V-VI	Braak stage III-IV- Braak stage V-VI
hsa-miR-185-3p	0.0079	0.0079
hsa-miR-425-3p	0.0079	0.0079
hsa-miR-425-5p	0.0079	0.0159
hsa-let-7i-5p	0.0079	0.0159
hsa-miR-185-5p	0.0079	0.0159
hsa-miR-1539	0.0079	0.0317
hsa-miR-212-3p	0.0159	0.0317
hsa-miR-503-5p	0.0159	0.0317
hsa-miR-622	0.0159	0.0317
hsa-miR-484	0.0159	0.0317
hsa-miR-877-5p	0.0317	0.0159
Total	11	